

Scaling Hydrologic Impacts from Road Segments to a Small Watershed

AN ABSTRACT OF THE THESIS OF

Timothy Adam Royer for the degree of Master of Science in Forest Engineering presented on February 27, 2006.

Title: Scaling Hydrologic Impacts from Road Segments to a Small Watershed.

Abstract approved:

Arne E. Skaugset III

The impact of forest roads on the hydrology of forested watersheds has long been studied. While forest roads have been reported to alter storm runoff at the road segment scale, the potential for changes to be detectable at the small watershed scale has been debated. The purpose of this study was to quantify the road affect at the road segment scale and estimate how those affects are expressed at the mouth of a watershed. This study took place in the McDonald-Dunn Research Forest located in the Oregon Coast Range near Corvallis, Oregon. Claire Creek, a small watershed within the Oak Creek Watershed, and two road segments with the associated inboard ditches and upslope contributing areas were selected to represent the roaded watershed. Runoff from both road segments enters small headwater streams at stream crossing culverts. Discharge was measured from the headwater streams and from the road segments at the stream crossing culvert for five storms during the winter of 2004 – 2005. Discharge was also measured at the mouth of Claire Creek, an adjacent roadless watershed, Finley Creek, and at a gauging station on Oak Creek near the boundary of the McDonald-Dunn Forest. The difference in time of occurrence of peakflows and the length of the stream between the culverts and the mouth of Claire Creek was used to estimate a ‘real’ travel time of the peakflows for all five storms. Kinematic wave equations were used to model travel times of peakflows from the culverts to the mouth of Claire Creek, with and without the influence of the road.

At the road segment scale the road affect was detectable for changes in peakflow magnitude, quickflow, and total stormflow, but the affect of the road on changes in the timing of occurrence of the peakflow was inconsistent. At the watershed scale the road affect could not be calculated for changes in peakflow magnitude, quickflow, or total stormflow because of the unavailability of pre-road runoff data. The modeled travel time of peakflows that included

discharge from the road were shorter than the modeled travel time of peakflows of stream discharge alone by less than 10 minutes for all five storms. The road effect on real travel times of peakflows was inconsistent and did not correlate to the magnitude of the increase at the road segment or at the mouth of the watershed. These findings agree with earlier studies that have reported a road affect on storm runoff at the road scale, and suggest that the road affect at the mouth of a watershed may not be detectable. The findings also suggest that other factors are influencing runoff at the mouth of a watershed more than the addition of ditch runoff at stream crossing culverts.

©Copyright by Timothy Adam Royer

February 27, 2006

All Rights Reserved

Scaling Hydrologic Impacts from
Road Segments to a Small Watershed

by

Timothy Adam Royer

A THESIS

submitted to

Oregon State University

in partial fulfillment of
the requirements for the
degree of

Master of Science

Presented February 27, 2006

Commencement June 2006

Master of Science thesis of Timothy Adam Royer presented on February 27, 2006.

APPROVED:

Major Professor, representing Forest Engineering

Head of the Department of Forest Engineering

Dean of the Graduate School

I understand that my thesis will become part of the permanent collection of Oregon State University libraries. My signature below authorizes release of my thesis to any reader upon request.

Timothy Adam Royer, Author

ACKNOWLEDGMENTS

The research presented in this thesis was made possible by a grant from the United States Department of Agriculture Center for Wood Utilization, funds administered by Dr. George Ice of the National Council for Air and Stream Improvement, and by an innovative grant from the College of Forestry at Oregon State University. I am grateful for the support given to me by these organizations.

I am grateful to my advisor and friend, Dr. Arne Skaugset, for giving me the opportunity to stretch my mind, and for patiently answering my questions. I am grateful to Dr. Skaugset and the other members of my committee for their time and suggestions on how to improve this project.

I am grateful to members of the Skaugset Lab and fellow Forest Engineering students for the assistance and friendship shown to me during the course of my time here at OSU, and especially with this project. Elizabeth Toman and other members of the Skaugset Lab had previously installed much of the infrastructure used in this study. Nicolas Zegre and Amy Simmons provided advice on the instrumentation of the study sites and analysis of the data. Amy Simmons support in the field and in the lab was especially helpful. Joanna Warren and Elizabeth Harper also spent many hours analyzing samples in the laboratory, samples that were analyzed but not included in this thesis.

I am grateful to my family for their patience and encouragement. Specifically, I am grateful to my wife Erica, and daughter Claire for brightening my life at the end of each day.

TABLE OF CONTENTS

	<u>Page</u>
1. INTRODUCTION	1
1.1 Objectives	2
2. LITERATURE REVIEW	3
2.1 Introduction.....	3
2.2 Hydrological Processes of Forested Watersheds	3
2.3 Forest Roads and Drainage	8
2.4 Impact of Forest Roads on Hydrological Processes.....	11
2.4.1 Impact of Forest Roads on Surface Runoff.....	11
2.4.2 Impact of Forest Roads on Subsurface Flow Paths.....	12
2.4.3 Road and Stream Connectivity	14
2.4.4 Altered Peakflows.....	15
2.5 Flow Routing with Kinematic waves.....	18
2.6 Conclusions.....	23
3. METHODS	24
3.1 Study Area	24
3.2 Site Description.....	25
3.3 Precipitation	30
3.4 Discharge Measurements	31
3.4.1 Peakflows.....	34
3.4.2 Quickflows.....	35
3.4.3 Total Stormflow.....	35
3.4.5 Travel Time of Peakflows.....	37
4. RESULTS	42
4.1 Instrumentation and Data Quality	42
4.2 Precipitation.....	43
4.3 Runoff.....	44
4.4 Road Effects at the Culverts.....	45
4.4.1 Peakflow Magnitude.....	45
4.4.2 Peakflow Timing.....	51
4.4.3 Quickflow Volume	52

TABLE OF CONTENTS (Continued)

	<u>Page</u>
4.4.4 Total Stormflow Volume	55
4.5 Road Effects for the Claire Creek Watershed	57
4.5.1 Peakflow Magnitude	57
4.5.2 Real Peakflow Travel Times	62
4.5.3 Quickflow Volume	65
4.5.4 Total Stormflow Volume	66
4.6 Discharge at Finley Creek and Oak Creek	68
4.7 Modeled Travel Time of Peakflows	70
4.7.1 Modeled Travel Times	71
5. DISCUSSION	84
5.1 Road Effects at the Culverts	84
5.1.1 Peakflow Magnitude	84
5.1.2 Peakflow Timing	85
5.1.3 Quickflow Volume	88
5.1.4 Total Stormflow Volume	88
5.1.5 Culvert 34 versus Culvert 35	89
5.2 Travel Time of Peakflows	90
5.2.1 Modeled Travel Times	90
5.2.2 Real and Modeled Travel Times	94
5.3 Instantaneous Peakflow versus Near Peakflow	97
5.4 Sensitivity of Kinematic Waves to Equation Parameters	98
5.4.1 Channel Slope	98
5.4.2 Manning Roughness Coefficient	100
5.4.3 Lateral Inflow	101
5.4.4 Discharge at the Confluence	102
6. CONCLUSION	105
7. LITERATURE CITED	106

LIST OF FIGURES

<u>Figure</u>	<u>Page</u>
1. Road cross sections (a, b, c) and designs (d, e) after Wemple (1994). The arrows indicate the direction of runoff	10
2. Visualization of dynamic and kinematic waves (after MacArthur and DeVries, 1993).	20
3. Map of the Oak Creek Watershed.....	26
4. Maps of stream channels below culverts 34 and 35, and Claire Creek below the confluence in a) plan view, and b) longitudinal profile.	28
5. Photograph of the flume installation in the road ditch at culvert 34 with a diagram of the flume and capacitance rod.	32
6. Photograph and diagram of pressure transducer installation at the stream crossing culvert above road segment 35.	33
7. Diagram of site layout above a road segment.	34
8. Storm hydrographs for above and below the road at culverts 34 and 35 in the Claire Creek Watershed for the December 6 th storm (a), the January 28 th storm (b), the March 25 th storm (c), the May 8 th storm (d) and the May 17 th storm (e) during the winter of 2004 – 2005.	48
9. Frequency distribution of changes in peakflow timing due to the road at culverts 34 and 35 in the Claire Creek Watershed during the winter of 2004 – 2005. Positive values indicate a delay in peakflow timing; negative values indicate an advance in peakflow timing.	52
10. Storm hydrographs for above and below the road at culverts 34 and 35 and at the mouth of the Claire Creek Watershed for the December 6 th storm (a), the January 28 th storm (b), the March 25 th storm (c), the May 8 th storm (d) and the May 17 th storm (e) during the winter of 2004 – 2005.	59
11. Frequency distribution of the real travel times from above and below culverts 34 and 35 to the mouth of Claire Creek during the winter of 2004 – 2005.	63
12. Scatterplots of real travel times from above and below culverts 34 and 35 to the mouth of Claire Creek relative to a) the magnitude of the peakflow at Claire Creek, and b) the magnitude of the peakflow at the culverts.	64

LIST OF FIGURES (Continued)

<u>Figure</u>	<u>Page</u>
13. The peakflow timing of the streams above and below the road at Culvert 35 for three storms in the winter of 2004-2005. Peakflow timing above the road was observed to be the same as below the road (a), to occur before peakflow below the road (b), and to occur after peakflow below the road (c).	87
14. Scatterplots of real travel times and average modeled travel times of peakflows from culverts 34 and 35 to the mouth of Claire Creek relative to a) peakflow magnitude observed at the mouth of Claire Creek, and b) peakflow magnitude observed above and below culverts 34 and 35 during the winter of 2004 – 2005.	96
15. Graph showing relationship between channel slope and average modeled travel times from the confluence of the streams below culverts 34 and 35 to the mouth of the Claire Creek Watershed for the December 6 th , 2004 storm, using the Wong (2001) equation and continuous method.	99
16. Graph of relationship between roughness coefficient, n , and average modeled travel time of kinematic wave from the confluence of the streams below culverts 34 and 35 to the mouth of the Claire Creek Watershed for the December 6 th , 2004 storm, using the Wong (2001) equation and continuous method.	101
17. Graph of initial upstream discharge at the confluence of the streams below culverts 34 and 35, and the modeled travel times from the confluence to the mouth of the Claire Creek Watershed for the December 6 th , 2004 storm, using the Wong (2001) equation and continuous method.	104

LIST OF TABLES

<u>Table</u>	<u>Page</u>
1. Stream characteristics within Claire Creek of the Oak Creek Watershed.....	29
2. Site characteristics of monitoring locations in the Oak Creek Watershed (Toman, 2004)	30
3. Summary of data availability at the monitoring locations in the Oak Creek Watershed for five storms during the winter of 2004 – 2005.....	42
4. Duration, maximum intensities, and total precipitation amounts for runoff producing storms from the Starker rain gauge at the top of the Finley Creek Watershed.....	44
5. Changes in peakflow magnitude and timing above and below the road at culverts 34 and 35 in Claire Creek Watershed during the winter of 2004 - 2005. Changes are caused by the introduction of ditch flow into the stream channel. Standard errors in parenthesis.....	47
6. Correlation coefficients between rainfall and the increase in peakflow above and below the road at culverts 34 and 35 in Claire Creek Watershed for five storms during the winter of 2004 – 2005.....	51
7. Changes in quickflow volume above and below the road at culverts 34 and 35 in Oak Creek watershed during the winter of 2004 - 2005. Changes caused by the introduction of ditch flow into the stream channel. Standard error in parenthesis.....	54
8. Total stormflow above and below the road at culverts 34 and 35 in Oak Creek watershed during the winter of 2004 – 2005. Standard errors in parenthesis.	56
9. Time of peakflow, real travel time of peakflows, peakflow magnitude, and quickflow volumes measured above and below culverts 34 and 35, and at the mouth of the Claire Creek Watershed during the winter of 2004 – 2005.....	58
10. Total stormflow volumes observed above and below culverts 34 and 35 and at the mouth of Claire Creek during winter of 2004 – 2005.....	67
11. Maximum instantaneous peakflow magnitude and timing at the mouth of Claire Creek, Finley Creek, and Oak Creek watersheds from five storms during the winter of 2004 – 2005..	69
12. Quickflow volumes at the mouth of Claire Creek, Finley Creek, and Oak Creek watersheds from five storms during the winter of 2004 – 2005.....	70

LIST OF TABLES (Continued)

<u>Table</u>	<u>Page</u>
13. Modeled travel times for peakflows above and below culvert 34 from the culvert to the confluence in the Claire Creek Watershed using the Chow (1988) and Wong (2001) kinematic wave equations and treating the stream as one continuous channel.....	72
14. Modeled travel times for peakflows above and below culvert 34 from the culvert to the confluence in the Claire Creek Watershed using the Chow (1988) and Wong (2001) kinematic wave equations and treating Claire Creek as discrete channel segments.	74
15. Modeled travel times for peakflows above and below culvert 35 from the culvert to the confluence in the Claire Creek Watershed using the Chow (1988) and Wong (2001) kinematic wave equations and treating Claire Creek as one continuous channel.	76
16. Modeled travel times for peakflows above and below culvert 35 from the culvert to the confluence in the Claire Creek Watershed using the Chow (1988) and Wong (2001) kinematic wave equations and treating Claire Creek as discrete channel segments.	78
17. Modeled travel times for peakflows above and below culverts 34 and 35 in the Claire Creek Watershed from the confluence to the mouth using the Chow (1988) and Wong (2001) kinematic wave equations and treating Claire Creek as one continuous channel.	80
18. Modeled travel times for peakflows above and below culverts 34 and 35 in the Claire Creek Watershed from the confluence to the mouth using the Chow (1988) and Wong (2001) kinematic wave equations and treating Claire Creek as discrete channel segments.	82
19. The average change in peakflow timing and the average percent increases in peakflow magnitude, quickflow volume and total stormflow below culverts 34 and 35 in the Claire Creek Watershed during the winter of 2004 – 2005. Percent increase is in parenthesis.....	84
20. Modeled travel times for peakflows from above and below culverts 34 and 35 to the mouth of Claire Creek using the Wong (2001) kinematic wave equation and treating Claire Creek as one continuous channel.	93
21. Time and duration of ‘near peak’ at the mouth of Claire Creek for five storms during the winter of 2004 – 2005.....	98

LIST OF EQUATIONS

<u>Equation</u>	<u>Page</u>
1	21
2	21
3	21
4	21
5	31
6	33
7	33
8	34
9	35
10	36
11	36
12	38
13	38
14	38
15	40
16	40
17	40
18	41
19	97

Scaling Hydrologic Impacts from Road Segments to a Small Watershed

1. INTRODUCTION

Forest roads are a common feature in the landscape of the Oregon Coast Range. Initially, roads were constructed to support timber harvesting activities. The vast road infrastructure still exists, and their effect on the hydrology of forested watersheds is a concern. A clear understanding of the effect of roads is complicated by the complex and non-exclusive hydrology processes occurring within a watershed and by the fact that construction of forest roads is often closely followed by timber harvesting.

Forest roads are hypothesized to increase the magnitude and advance the timing of peakflows by routing surface and subsurface runoff to stream channels. Surface runoff may be generated when precipitation lands on road surfaces which have infiltration capacities that are lower than the precipitation intensity (Luce and Cundy, 1994). The low intensity precipitation patterns, coupled with high infiltration capacities of forest roads in the Coast Range of Oregon result in little to no road-surface runoff (Marbet, 2003). The infiltration capacity of the forest floor often exceeds the infiltration capacity of the road surface (Ziegler and Giambelluca, 1997). Precipitation thus infiltrates into the soil and travels through subsurface pathways. Otherwise, roads may intercept subsurface flow paths and transfer the water as concentrated surface runoff in roadside ditches (Megahan, 1972). Both road surface runoff and intercepted subsurface flow may be deposited onto the forest floor by cross drain culverts, or directly into a stream channel at stream crossing culverts (Wemple et al., 1996). When surface runoff that otherwise would not have been delivered to the stream channel at the same location or time in the absence of the road enters a stream, the peakflows may increase in size and advance in timing at that location (Wemple and Jones, 2003; Toman 2004).

While the magnitude of changes to peakflow and time of peakflow remains unknown, it is hypothesized to be proportional to factors such as the level of connectivity between the road drainage features and the streams (Croke and Mockler, 2001). Forest roads impact watershed hydrology by

affecting several processes. These impacts can be enumerated and quantified on the scale of an individual road segment, but it is not currently possible to predict the aggregated impact at the watershed scale.

1.1 Objectives

The objectives of this study are to: 1) Quantify the impacts of individual road segments on the hydrology of specific streams at stream crossing culverts, 2) Model travel times of peakflows from the stream crossing culverts to the mouth of the watershed with and without the road effect, and 3) Investigate whether the effects at individual road segments correlate to observed patterns of runoff at the watershed outlet.

2. LITERATURE REVIEW

2.1 Introduction

Prior studies have demonstrated the changes in both surface and subsurface hydrology that result from the construction of forest roads (Megahan, 1972; Ziemer, 1981; King and Tennyson, 1984; Thomas and Megahan 1998, Jones, 2000). Forest roads have been hypothesized to increase the drainage density of roaded watersheds (Wemple et al., 1996). The impacts of forest roads have been studied at the road segment scale (Reid and Dunne, 1984; Wemple and Jones, 2003; Toman, 2004). Other studies have examined the correlation between road construction and changes in runoff at the mouth of a watershed (Harr, et al., 1975; Ziemer, 1981; Wright et al., 1990; Wemple and Jones, 2003). This review will summarize the hydrological processes that occur in forested watersheds, the basic types of road design, and the ways in which forest roads impact hydrological processes including peakflow magnitude and timing. A summary will also be made of the use of the kinematic wave theory and its application in modeling the travel time of runoff flowing along a stream channel.

2.2 Hydrological Processes of Forested Watersheds

Understanding the hydrological processes of forested watersheds is essential to improving management practices and maintaining the overall health of forests that are managed for multiple purposes. An important part of watershed management is understanding the runoff response to storms. The depiction of runoff over time at a point is called a hydrograph. After examining hydrographs from numerous watersheds, Hewlett and Hibbert (1967) devised an arbitrary, universal method for humid regions that quantifies how much runoff is produced by specific storms. Using this method, the hydrograph is separated with a line beginning at the initial rise of the hydrograph and continuing until it intersects the recession limb of the hydrograph. The separation line has a slope of 0.0055 l/s/ha/hour and thus takes into account the area of the watershed. Although other methods of separating a hydrograph have been successfully used, the Hewlett and Hibbert line is still used to compare storm responses between watersheds, or against previous responses within the same watershed .

Forested watersheds are unique because the soils have low bulk densities and have a layer of organic matter that covers the mineral soil. Pritchett (1979) designates the organic layer to be the feature that distinguishes forest soils from agricultural soil. Forested watersheds in the Pacific Northwest (PNW) are further distinguished by steep topography. Storms in the PNW are characterized by low precipitation intensities, though short-duration high-intensity bursts may occur. All of these characteristics contribute to conditions in which subsurface flow is the dominant, but not the only, runoff pathway.

There are some conditions in which surface runoff has been observed in forested watersheds. For example, rain falling directly on the stream channel contributes a small percentage to the overall amount of storm runoff (Brooks et al., 1997). Surface runoff in the form of overland flow can be described as either infiltration excess overland flow or saturation excess overland flow.

Infiltration excess overland flow, also called Hortonian overland flow, occurs when the rainfall intensity is greater than the infiltration capacity of the soil. It was reported in the literature by Horton (1933) for agricultural lands of Iowa. However, the structure and texture of forest soils create high infiltration capacities. This, coupled with low precipitation intensities, results in the absence of Hortonian overland flow on undisturbed soils in humid forests (Hewlett and Hibbert, 1967; Dunne and Black, 1970; Harr, 1977). Betson (1964) and Ragan (1967) each reported that Hortonian overland flow occurs where the infiltration capacity of the forest soil has been changed—as with the construction of a road—or is naturally low. Since surface runoff was only being generated by part of the watershed, this process has been termed partial area flow (Ragan, 1967). Overland flow may also be generated when wildfires create hydrophobic soils (Ice et al., 2004).

Saturation excess overland flow occurs when the subsurface flow from upslope areas exceeds the capacity of the soil profile to transfer the water down slope, resulting in the exfiltration of the excess subsurface flow. Saturation excess overland flow was found to be a major contributor to runoff in the glaciated region of Vermont (Dunne and Black, 1970). Dunne and Black (1970) concluded that saturation excess overland flow was similar to the partial flow observed by Betson

(1964) and Ragan (1967) in that both processes occurred consistently from specific portions of the watershed and were thought to be the delivery mechanism of runoff to the storm hydrograph.

Although subsurface flow pathways dominate forested watersheds, they are more challenging to understand than surface flow pathways. Numerous studies have been conducted to determine the mechanisms and flow paths by which subsurface flow arrives at the stream and to calculate the length of time required for the subsurface flow to reach the stream. Early studies examined the limitations of vertical infiltration of rainwater and the conditions that would change the flow from vertical to lateral. Whipkey (1965) and Weyman (1970) both excavated troughs along hillslopes to observe subsurface flow through the different soil horizons. Subsurface flow infiltrated vertically through coarse textured soils until it reached an impeding layer: either an impermeable layer (Weyman, 1970) or one with significantly reduced hydraulic conductivity (Whipkey, 1965) and then flow became lateral.

The alteration of subsurface flow from vertical to lateral was also observed to occur as the soil profile reached saturation (Weyman 1973), or in response to rainfall (Harr 1977). Weyman (1973) observed that runoff initially drained vertically, and then flowed laterally down the slope at an impeding layer. With continued lateral drainage, a saturated, wedge-shaped zone extended upslope, and flow within the saturated zone was lateral. Harr (1977) reported that during the interstorm period, drainage in the upper 30 cm of soil was predominantly lateral, and became vertical during storms. The opposite occurred at depths greater than 30 cm; during the interstorm period drainage was predominantly vertical and became lateral during storms (Harr 1977).

One of the most contested topics in hillslope hydrology has been mechanism responsible for the rapid delivery of runoff to streams during storms. At the center of the debate is the discussion over whether the fast response in runoff is the result of event water traveling to the stream or of a displacement of pre-event water from the soil storage. In this context, event water is rainfall that is associated with an occurring storm, and pre-event water is rainfall that was associated with earlier storms and has since been stored in the hillslope as soil moisture.

A mechanism explaining the delivery of pre-event water to storm runoff was proposed by Hewlett and Hibbert (1967) and is called translatory flow or displacement (Pearce et al., 1986). As new inputs of rainfall are added to the soil profile, they displace water that was present as soil moisture. The displacement continues through the hillslope until water exfiltrates at the surface or is displaced into the stream (Hewlett and Hibbert, 1967). As support for the process of translatory flow Hewlett and Hibbert (1967) cite a study done by Horton and Hawkins in 1965 in which the flow of tritium was observed through 4-foot soil columns. In the Horton and Hawkins study, after the soil was drained to field capacity, an inch of tritiated water was added to the surface. Subsequently, an inch of pure water was added each day to the top of the soil column and the discharge was monitored for tritium. Nearly all of the original soil water (87 percent) drained from the soil column before the tritiated water was recovered (Hewlett and Hibbert, 1967).

In a dye-tracer experiment in the Maimai Watershed of New Zealand, Mosley (1979) observed the arrival of dyed water downslope to be so rapid that it could not be accounted for by translatory flow. When the author calculated subsurface flow velocities, they were two orders of magnitude greater than flow through the soil matrix. It was determined that when the flow was through macropores (root channels, animal burrows, etc.) event runoff traveled fast enough to arrive in the stream and contribute to the storm runoff (Mosley, 1979).

In a later study in the same watershed, Pearce et al. (1986) questioned the results of the Mosley (1979) experiment and suggested that translatory flow, and not rapid macropore flow, was the dominant runoff mechanism. Pearce et al. (1986) used oxygen-18 isotopic tracers to determine that most of the water (97 percent) discharged at the bottom of the hillslope during storms was pre-event water. The authors concluded that rapid macropore flow does not explain the stream flow response in the study area because only 3 percent of the storm runoff was new water.

The conflicting results of Pearce et al. (1986) and Mosley (1979) were resolved by a third study in the Maimai Watershed. McDonnell (1990) observed that event water enters vertical cracks in the soil matrix and bypasses to the impermeable horizon, contributing to a buildup of a transitory, perched water table. At the perched water table, the event water mixes with pre-event water that was

stored from previous rainfall events. Associated with the perched water table is an increase in localized pressure potential, which is dissipated through preferential flowpaths located between the mineral soil and the impermeable bedrock. McDonnell's 'cracked pipe' mechanism explains how macropore flow can occur and deliver pre-event water that had been stored in the soil prior to a storm (McDonnell, 1990), and has been observed to occur in other studies (Keppeler and Brown, 1998).

Still other studies have observed that although macropore flow can account for the rapid delivery of pre-event and event water, other processes may be happening at the same time and may also be contributing to the rapid delivery of both pre-event and event water. In a study by Megahan and Clayton (1983), the hydraulic conductivity of the hillslope above a road cut as measured by the tracer velocity was an order of magnitude greater than the hydraulic conductivity of undisturbed soil cores. The increased hydraulic conductivity was attributed to flow through macropores. However, an analysis of the runoff revealed that Darcian, or matrix, flow conditions existed at the time of the tests such that flow was not limited to the macropores (Megahan and Clayton, 1983).

Anderson et al. (1997) used deuterium- and bromide-enriched water to trace the movement of event and pre-event water in the Coast Range of Oregon. The authors reported that the movement of event water through the unsaturated zone was similar to the plug, or translatory flow, hypothesized by Hewlett and Hibbert (1967). In response to the addition of event water, pre-event water flowed through fractures and preferential flowpaths in the bedrock and resurfaced in the colluvium further down the slope. The event and pre-event waters mixed in the colluvium layer, but only 8 percent of the event water was discharged from the hillslope (Anderson et al., 1997).

Torres et al. (1998) explained yet another mechanism in which the rapid delivery of pre-event water is related to changes in pore pressures within the soil column. Torres et al. (1998) demonstrated that the discharge of runoff was related to the pore pressure in the unsaturated portion of the soil column. When pore pressures and discharge from the saturated and unsaturated zones reached steady state conditions, a spike in precipitation created a pressure wave that was rapidly transmitted through the soil. The pressure wave resulted in a slight change in pressure head and large changes in the hydraulic conductivity of the unsaturated zone. Water that had been stored in the

unsaturated zone was rapidly delivered to the saturated zone and discharged from the hillslope at rates greater than matrix flow (Torres et al., 1998).

The results of Anderson et al. (1997) and Torres et al. (1998) coincide with the results of McDonnell (1990) and others who have observed storm runoff to be dominated by a rapid discharge of pre-event water (Sklash and Farvolden, 1979; Abdul and Gillham, 1984; Pearce et al., 1986; Buttle, 1994). Other studies have reported that while pre-event water did not dominate the storm runoff, it was a significant portion (Pinder and Jones, 1969; Brown et al., 1999).

While many of the studies mentioned in this review have focused on explaining the dominant mechanism for the rapid hydrologic response of a watershed, these mechanisms are not likely to be occurring in an exclusive manner. As observed by Megahan and Clayton (1983), macropore flow and matrix flow may occur simultaneously. It is also possible that the pressure wave observed by Torres et al. (1998) and the creation of pressure observed by McDonnell (1990)—both of which result in the release of pre-event water—occur at the same time. Thus, subsurface runoff along a hillslope may be dominated by any one of the mechanisms described, or by a combination of them.

2.3 Forest Roads and Drainage

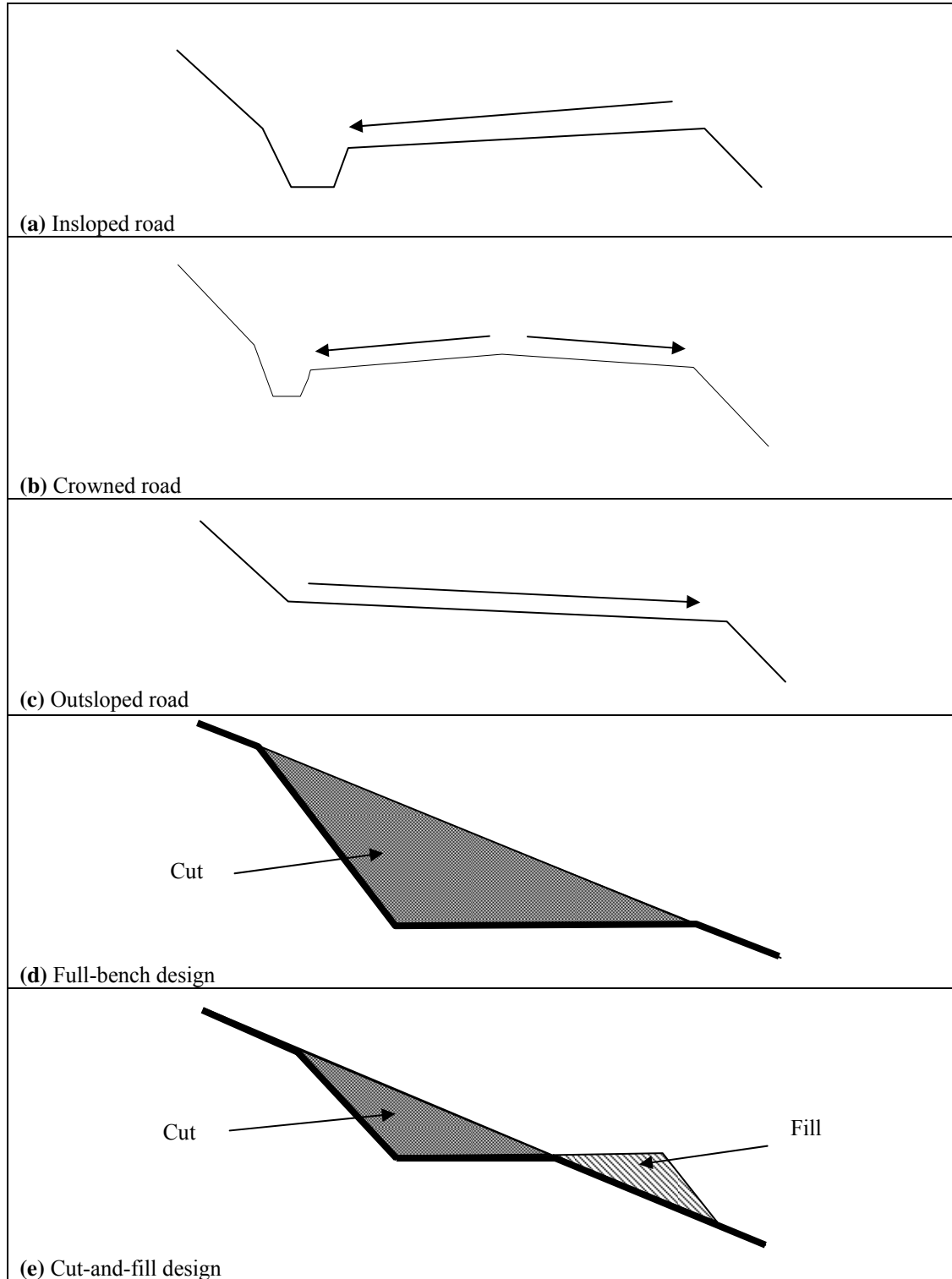
Watershed management includes the construction and maintenance of roads for logging, fire control, timber stand improvement, recreation, and many other purposes. Forest roads have three basic cross-sections or prisms: insloped, crowned, and outsloped (Figure 1). Insloped roads slope towards the hillslope, and runoff from the entire prism is collected in an inboard ditch. Crowned roads differ from insloped roads in that half of the prism slopes away from the hillslope, and only half of the runoff from the road surface enters the inboard ditch. The runoff collected in the inboard ditches of either insloped or crowned road prisms is then delivered to the forest floor at culvert outlets. Outsloped roads slope away from the hillslope, and all the runoff flows to the downhill side of the road. Depending on the topography of the hillslope, all three prism types may have a cut slope on the uphill side of the road. When a crowned or insloped road intercepts a subsurface flow path, the intercepted runoff will be redirected and flow through inboard ditches. When an outsloped road

intercepts a subsurface flow path, the intercepted runoff will flow across the prism and onto the hillslope below the road.

Roads are primarily constructed by excavating the hillslope in two ways: full-bench endhaul and cut-and-fill. Full-bench endhaul design is constructed by excavating the entire road surface into the hill, and transporting the material to a stable disposal area. The material from full-bench roads may also be sidecast onto the hillslope, but the material does not form a part of the road surface. A cut-and-fill section is constructed by removing hillslope material from above the road corridor, and placing it below the road corridor to serve as the road surface (Figure 1).

Cross drain culverts and stream crossing culverts are two types of culverts used in road designs. Cross drain culverts are used to transfer water from the ditch above the road to the hillslope below the road. Stream crossing culverts are used when the road crosses an existing stream channel. The placement of cross drain culverts is important in maintaining road stability and must be done in a way such that adjacent streams are not degraded (Oregon Department of Forestry, 2004). In Oregon, stream crossing culverts are required to be large enough to accommodate runoff from a 50-year storm event (Oregon Department of Forestry, 2004). Culverts, including those designed to accommodate a 50-year storm event may become blocked and have the potential to result in road failures during large storms (Donahue and Howard, 1987). Installing culverts that are sized for less than a 50-year storm event increases the probability of culvert failures because storms with lower return intervals have a higher probability of occurring in any given year. Cross drain culverts can also be used near stream crossing culverts to lessen the length of the road segment that will deliver runoff to the stream (Oregon Department of Forestry, 2004).

Figure 1. Road cross sections (a, b, c) and designs (d, e) after Wemple (1994). The arrows indicate the direction of runoff



2.4 Impact of Forest Roads on Hydrological Processes

Several studies have been conducted to better understand the impact of forest management activities, including forest road construction, on the hydrological processes. Many of the studies have examined the dual impacts of timber harvesting and road construction. Separating the impact of harvesting from road construction is complicated by the short period of time between the end of road construction and the beginning of the harvest.

Forest roads have been shown to affect hydrological processes. Overland flow may occur on the road surface, subsurface flow may be intercepted, and the drainage features associated with the road may be connected to a nearby stream, all of which may result in an alteration of existing flow paths. These impacts have been hypothesized to increase the peakflow magnitude and advance the peakflow timing of the streams in a roaded watershed.

2.4.1 Impact of Forest Roads on Surface Runoff

During road construction and subsequent timber harvest activities forest roads become compacted with the passage of heavy equipment. As a result, forest roads have a reduced infiltration capacity when compared to the surrounding forest soil (Rothacher, 1965) and may generate more surface runoff (Ziegler and Giambelluca, 1997). When the rainfall intensity of a storm exceeds the infiltration capacity of a road segment, Hortonian overland flow will be generated from the road. In the PNW, surface runoff on graveled roads has been observed when short periods of high-intensity rainfall occur during a storm, or during storms with large return intervals (Reid and Dunne, 1984; Luce and Cundy 1994). However, Marbet (2003) reported that rainfall intensity is less than the infiltration capacity of forest roads for an average of 80 percent of the storm duration. This means that high-intensity short-duration bursts represent an average of 20 percent of the storms.

The amount of rainfall that becomes road surface runoff and enters a stream has been found to vary. Studies conducted in the PNW have reported that surface runoff from roads is a minor component of the storm runoff (Wemple, 1998; Marbet, 2003). Wemple (1998) modeled surface runoff from road segments in Watershed 3 of the H.J. Andrews Experimental Forest and reported that with the exception of small storms, surface runoff was estimated to account for no more than 10

percent of the storm runoff. Marbet (2003) found that surface runoff from road segments accounted for approximately 5 percent of the rainfall recorded during storms. Although the rainfall intensities were greater than the infiltration capacity of the road for an average of 20 percent of the storm duration, Marbet (2003) hypothesized that some of the surface runoff had infiltrated into the ditch. Thus, forest roads in the PNW may generate surface runoff when the infiltration capacity of the road is less than the rainfall intensity, and it is possible that only a portion of the surface runoff will become storm runoff.

2.4.2 Impact of Forest Roads on Subsurface Flow Paths

In a watershed the rate of subsurface flow is a function of the hydraulic conductivity of the medium through which it is flowing. Typically, the flow velocities of runoff in the medium may be anywhere from two to four orders of magnitude less than surface water velocities in streams and ditches (Hillel, 1998). When subsurface flow is intercepted by a road cut, and is then redirected to the stream via inboard ditches and culverts as surface flow, the rate of delivery has been hypothesized to increase (Wemple et al., 1996; Wemple and Jones, 2003). However, Mosely (1979) observed subsurface travel velocities of runoff that was 3 orders of magnitude faster than the velocity of flow in the subsurface matrix of the mineral soil being studied, and were only one order of magnitude slower than the surface velocity of mountain streams observed by Marcus et al., (1992). Thus it appears that the increased rate of delivery of intercepted subsurface flow does exist, but may not be as large as hypothesized by Wemple et al. (1996) and Wemple and Jones (2003).

The location of a forest road may determine the extent of the impact on subsurface flow paths. Roads constructed near the ridge of a hillslope intercept short flow paths and are thus expected to deliver a small amount of water into the stream. Jones (2000) found that the density of mid-slope roads is related to an increase in peakflow magnitude at the mouth of the watershed, an indication of a change in the hydrologic behavior of the hillslope. Roads constructed at the bottom of a slope intercept the longest flow paths. However, they are expected to have less of an impact on the hillslope processes and storm runoff because the majority of the flow path is left unchanged (Wright et al., 1990).

The amount of subsurface flow that is intercepted by a road cut is difficult to predict. Several studies have examined the amount of subsurface flow intercepted by road segments and have reported that the amount varies temporally and spatially (Bowling and Lettenmeier 1997; Gilbert 2002; Marbet, 2003; Toman, 2004). In studies of the variability of subsurface flow interception along mid-slope road segments in the Oregon Coast Range, Gilbert (2002), Marbet (2003), and Toman (2004) selected road segments that had hillslope characteristics that were believed to have a high potential to intercept subsurface flow. These studies reported that the amount of intercepted subsurface flow intercepted by the road was correlated to rainfall intensities and amounts and the presence of existing subsurface flow paths, but not the road and hillslope characteristics (Gilbert 2002; Marbet, 2003; Toman, 2004). The correlation was made by assuming that all road cuts with consistent, seasonal runoff production were intercepting subsurface flow. These results suggest that identifying road segments that will intercept subsurface flow may not be done from the hillslope characteristics alone.

The impact of forest roads on subsurface flow extends beyond the impact of redirecting runoff to roadside ditches and stream channels. Several studies have investigated the change in soil moisture on the downslope side of forest roads that result from the interception of subsurface runoff above the road (Megahan, 1972; McGee, 2000; Tague and Band, 2001). The magnitude of change in soil moisture is thought to correspond with the proportion of subsurface flow intercepted by the road. Megahan (1972) estimated that approximately 35 percent of the subsurface flow was intercepted by a forest road in the Idaho Batholith, and the remainder passed beneath the road prism. Tague and Band, (2001) used a conceptual model to simulate the change in the soil wetness index below a road and found that the model simulated a potential decrease in summer soil moisture in localized areas below the road. Tague and Band (2001) also inferred that intercepted subsurface runoff could be redirected by a cross drain culvert onto an area of the hillslope that had lower soil wetness indices before the road was constructed.

McGee (2000) used wells to monitor soil moisture above and below forest roads in Southeast Alaska and reported that the peak water levels decreased slightly below the road and that low water

levels were not consistently affected. Both the peak water levels and the low water levels were most affected immediately above and below the road (McGee, 2000). These studies demonstrate that forest roads may not intercept all of the subsurface runoff, and that the effect of the road on soil moisture downslope of the road is largest within a narrow corridor adjacent to the road. Furthermore, Parizek (1971) speculated that if intercepted subsurface runoff is transferred out of the watershed, the forest road may decrease the soil moisture below the road in one watershed and increase the soil moisture below the road in an adjacent watershed.

2.4.3 Road and Stream Connectivity

Forest roads have the potential to increase the drainage density of a watershed when the drainage features of the road are connected to the stream system (Wemple et al., 1996). The degree of connectivity is frequently expressed as the percent of the total road length that is connected to the stream channel network. It is correlated to the size of the storm and the antecedent soil conditions (Wemple and Jones, 2003). Other factors that influence the connectivity include hillslope position, road design and contributing length, geology, topography, and soil properties (Wemple et al., 1996; Veldhuisen and Russell, 1999; Croke and Mockler, 2001). Two processes have been observed that increase connectivity: the direct transport of inboard ditch flow to the stream channel, and the transport of ditch relief culvert water to the stream via a channel or gully at the outlet of a relief culverts (Wemple, 1994; Croke and Mockler, 2001).

Inventories have been conducted throughout western Oregon and Washington to determine the degree of existing connectivity, and have reported a range of percentages (Reid and Dunne, 1984; Bilby et al., 1989; Wemple et al., 1996; and Skaugset and Allen, 1998). Reid and Dunne (1984) report that of the insloped and crowned roads sampled in the Clearwater Basin of Washington, 75 percent are connected directly to the stream. Wemple et al. (1996) conducted a summer inventory of connectivity, and later a winter inventory of a subset of the road segments, and reported that 57 percent of the road drainage was connected to the streams in the western Cascades, Oregon. Skaugset and Allen (1998) conducted an inventory of connectivity in Western Oregon during the summer of 1995 and classified road segments as either connected, potentially connected, and not connected. The

connected and potentially connected road segments accounted for 31 percent of the sampled road segments (Skaugset and Allen, 1998). Remaining studies have reported 34 percent connectivity (Bilby et al., 1989), and 39 percent connectivity (Oregon Department of Forestry, 1996).

The dissimilarities reported in these studies may be attributed to the time of year that the inventories were conducted and to the age of the road. An inventory conducted during the dry summer months may report lower percent connectivity than an inventory conducted in the wet winter months. Likewise, roads that were constructed earlier would be expected to have a higher percent connectivity because of the different road design practices that existed. For example, the inventory conducted by Reid and Dunne (1984) was on road segments that were constructed before 1968, and the road segments inventoried by Skaugset and Allen (1998) were constructed during the 1980s.

2.4.4 Altered Peakflows

Forest roads that generate surface runoff and/or intercept subsurface runoff and redirect it into streams have been hypothesized to influence the arrival of the peakflow and increase the peakflow magnitude (Harr et al., 1975; Jones, 2000; Wemple and Jones, 2003; Toman, 2004). As mentioned in section 2.4, isolating the hydrologic impact of forest roads from timber harvesting is complicated. Often there is only a short amount of time between the time when roads were constructed and the harvest. Even in studies that have been specifically designed to investigate the road impact, the time between road construction and harvesting has been one (Harr et al., 1975) to four years (Ziemer, 1981; Wright et al., 1990). Thus it is difficult to measure the road effect at a given location while incorporating the climatic variations that could occur over a long period of time.

Changes in either the peakflow timing or magnitude may negate management activities aimed at protecting the road infrastructure and the forest resources. As previously mentioned, the Oregon Department of Forestry requires that culverts be sized to accommodate the discharge associated with a 50-year storm event. If the construction of forest roads does increase the magnitude of the peakflows, then the capacity of a downstream culvert may be exceeded by the runoff generated during a storm with less than a 50-year return interval. However, if an increase in peakflow magnitude does occur following road construction, it is reasonable to expect a decrease to occur

elsewhere as inferred by Parizek (1971) and Tague and Band (2001). Thus the change imposed on peakflows by forest roads may be an issue of scale.

Studies have shown that the magnitude and timing of the peakflow might be affected at the road segment scale. Toman (2004) measured the runoff in streams above road segments and quantified the addition of ditch runoff into the stream at stream crossing culverts. Toman (2004) reported that the peakflow timing of streams just below road segments was advanced so long as the road segment intercepted subsurface groundwater. Peakflow magnitude was also greater at streams that received intercepted groundwater from an adjacent ditch (Toman, 2004). The peakflow magnitude and timing were less changed in streams that were connected to road segments that did not intercept subsurface flow (Toman, 2004). The study design employed by Toman (2004) did not allow for the measurement of runoff at the mouth of watersheds below the road segments and was thus unable to correlate the change in peakflows at the road scale to changes at the watershed scale.

Wemple and Jones (2003) measured runoff at the outlet of ditch relief culverts found that during large precipitation events, intercepted subsurface flow measured at individual road segments was synchronized with and exceeded the unit-area runoff of the entire watershed. The authors interpreted the results to indicate that the road segments were advancing peakflow timing and increasing peakflow magnitude at the road segment scale (Wemple and Jones, 2003). The study design employed by Wemple and Jones (2003) did not include runoff measurements in existing streams, or the amount of runoff exiting the culvert outlet that was delivered to existing streams, and was thus unable to establish a causal relationship between the runoff intercepted at the road segment and peakflows at the mouth of the watershed.

Other studies have investigated the effect of forest roads on the peakflow magnitude and or timing at the watershed scale. This is typically done by comparing the runoff at the mouth of a watershed (rather than from road segments and streams within the watershed) before and after road construction and then analyzing the runoff data for a correlation to the construction of the road. To examine the impact of roads on the peakflows at the watershed scale one approach has been to investigate if there is a threshold response to the amount of the watershed area that is converted to

roads, skid trails, and landings. Ziemer (1981) and Wright et al. (1990) conducted separate analysis of data from Caspar Creek and reported that road construction had no effect on any storm flow parameter when roads and landings occupied 15 percent of the watershed area, and roads alone occupied 5 percent of the watershed area. A road effect may have been detectable if a larger percentage of the watershed had been converted to road surface (Ziemer, 1981), or if the roads were located away from the valley bottoms (Wright et al., 1990). Wright et al. (1990) suggested that peakflows were unchanged because the flow paths were only changed for the short distance below the road, but remained unchanged for the area above the road. A different study found that when roads occupied 12 percent or more of the watershed area, peak discharges increased (Harr et al., 1975). King and Tennyson (1984) reported no consistent pattern of change to peakflows resulting from road construction when roads occupied five percent of the watershed area.

Three groups of researches have investigated the impact of road construction and timber harvesting on both small and large watersheds in the Cascade Range of Oregon. Although all three groups have begun the analysis with the same historical runoff data, the researches have reached different conclusions. The first study was conducted by Jones and Grant (1996), and they concluded that increases in peakflows were not statistically significant following road construction and harvesting in small watersheds. The authors interpreted the results of their analysis in large watersheds to suggest that the combination of road construction and harvesting activities could increase peakflows by up to 100 percent (Jones and Grant, 1996). In the second analysis Thomas and Megahan (1998) concluded that the forest roads did not alter the peakflows in the small basins, and that the data from the large basins provided inconclusive results. Furthermore, Thomas and Megahan (1998) concluded that the increase in peakflows was greatest for small storms, and that the increase decreased for large events. In the third analysis Beschta et al. (2000) also concluded that in the small basins, the amount of increase in peakflows following road construction and timber harvesting depended on the return interval for the peakflow magnitude. Small storms yielded a greater increase in peakflow than large storms (Beschta et al., 2000). The different conclusions reached in these three analyses of the same data can be attributed in part to the type of statistical analysis used and the

designation of large storm events. For example, Jones and Grant (1996) designate storms with return intervals ranging from 0.4 to 100 years as large storm events, whereas Thomas and Megahan (1998) designate large storms as those having return intervals of at least 2 years. Also, Jones and Grant (1996) used analysis of variance in order to detect a treatment effect, whereas Thomas and Megahan (1998) used analysis of co-variance, and Beschta et al. (2000) used regression analysis.

As mentioned, studies have examined the hydrologic impact of forest roads at the at the road segment scale, and have not been able to establish a causal relationship to changes in peakflows at the mouth of the watershed. Others have analyzed the runoff at the mouth of a watershed before and after roads are constructed and have studied the correlation between the road construction and changes in peakflows at the watershed outlet. However, no study has measured runoff from the streams and runoff contributed from road segments and correlated them to changes in peakflows at the mouth of the watershed.

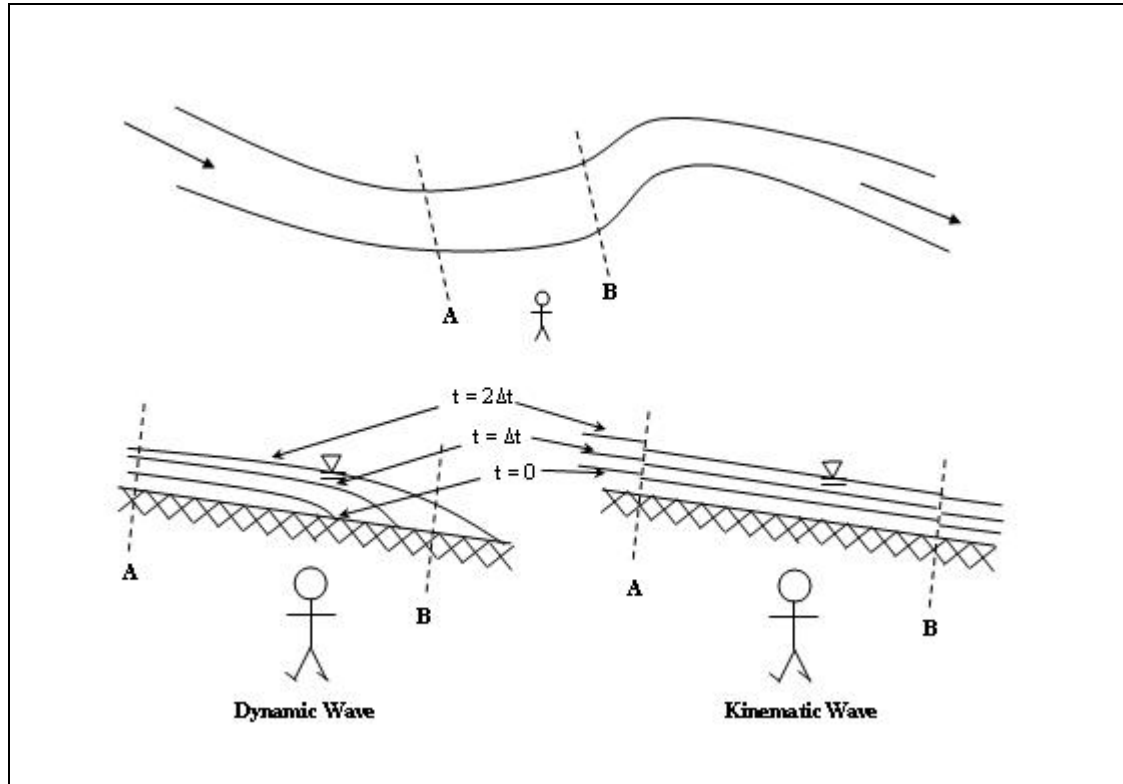
2.5 Flow Routing with Kinematic waves

Kinematic wave models are used to route water, generate downstream hydrographs, and to model the time of travel of the peakflow (Lighthill and Whitham, 1955; MacArthur and DeVries, 1993; Singh 1996; Wong 2001). Kinematic waves dominate the flow characteristics in small watersheds with channel slopes greater than 0.2 percent (ASCE, 1996). Kinematic waves have been observed for flows with Froude numbers less than two (Lighthill and Whitham, 1955) and for flows with Froude numbers less than one (Gburek and Overton, 1973). Thus, kinematic waves can occur when flows are both subcritical and supercritical. Supercritical flows exist when the water molecules travel faster than the speed of the energy wave, and subcritical flows occur when the speed of the energy wave travels faster than the water molecules. The rate at which the water molecules move is the flow velocity and the rate at which the energy wave moves is the wave celerity.

To an observer on the stream bank, the kinematic wave would appear as a uniform rise and fall in the water height over a long period of time (Figure 2). The observer would not see an advancing surface wave, as would be the case with a dynamic wave. Kinematic waves do attenuate as they move down the stream, though the attenuation is less than occurs with a dynamic wave

(MacArthur and DeVries, 1993). The weight component of the flow within a kinematic wave cancels the resistive forces from the channel bed so that inertia does not influence the wave. As a result, flows do not accelerate significantly and remain uniform across the channel. Flows in kinematic waves are then classified as uniform, unsteady flows.

Figure 2. Visualization of dynamic and kinematic waves (after MacArthur and DeVries, 1993).



Uniform, unsteady flow equations assume that depth of flow and velocity does not vary along the length of the channel, but may change with respect to time. Other assumptions include:

- No superpositioning of flow at any cross section;
- Flows vary gradually with hydrostatic pressure dominating at all points within the flow such that changes in velocity within the water column are neglected;
- The longitudinal flow axis can be approximated by a straight line;
- The stream banks are noneroding and the bed is nonaggrading;
- Flow resistance may be described empirically through the Manning or Chezy equations;
- The flow has constant density and is incompressible;
- Channel slopes do not exceed 10 percent (MacArthur and DeVries, 1993).

When channel slopes do exceed 10 percent, the kinematic wave equations can be corrected by adjusting the roughness coefficient (Jarrett, 1984).

The general kinematic wave equations for streamflow routing incorporate the continuity equation for unsteady flow (Equation 1) and momentum (Equation 2) equations:

$$\frac{\partial A_c}{\partial t} + \frac{\partial Q}{\partial x} = q \quad (1)$$

$$Q = \alpha * A_c^m \quad (2)$$

where A_c is the cross-sectional area of flow (m^2); t is time (seconds); Q is discharge (m^3/s); x is distance along the channel (m); q is the lateral inflow (m^3/s); and α and m are kinematic wave parameters for a given cross sectional shape, slope, and roughness (MacArthur and DeVries, 1993).

The Manning equation (Equation 3) is used to determine the values of α and m as follows:

$$Q = \frac{S^{1/2} * R^{2/3} * A_c}{n} \quad (3)$$

where Q is discharge (m^3/s); S is the slope of the energy line and is approximated by the channel slope (m/m); R is the hydraulic radius and is equal to the cross-sectional area of the flow, A_c (m^2), divided by the wetted perimeter, WP (m); and n is the roughness coefficient (dimensionless). Substituting A/WP for R yields:

$$Q = \frac{S^{1/2}}{n * WP^{2/3}} * A_c^{5/3} \quad (4)$$

such that $\alpha = [S^{1/2} / (n * (WP^{2/3}))]$ and $m = 5/3$ in Equation 2.

As mentioned previously, kinematic wave equations have been used to construct downstream hydrographs from known hillslope and rainfall characteristics (Chow, 1988; MacArthur and DeVries, 1993), and are appropriate for calculating wave celerities in small watersheds (Woolhiser and Liggett, 1967; Loukas and Dalezios, 2000). However, when both the upstream and downstream hydrographs are known, kinematic equations may also be used to model the travel time of a flood wave or peakflow (Wong, 2001). The advantage of modeling travel times for peakflows using both the upstream and downstream discharge is that the discharge values function as boundary conditions and

yield more representative travel times when compared to travel times modeled using only the upstream discharge.

The complexity of the kinematic wave theory may act as a deterrent to land managers and others who consider using the theory to model travel times in open channels. Wong (2001) recognized that a simplified application was needed and developed a form of the kinematic wave equation that could be readily applied by land managers. Formulas for seven different cross sections were calculated and verified against rainfall and runoff data of a section of freeway in the United Kingdom. The modeled travel times were within 5 percent of the travel times as indicated by the runoff data (Wong, 2001).

2.6 Conclusions

The following conclusions may be drawn from the reviewed studies and have application to this study:

- Although dominant hydrologic pathways that deliver runoff to streams have been observed, the pathways are complex and non-exclusive.
- Forest roads in the Pacific Northwest generate little surface runoff because the infiltration capacities of the roads are greater than the rainfall intensity of most winter storms.
- The percentage of road drainage features that are connected to stream systems may vary spatially and temporally.
- Forest roads may alter runoff pathways by intercepting subsurface flow and redirecting it to inboard ditches and stream channels or the forest floor.
- The impact of forest roads on soil moisture appears to be most concentrated in a narrow corridor adjacent to the road and may be related to the percentage of the watershed converted to roads.
- Roads that are connected to streams have been hypothesized to advance the arrival of the stream peakflow by increasing the velocity of groundwater and to increase the maximum instantaneous peakflow volume.
- Hillslope characteristics alone may not be sufficient to predict which road segments intercept subsurface flow.
- No study has measured runoff from the streams and runoff contributed from road segments and correlated them to changes in peakflows at the mouth of the watershed.
- Kinematic waves have been used to model a travel time of peakflows from one point in a watershed to another.

3. METHODS

3.1 Study Area

This study took place in the Oak Creek Watershed of the McDonald-Dunn Research Forest. The McDonald-Dunn Research Forest is the school forest for the College of Forestry at Oregon State University and is located approximately 10 miles northwest of Corvallis, Oregon. The Oak Creek Watershed has an area of 824 hectares and the topography is dominated by short, highly dissected slopes with gradients between 20 and 60 percent. Elevation ranges from 140 to 655 meters.

The Oak Creek watershed is underlain by the Siletz Volcanics, which is a basalt formation. Overlaying the Siletz Volcanics are the Jory, Price, Ritner, Witzel, Dixonville, and Philomath soil series. The river bottoms are recent alluvium and form the basis for McAlpin, Abiqua and Waldo soil series. These soil series range in texture from coarse-grained mineral soils to fine, highly organic soils, and silty clay loams are the most common soil texture. Bulk densities range from 1.10 – 1.30 g/cm³, and porosities are low. The average soil depth throughout the watershed is 125 centimeters (NRCS, 2005).

The climate for the Oak Creek watershed is a Pacific Maritime climate with cool, wet winters, and warm, dry summers. Mean annual precipitation is 1400 mm, which occurs as low intensity/long duration, frontal storms from October to April. Precipitation occasionally occurs as snow at higher elevations in the Oak Creek watershed, although the snow pack seldom exists for more than a few days. Mean maximum temperature is 15°C and mean minimum temperature is 4°C (NRCS, 2005)

Vegetation in the Oak Creek watershed was historically an oak-savannah ecotype maintained by periodic burning by the aboriginal population (Longwood, 1940). Stand composition changed with the cessation of burning and it is now dominated by Douglas-fir (*Pseudotsuga menziesii*), with minor stand components of bigleaf maple (*Acer macrophyllum*) red alder (*Alnus rubra*) and Oregon white oak (*Quercus garryana*). The road system in the Oak Creek Watershed was constructed in the 1950's and 1960's with contemporary methods and it currently supports primarily light recreational traffic including pedestrians, cyclists, and horse-back riders. The roads have a crowned cross-section with a

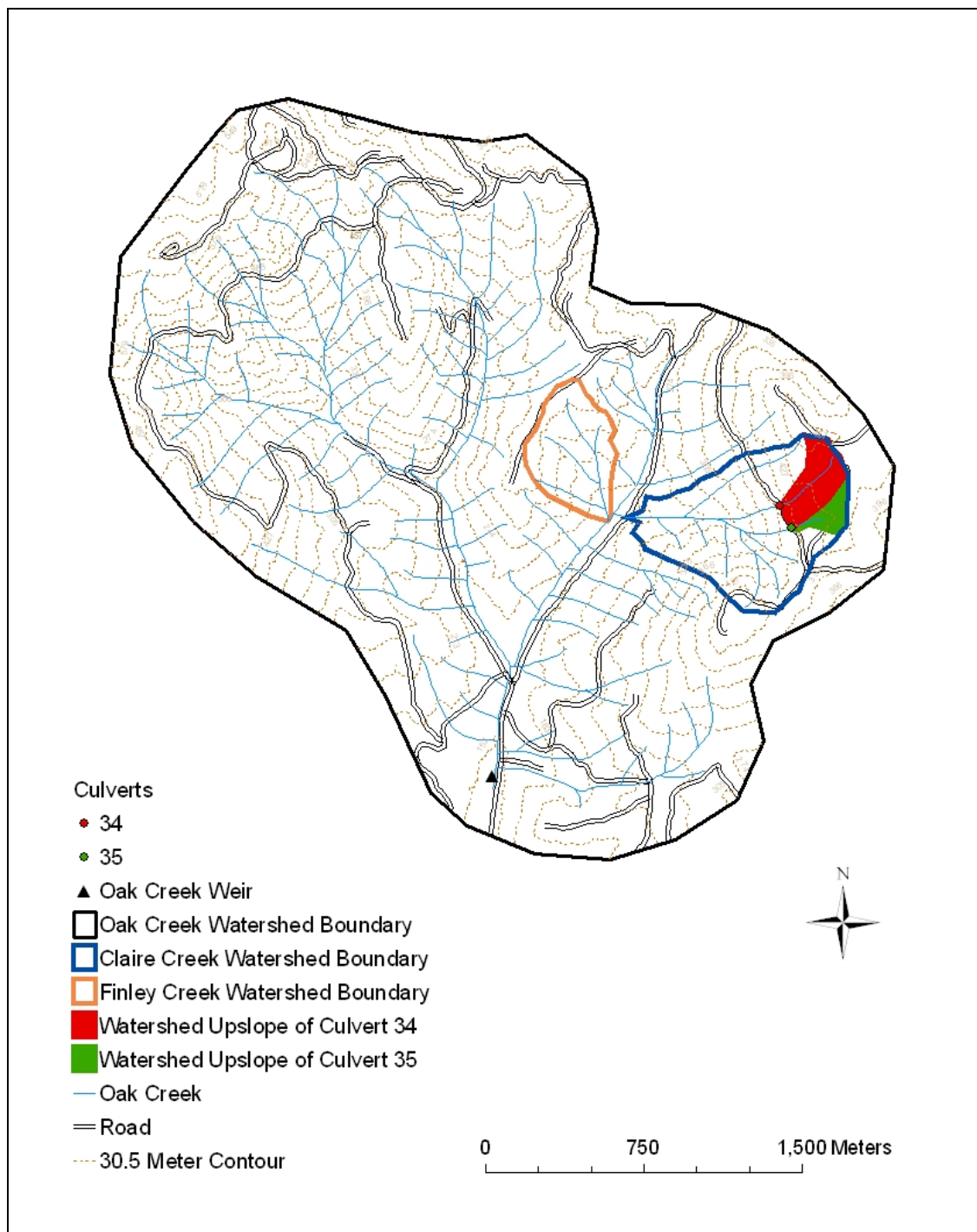
mean width of 5 meters. Average road segment gradient ranges from 1 – 13% (Amann, 2004). The forest canopy is nearly closed over most portions of the road throughout the study area. Though the forest is actively harvested, the road segments in this study were not used as haul roads during the study period.

3.2 Site Description

This study was conducted in two adjacent watersheds within the Oak Creek watershed; Claire Creek and Finley Creek. The Finley Creek Watershed is a roadless watershed with an area of 19.6 ha (Figure 3). Elevation ranges from 330 m to 200 m and the aspect is to the east.

The elevation of Claire Creek ranges from 455 to 205 meters, and the watershed aspect is to the west. The area of the Claire Creek watershed is 51.5 hectares. A road (HR#600) crosses the Claire Creek watershed about 2/3 of the way up the hillslope, and has a surface area of 0.5 hectares (Figure 3). Approximately one percent of the Claire Creek Watershed area is occupied by the road.

Figure 3. Map of the Oak Creek Watershed.



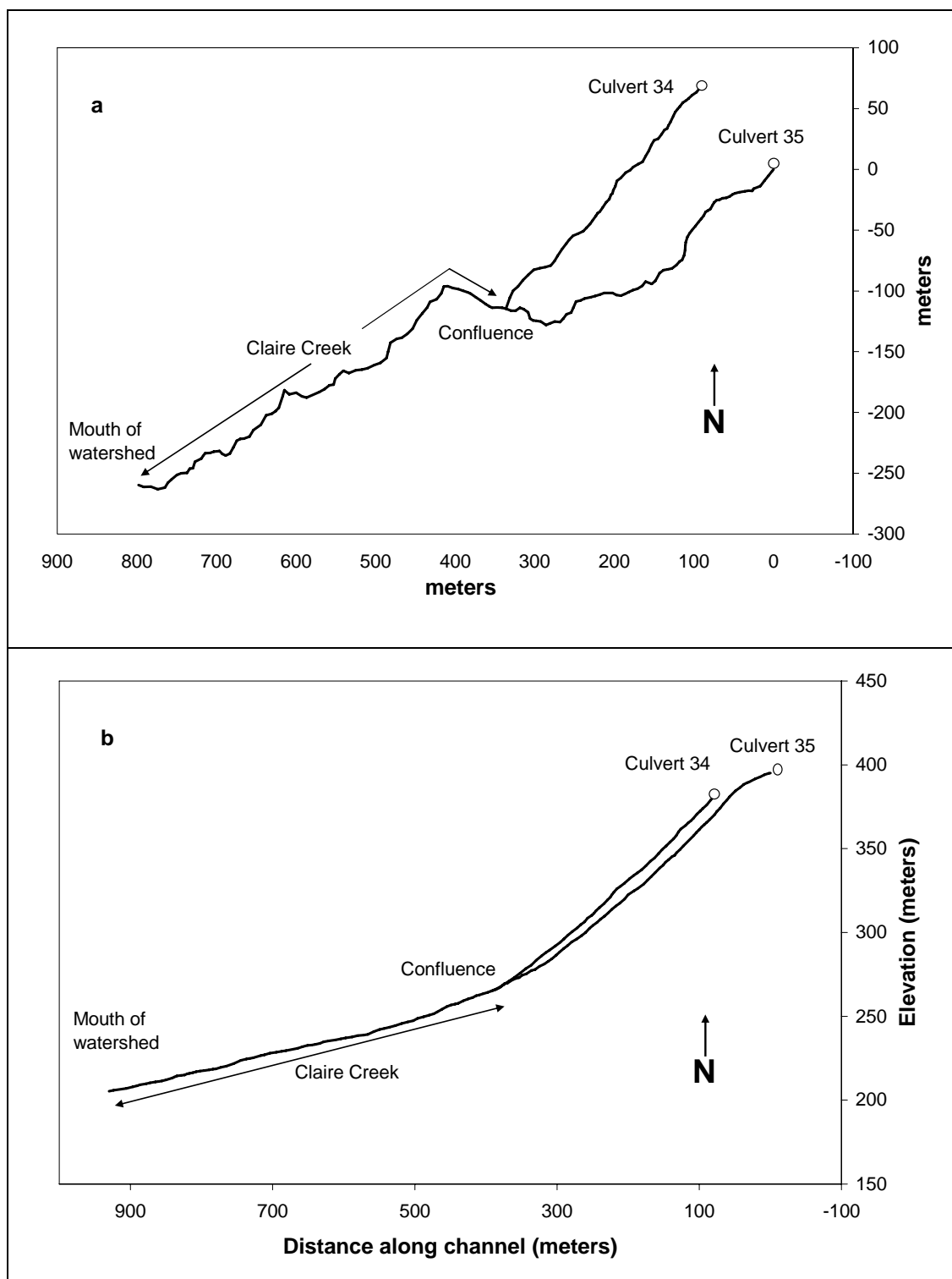
Two segments of the #600 road were studied during this project; segments 34, and 35. These segments cross stream channels and are associated with ditch flow that enters the streams at stream crossing culverts. Discharge in the stream crossing culverts at road segments 34 (culvert 34) and 35 (culvert 35) is composed of stream and ditch flow. The streams that flow through culverts 34 and 35 come together further down the slope (Figure 4a). The stream channel characteristics below culverts 34 and 35, and below the confluence of the two (Claire Creek) is presented in Table 1.

The stream that passes through culvert 34 is a first order stream. The distance from the outlet of culvert 34 to the confluence with the stream that passes through culvert 35 is 317 m (Figure 4b). The gradient of this section of the stream averages 37 percent and ranges from 18 to 72 percent. The active channel width of this section of the stream averages 1.4 m and ranges from 0.4 to 3.3 m. The bed of the stream is cobble sized with little gravel or fines and has an estimated D_{84} of 110 mm, meaning that 84 percent of the stream bed particles have a diameter of 110 mm or smaller (Wolman, 1954).

The stream that passes through culvert 35 is also a first order stream. The distance from the outlet of culvert 35 to the confluence with the stream that passes through culvert 34 is 393 m. The gradient for this section of the stream averages 34 percent and ranges from 6 to 57 percent. The width of this segment of the stream averages 0.9 m and ranges from 0.35 to 3.0 m. The bed of the channel is also cobble sized with little or no gravel or fines and has an estimated D_{84} of 72 mm.

The stream below culvert 34 is shorter, steeper, wider, and the bed has a larger average particle size than the stream below culvert 35 (Figure 4b). The riparian areas of both streams are dominated by brush that includes, vine maple (*Acer cincinatum*), poison oak (*Rhus diversiloba*), and common snowberry (*Symphoricarpos albus*). Both streams have woody debris in the channel.

Figure 4. Maps of stream channels below culverts 34 and 35, and Claire Creek below the confluence in a) plan view, and b) longitudinal profile.



The channel length of Claire Creek (below the confluence) is 538 m, the gradient averages 11 percent, and ranges from 4 to 24 percent. The width of the channel averages 1.8 m and ranges from 0.4 to 3.6 m. In Claire Creek, bedrock makes up an increasing and distinct portion of the stream bed. Approximately 20 percent of the stream length is bedrock, and the remainder is cobble-sized material with little gravel or fines and it has an estimated D_{84} of 155 mm. The stream channel has a trapezoidal shape at low flows and at high flows the shape of the channel can be approximated as a wide, shallow rectangle. The stream channel is incised and the depth of incision ranges up to 1.6 m.

Table 1. Stream characteristics within Claire Creek of the Oak Creek Watershed.

Stream channel	Channel length (m)	Average channel gradient (%)	D_{84} particle projection (mm)	Average channel width (m)
Stream below culvert 34	317	37.2	110	1.4
Stream below culvert 35	393	33.6	72	0.9
Claire Creek	538	11.3	155	1.8

In addition to stream characteristics, the site characteristics at each stream crossing culvert were also obtained by Toman (2004) using GIS. Culvert 34 is at an elevation of 383 m and has a topographically-based upslope contributing area of 5.0 hectares with an average hillslope gradient of 13 percent (Table 2). The road and associated ditch that drains to culvert 34 are both 122 meters long and have a gradient of 10 percent. Culvert 35 is at an elevation of 395 meters and has a topographically-based upslope contributing area of 3.0 hectares with an average hillslope gradient of 12 percent. The road and the associated ditch that drains to culvert 35 are both 86 meters long and have a gradient of 4 percent. Measured from a road crossing near the confluence with Oak Creek, Claire Creek has an upslope contributing area of 51.5 hectares, an average hillslope gradient of 45 percent, and the outlet of the Claire Creek watershed is at an elevation of 204 m.

Table 2. Site characteristics of monitoring locations in the Oak Creek Watershed (Toman, 2004)

Site	Upslope Contributing Area (ha)	Elevation (m)	Associated Road and Ditch Length (m)	Average Hillslope Gradient (%)
Culvert 34	5.0	383	122	13
Culvert 35	3.0	395	86	12
Claire Creek	51.5	204	NA	45
Finley Creek	19.6	200	0	30
Oak Creek Weir	824	147	NA	22

3.3 Precipitation

Rainfall was measured using an eight-inch diameter tipping-bucket rain gauge (NovaLynx Corporation, Grass Valley, CA). The rain gauge was equipped with an electronic data logger that affixed date and time stamps to rain events in .254 mm increments (Onset Computer Corporation, Pocasset, MA). The gauge was located near the centroid of the Oak Creek Watershed, near the top of the Finley Creek Watershed at an elevation of 325 meters.

Precipitation data were analyzed for maximum 1-hour intensities, maximum 15-minute intensities, total precipitation and storm duration using a Microsoft Excel © macro written by Richard Keim. For this study, storms were defined as beginning with the precipitation that preceded the rise of the discharge hydrographs and were considered to be over when a period greater than 12 hours occurred without measurable precipitation. Probability of occurrence for each storm was estimated by comparing the maximum 1-hour storm intensity to the 1-hour storm intensities observed by Toman (2004) and to a frequency analysis conducted on a 117-year precipitation record from the Oregon Climate Service at Corvallis, Oregon (HYSLOP). The HYSLOP station is located at an agricultural experiment station in the Willamette Valley approximately 9 kilometers to the east of the Oak Creek Watershed.

3.4 Discharge Measurements

Discharge was measured at the inlet of culverts 34 and 35 and in the road ditches that drained into culverts 34 and 35. Using these measurements it was possible to calculate the discharge in the streams above culverts 34 and 35 above the influence of the road. In this manner the parameters of interest are the discharge in the streams not influenced by the road or the discharge ‘above the culverts’ and the discharge in the culvert that is influenced by the road or the discharge ‘below the roads’. The discharge below the culverts is composed of the streamflow above the culverts plus the contribution from the associated road ditch.

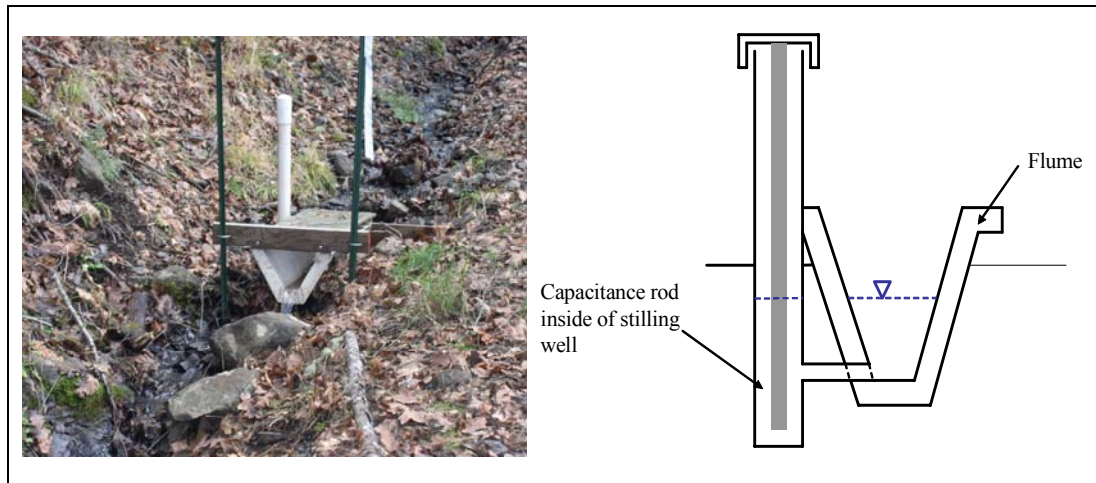
Discharge was measured in the road ditches that drain to culverts 34 and 35 using flumes as described by Toman (2004). The flumes are fiberglass, 60° V-notch trapezoidal flumes (Tracom Incorporated, Alpharetta, GA). The flumes were installed in the ditches of road segments 34, and 35 above the confluence of the ditch and the stream flow (Figure 5). Water height in each flume was measured by capacitance rods (TruTrack Ltd., New Zealand) in an attached stilling well. Water height was verified and noted whenever data from the capacitance rods were downloaded. The sampling interval for the capacitance rod was 10 minutes.

Discharge for the flumes was calculated using the equation:

$$Q = 1.55H^{2.58} \quad (5)$$

where H is water height in the flume (m) measured by the capacitance rod and Q is discharge (m^3/s) (Robinson and Chamberlain 1960). The rating curve for the flumes was provided by the manufacturer (Tracom Incorporated, Alpharetta, GA).

Figure 5. Photograph of the flume installation in the road ditch at culvert 34 with a diagram of the flume and capacitance rod.



Discharge was measured at the inlet of the stream crossing culverts labeled culverts 34 and 35. The flow at these culverts is composed of the flow in the stream above the road and the flow in the road ditch that drains at the culvert.

Water height or stage was measured at the inlet of culverts 34 and 35 with 2.5 psig pressure transducers (Druck Incorporated, New Fairfield, CT). The pressure transducers were secured to a concave polyvinyl chloride (PVC) rod and placed inside a second PVC casing. Slits were cut in the PVC casing to allow water to move easily into and out of the casing. The casing was countersunk into the stream channel so that the water height measured by the pressure transducer was always greater than the actual water height in the channel (Figure 6). The depth of the offset was measured and recorded so that water height values could be corrected during analysis. The pressure transducer assembly was fastened to a steel fence post at the culvert inlet. Water height at each culvert location was measured every week on fixed staff plates (Figure 6) to detect sensor drift in the pressure transducers. When a pressure transducer was in error, the data were corrected using the observations from the staff plate and applied as linear drift since the last staff plate reading. The pressure transducers at the inlet of the culverts had a sampling interval of ten minutes. The layout of the flume in the road ditch and the pressure transducers at the culvert inlet are shown in Figure 7.

Discharge at the culvert inlets of culverts 34 and 35 was calculated using the Henderson (1966) equation. Toman (2004) showed that the Henderson (1966) equation was the most appropriate model and works quite well to convert water height to discharge at the inlet of 18 and 24 inch culverts. The Henderson (1966) equation is:

$$Q = 0.432\sqrt{g}H^{1.9}D^{0.6} \quad (6)$$

where H is the height of the water above the invert of the culvert (m) measured by the pressure transducer, D is the diameter of the culvert (m), g is the acceleration of gravity (m/s^2), and Q is culvert discharge (m^3/s). The discharge in the streams above the culverts was calculated as the difference in the discharge at the culvert inlet and the discharge in the ditch:

$$Q_{\text{AboveRoad}} = Q_{\text{Culvert}} - Q_{\text{Ditch}} \quad (7)$$

Discharge below the road is simply the discharge calculated at the culvert inlet.

Figure 6. Photograph and diagram of pressure transducer installation at the stream crossing culvert above road segment 35.

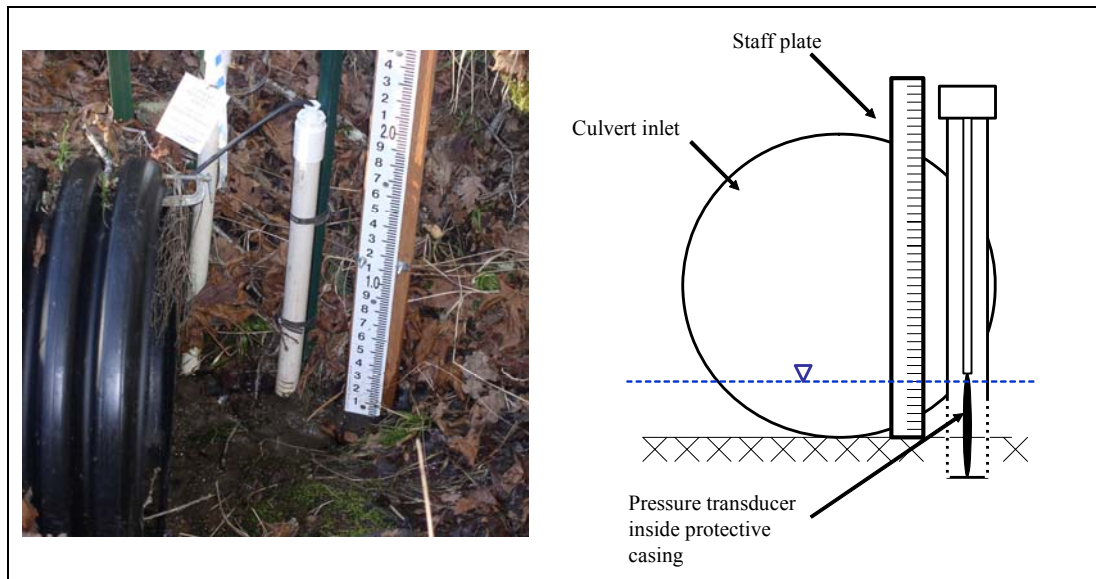
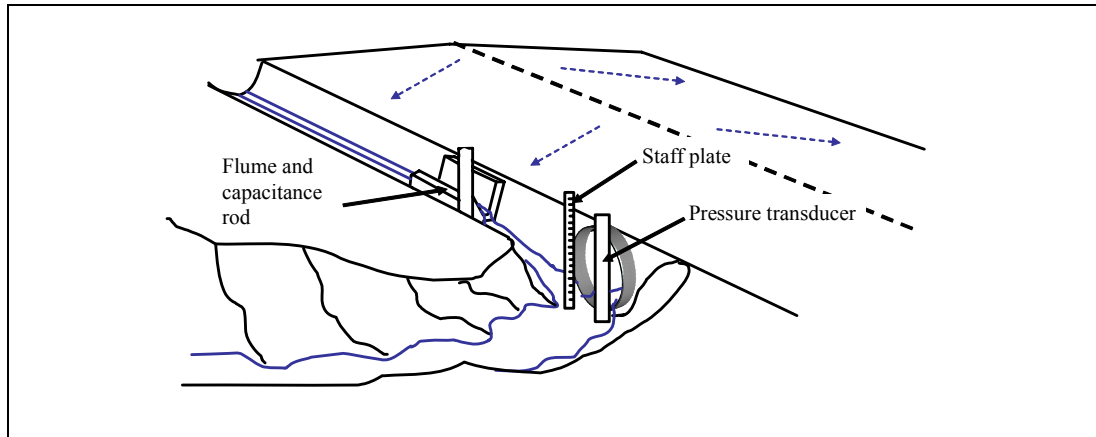


Figure 7. Diagram of site layout above a road segment.



Discharge was also measured at the mouths of Claire Creek and Finley Creek and at the gauging station for Oak Creek located near the research forest boundary (see map Figure 3). Pressure transducers were used to measure the height of the water in the streams at the mouth of the Claire Creek and Finley Creek, and at the Oak Creek gauging station. The streams at the mouths of these watersheds are natural channels so water height was converted to discharge using a stage/discharge relationship. Discharge was measured with current meters and with standard stream gauging techniques and by using tracer dilution techniques (Rantz, 1982).

3.4.1 Peakflows

For each storm, the magnitude and time of occurrence of the peakflow were identified at each monitoring location where discharge was measured. The peakflow was identified as the maximum instantaneous discharge at that location during a storm. The magnitude and time of occurrence of the peakflows below the culvert were compared to the magnitude and time of occurrence of peakflows above the culvert. The change in timing of the peakflows between above and below culverts 34 and 35 was calculated as:

$$\Delta t = t_b - t_a \quad (8)$$

where Δt is the change in the timing of the peakflow timing (min), t_a is the time of occurrence of the peakflow above the culvert, and t_b is the time of occurrence of the peakflow below the culvert. A positive Δt means that the discharge below the culvert peaked later than the stream above the culvert.

A negative Δt means that the discharge below the culvert peaked before the stream above the culvert. Comparisons in the magnitude and time of occurrence of peakflows were also made between above and below the culverts and the mouth of Claire Creek and between Oak, Finley, and Claire Creeks.

In order to investigate how the #600 road influences peakflows in Claire Creek, a parameter was calculated that is labeled the 'real' travel time of peakflows. This parameter is the difference in time of occurrence of the peakflows above and below culverts 34 and 35 and at the mouth of Claire Creek:

$$T_r = t_{pc} - t_{pw} \quad (9)$$

where T_r is the real travel time of the peakflow (minutes), t_{pc} is the time of occurrence of the peakflow at the appropriate culvert, and t_{pw} is the time of occurrence of the peakflow at the mouth of Claire Creek.

3.4.2 Quickflows

In addition to looking at the magnitude and time of occurrence of peakflows, quickflow volumes of the storm flows were also calculated. Quickflow was calculated using the method described by Hewlett and Hibbert (1967) so that comparisons could be made between Claire Creek, Finley Creek, and the Oak Creek Watershed, and against the results of Toman (2004). As discussed in section 2.2, the Hewlett and Hibbert (1967) hydrograph separation method is an appropriate method when comparisons of this kind are made. The calculations were done in a Microsoft Excel spreadsheet using a macro written by Elizabeth Toman (2004). Quickflow was calculated for the streamflow above the culverts using the Hewlett and Hibbert method. For the streamflow below the culverts, the quickflow was calculated as the sum of the quickflow above the culvert plus all the ditchflow. The reason that all ditchflow was considered as quickflow is that there would be no ditchflow without the road.

3.4.3 Total Stormflow

The total volume of stormflow was also calculated for each storm. The total volume of stormflow is defined as the amount of discharge that occurred between the initial rise of the hydrograph and the recession limb at the same discharge. An alternative parameter to quickflow was

needed because in the definition of quickflow the baseflow separation line is a function of the area of the contributing watershed. Thus, comparing quickflow volumes between watersheds with different areas can be problematic because the method of calculation isn't consistent. The calculation of the total volume of stormflow circumvents this problem because watershed area is not considered in the calculation of total stormflow.

During some storms additional precipitation fell after the peak on the hydrograph occurred, resulting in small rises in the recession limb of the hydrograph. However, since the precipitation occurred after the storm was determined to be over, an exponential decay function was used to estimate the recession limb without the additional runoff. In this way only the runoff that resulted from the initial storm could be analyzed. The decay function is as follows:

$$Q = Q_0 * e^{(-kt)} \quad (10)$$

where Q is the discharge (m^3/s) at time t , Q_0 is the initial discharge (m^3/s), and k is the decay constant.

The decay coefficient, k , is defined by:

$$k = \frac{LN\left(\frac{Q_0}{Q}\right)}{t_0 - t} \quad (11)$$

where t_0 is the initial time, and other variables are as previously defined. In this manner, the recession limb was extended until the pre-storm was reached and the total volume of stormflow could be calculated.

All the hydrology parameters, maximum instantaneous peakflow, quickflow, and total volume of stormflow, were expressed as raw values and normalized by the upslope contributing area. The peakflows were expressed as l/s/ha , and volumes of quickflow and total stormflow were expressed in mm as an area depth. Streamflow labeled 'above the culvert' was divided by the nominal area of the watershed for the stream above the road. Streamflow labeled 'below the culvert' was divided by this same nominal area. No effort was made to discern the increase in watershed area above the road due to the interception of subsurface water by the road because the effect is not

consistent across road segments, making the resulting values somewhat meaningless (see Toman 2004).

3.4.5 Travel Time of Peakflows

In a previous study (Toman, 2004) and as a part of this study, the influence of the #600 road on the magnitude and time of occurrence of peakflows and the volume of stormflows at culverts 34 and 35 was quantified. However, the previous study did not address the relationship between the effects at the culverts and the possible effects at the watershed mouth. This study attempts to establish that relationship using kinematic wave equations to calculate the time of travel of the peakflows that occur at culverts 34 and 35.

Since there is no information on the hydrology of Claire Creek before the #600 road was constructed, an analytical method was needed to assess the impact of the road in the absence of pre-treatment data. Using kinematic wave equations, it is possible to model how long it takes for each peakflow—above and below culverts 34 and 35—to reach the mouth of Claire Creek. The assumptions were made that the modeled travel time for the peakflows above the culverts represents data from before the road was constructed and that travel times of peakflows below the culverts represents data after the road was constructed in the watershed. Thus, it is possible to compare the travel times for peakflows from the culverts to the watershed mouth before and after the #600 road was constructed. In this manner it is possible to conclude whether or not it is reasonable to expect that the impact of the #600 road on streamflow at culverts 34 and 35 will also have an impact on streamflow at the mouth of Claire Creek.

Two equations were used to model the travel time of peak discharges in Claire Creek as kinematic waves: an equation by Chow (1988) and an equation by Wong (2001). As described in the literature review, kinematic wave equations are appropriate for modeling the travel time of peakflows in small, steep channels, like the ones in the Claire Creek Watershed.

The equation by Chow (1988) takes the form:

$$T = \frac{3}{5} \left(\frac{nB^{2/3}}{S^{1/2}} \right)^{3/5} Q^{-2/5} L \quad (12)$$

where T is travel time (seconds), n is the Manning roughness coefficient (dimensionless), B is the width of the stream channel (m), S is the slope of the stream channel (m/m), Q is discharge (m^3/s), and L is the length of the stream reach that the travel time is being calculated for (m). For this equation, there is only one value of discharge used to calculate the travel time.

The equation by Wong (2001) differs from the Chow (1988) equation in that the initial upstream discharge value can be assigned, and travel time is then calculated as:

$$T = 0.0167 \left(\frac{n}{S^{1/2}} \right)^{3/5} L * b^{2/5} \left[\frac{Q_d^{3/5} - Q_u^{3/5}}{Q_d - Q_u} \right] \quad (13)$$

where T is travel time (minutes), b is the channel width (m), Q_d is the discharge at the downstream end of the segment (m^3/s), and Q_u is the discharge at the upstream end of the segment (m^3/s), and all other variables are as previously defined. Since initial upstream discharge was not measured at the confluence, this study uses discharge measured downstream at the mouth of the Claire Creek Watershed and the continuity equation to derive Q_u as follows:

$$Q_u = Q_d - (q * L) \quad (14)$$

where q is the lateral inflow per unit length of channel (l/s/m) and all other variables are as previously defined. The lateral inflow is the amount of water entering the stream incrementally, and in order to comply with the constraints of the kinematic wave equation, is assumed to be constant and evenly distributed along the stream channel.

One reason that these equations were selected is that the only parameter that is changed in order to model the road effect is the peakflow magnitude. If the introduction of ditch runoff into streams is the mechanism responsible for changes in peakflow timing, then the modeled travel times with and without the road would reflect that.

Because the slopes above the confluence are so much greater than the slopes below the confluence (Table 1), calculations were made first for peakflows traveling from culverts 34 and 35 to

the confluence and then from the confluence to the mouth of Claire Creek. Since the discharge at the confluence was unknown and in order to calculate a maximum road effect, the travel times were modeled based on the assumption that the peakflows from the streams below culverts 34 and 35 arrived at the confluence at the same time. The simultaneous arrival of the peakflows from these two streams was believed to generate the largest peakflow in Claire Creek which then result in the shortest possible travel time and greatest road effect.

Travel times of peakflows were modeled for the stream channels between culverts 34 and 35 and the confluence and between the confluence and the mouth of Claire Creek using Equations 12 and 13 in two ways. In the first method, each stream channels was treated as one continuous reach: a 317 meter reach between culvert 34 and the confluence, a 393 meter reach between culvert 35 and the confluence, and a 538 meter reach between the confluence and the mouth of Claire Creek. In the second method each stream channels was discretized into a number of shorter stream segments, and the travel time was modeled for each discrete stream segment. Then for each stream channel, the total travel time was the sum of the travel times for all of the discrete stream reaches. The discrete segments were designated during a survey of the stream segments as the distance between a hand level and a stadia rod without exceeding the height of the stadia rod. Stream width, channel shape, gradient, and roughness were also estimated for each stream segment during the survey.

For each storm a range of travel times and an average travel time were made for the stream channels between culvert 34 and the confluence and culvert 35 and the confluence. The shortest, longest, and average travel time calculations were modeled by estimating the greatest possible, smallest possible, and average discharge, respectively, at the confluence. These discharge estimates were made by maintaining a constant Q_u (defined here as the peakflow observed above or below the appropriate culvert) and varying the downstream discharge, Q_d , (defined here as the estimated peakflow in the appropriate channel, just above the confluence).

The method for estimating Q_d was to adjust the lateral inflow entering the channel. In order to meet the assumptions of Equation 13, the lateral inflow was allocated between the stream below culverts 34 and 35 based on the channel length as follows as:

$$q = \frac{Q_{CC} - (Q_{34} + Q_{35})}{(L_{34} + L_{35})} \quad (15)$$

where Q_{CC} is the peakflow observed at the mouth of Claire Creek (l/s), Q_{34} is the peakflow above culvert 34 (l/s), Q_{35} is the peakflow above culvert 35 (l/s), L_{34} is the length of the channel between culvert 34 and the confluence (m), and L_{35} is the length of channel between culvert 35 and the confluence (m) and all other variables are as previously defined. To estimate the greatest possible Q_d for the above the road peakflow, all the lateral inflow was assigned to occur above the confluence, such that lateral inflow in Claire Creek was zero, and Q_d was:

$$Q_{d34} = Q_{34} + (L_{34} * q) \quad (16)$$

where Q_{d34} is the downstream discharge for the channel below culvert 34 (l/s) and all variables are as previously defined. Equation 16 was repeated with the appropriate variables to solve the downstream discharge for the channel below culvert 35, Q_{d35} . To determine the smallest possible Q_d for the above the road peakflow, all lateral inflow was assigned to occur in Claire Creek below the confluence, such that Q_d was equal to Q_u . However, the Wong (2001) equation requires that $Q_u \neq Q_d$; so Q_d was set to equal $Q_u + 0.01$ l/s. The average Q_d was modeled as follows:

$$\bar{Q}_{d34} = \frac{Q_{34} + (Q_{34} + L_{34} * q)}{2} \quad (17)$$

where \bar{Q}_{d34} is the average downstream discharge in the channel below culvert 34. Equation 17 was used to calculate the average downstream discharge for the stream below culvert 35, \bar{Q}_{d35} . The greatest possible, smallest possible, and average downstream discharges were then used in Equations 12 and 13 to model the shortest, longest, and average travel time, respectively. The range and average modeled travel times were then calculated using the peakflow values from below the culverts. The difference in travel times from above and below the culverts was attributed to the #600 road.

Travel times were modeled in a similar manner for Claire Creek below the confluence. For each storm a range of travel times and an average travel time in Claire Creek were modeled for both the above and below the road peakflows by estimating the greatest possible, smallest possible, and

average initial upstream discharge, Q_u (defined here as the estimated peakflow at the confluence), and maintaining the downstream discharge, Q_d , constant (defined here as the peakflow observed at the mouth of Claire Creek). To determine the greatest possible Q_u for the above the road peakflows, all lateral inflow was assigned to enter the stream channels below culverts 34 and 35 and above the confluence, such that lateral inflow in Claire Creek was zero and Q_u was equal to Q_d . However, the Wong (2001) equation requires that $Q_u \neq Q_d$; so Q_u was set to $Q_d - 0.01$ l/s. Second, to determine the smallest possible Q_u all lateral inflow was assigned to enter Claire Creek below the confluence, such that Q_u was equal to the sum of the peakflows observed above the road at culvert 34 and 35. Third, the average Q_u was estimated by inputting the mean Q_u of the boundary estimates derived in the first two steps:

$$\overline{Q_u} = \frac{(Q_{34} + Q_{35}) + (Q_d - 0.01 \text{ l/s})}{2} \quad (18)$$

where $\overline{Q_u}$ is the average upstream discharge (l/s), and all other variables are as previously defined.

The greatest possible, smallest possible, and average Q_u values were then input into Equations 12 and 13 to model the shortest, longest, and average travel times, respectively. The range and average modeled travel times were then calculated using the peakflow values from below the culverts. The average modeled travel times, as modeled by the continuous channel method and using equation 13, were then compared to the real travel times.

4. RESULTS

4.1 Instrumentation and Data Quality

During the study period data were subjected to quality control. Water height measured by the pressure transducers and the capacitance rods were verified using staff gauges during downloads and maintenance. Precipitation data were compared to data from rain gauges in the watershed and at the HYSLOP farm, a long-term meteorological station. Hydrographs from all the monitoring locations were compared for consistency for each storm.

Because of equipment malfunction and sedimentation around sensors some data was lost and the quality of other data is questionable. Table 3 shows the array of data collected and the storms for which data was analyzed. The presence and quality of the data for each sampling location and storm is shown in the table.

Table 3. Summary of data availability at the monitoring locations in the Oak Creek Watershed for five storms during the winter of 2004 – 2005.

Site	Storm #1	Storm #2	Storm #3	Storm #4	Storm #5
Culvert 34					
Ditch 34					
Culvert 35					
Ditch 35					
Claire Creek					
Finley Creek					
Oak Creek					
Rain Gauge					

Included	Data Questionable	Data Lost
----------	-------------------	-----------

An error downloading the data from culvert 34 resulted in the loss of the ditch flow data during the March 25th storm. As a result, the stream contribution to quickflow above the road and the peakflow magnitude and the timing of the first peak in the hydrograph are unknown.

The stream channel in Finley Creek is actively eroding in a series of one to three meter high head cuts 100 meters upstream from the monitoring location. Sediment eroded from the head cuts

deposited in the channel at the monitoring location during the December 6th storm. The establishment of the stage/discharge relationship on Finley Creek came from discharge measurements made after this deposition occurred during the recession limb of the hydrograph. Thus, during the storm the bottom two inches of the pressure transducer was buried, causing an unknown shift in the stage/discharge relationship.

The pressure transducer at Finley Creek was in error for the recession limb of the May 17th storm. By comparing the hydrograph at Finley Creek to the hydrographs from the other monitoring locations it appears that the peak discharge value was not affected, but the quickflow and total stormflow volumes were.

4.2 Precipitation

The precipitation in the Oak Creek Watershed during the winter of 2004 – 2005 was not typical for either total amount or distribution. At HYSLOP, a proximal, long-term weather station managed by the Oregon Climate Service, the amount of precipitation measured from October 1, 2004 to October 1, 2005 (Water Year 2005) was 65 percent of the long-term average. During the winter and spring of Water Year 2005 only five storms occurred that produced runoff at the culvert locations. Two of these storms occurred in May, one in March, one in January, and one in December (Table 4). Only two of the storms occurred during the three month time period when the majority of winter storms occur in the Pacific Northwest; November, December, and January (Goard, 2004). The amount of rainfall during these three months of Water Year 2005 was only 48 percent of the long-term average for those same months at the HYSLOP station. These runoff producing storms were separated by extended periods of time when rainfall did not occur and runoff at the culverts decreased markedly or ceased altogether. All of the storms that occurred during the Water Year 2005 had a recurrence interval that was subannual. In other words, the storms have a high probability of occurring in any given year (see Table 4) (Toman, 2004).

Table 4. Duration, maximum intensities, and total precipitation amounts for runoff producing storms from the Starker rain gauge at the top of the Finley Creek Watershed.

Storm number	Storm begin date	Storm end date	Total rainfall (mm)	Maximum 1-hour intensity (mm/hr)	Maximum 24-hour intensity (mm/hr)	Storm duration (hours)
1	12/06/2004	12/11/2004	117	8	53	137.3
2	1/28/2005	1/29/2005	34	6	34	24.0
3	3/25/2005	3/30/2005	92	5	35	114.4
4	5/08/2005	5/10/2005	61	6	48	45.8
5	5/17/2005	5/19/2005	41	5	21	52.7

As determined by the tipping bucket rain gauge located at the centroid of the Oak Creek Watershed, the mean total rainfall for all five runoff producing storms was 69 mm and ranged from 34 mm to 117 mm. The average 1-hour rainfall intensity was 6 mm and ranged from 5 mm to 8 mm. The average 24-hour rainfall intensity was 38 mm and ranged from 21 to 53 mm. As a comparison, the 24-hour rainfall intensity associated with a storm event with a two-year return interval at the HYSLOP station is 55 mm (G. Taylor, Oregon Climate Services, personal communication, October 2005). On average, the storms lasted 74.8 hours and ranged from 24.0 to 137.3 hours. The January 28th storm had the most constant rainfall, delivering 1.4 mm/hr on average.

4.3 Runoff

For this study, runoff was measured throughout the winter of 2004 – 2005 at culverts 34 and 35, in the road ditches adjoining culverts 34 and 35, and at the mouth of the Claire Creek Watershed. Runoff was also measured at an adjacent roadless watershed, Finley Creek, and in Oak Creek at the Research Forest Boundary (see map in Figure 3).

Toman (2004) measured runoff at culverts 34 and 35 and in the adjoining ditches to determine the effect of the road on flow in the streams at culverts 34 and 35. Toman (2004) did discern an impact of the road on the magnitude and timing of peakflows and streamflow volume. However, it was not possible to scale these impacts up to a watershed scale because, for that study,

discharge was not measured at the watershed outlets. These measurements were included in this study to investigate the possibility that the impacts of the road on streamflow at culverts 34 and 35 could be put into hydrologic context at a watershed scale.

To do this, first the impacts of the road on streamflow, specifically peakflow magnitude and timing and storm flow volumes (quickflow and total stormflow), were quantified for the latest water year. Then the streamflow at the culverts was compared with streamflow at the watershed mouth. Finally, peakflows at the culverts, those affected and unaffected by the road, were routed to the mouth of the watershed to investigate their role in the hydrology of the watershed.

4.4 Road Effects at the Culverts

Discharge was measured at culverts 34 and 35 and in the road ditches adjoining culverts 34 and 35. To determine the effect of the road on streamflow at the culverts, the discharge in the ditch was subtracted from the discharge at the culvert. The difference in these two values resulted in a hydrograph for the stream that is unaffected by the road. By comparing the hydrographs for above the road with those from below the road, the impact of the road on the hydrology of the stream at the stream crossing culvert can be discerned.

4.4.1 Peakflow Magnitude

To determine the effect of the road on peakflow magnitude, the magnitude of the peakflow for each storm for the above the road hydrographs was compared with the magnitude of the peakflow for the hydrographs below the road. For all five storms and for both culverts the effect of the road was to increase the magnitude of the peakflow (Table 5). These results are consistent with the results of Toman (2004).

Increases in peakflow magnitude were more pronounced below culvert 34 than below culvert 35. For example, peakflow magnitude at culvert 34 increased from 1.4 l/s above the culvert to 6.4 l/s below the culvert in the May 8th storm, an increase of 357 percent. For the same storm, peakflow magnitude at culvert 35 increased from 5.7 l/s above the culvert to 9.7 l/s below the culvert, an increase of 70 percent (Table 5). The average increase in peakflow magnitude as a result of the road was 196 percent below culvert 34 and ranged from 61 to 357 percent. The average increase below

culvert 35 was 66 percent and ranged from 29 to 120 percent. The hydrographs showing the effect of the road on peakflow magnitude at culverts 34 and 35 for all five storms are shown in Figure 8a-e.

Table 5. Changes in peakflow magnitude and timing above and below the road at culverts 34 and 35 in Claire Creek Watershed during the winter of 2004 - 2005. Changes are caused by the introduction of ditch flow into the stream channel. Standard errors in parenthesis.

Storm	Location	Time of peak (hh:mm)	Change in timing (hh:mm)	Peakflow magnitude (l/s)	Unit area peakflow magnitude (l/s/ha)	Percent increase in peakflow magnitude (%)
12/06/04	34 above road	12/8/04 3:30	0:30 after	5.0	1.0	191
	34 below road	12/8/04 4:00		14.6	2.9	
	35 above road	12/8/04 3:50	0:00	11.3	3.8	71
	35 below road	12/8/04 3:50		19.3	6.5	
1/28/05	34 above road	1/29/05 9:30	0:00	2.3	0.5	61
	34 below road	1/29/05 9:30		3.7	0.7	
	35 above road	1/29/05 8:10	0:00	2.5	0.8	40
	35 below road	1/29/05 8:10		3.5	1.2	
Peak 1 3/25/05	34 above road	--	--	--	--	--
	34 below road	3/27/05 7:10		4.4	0.9	
	35 above road	3/27/05 9:00	1:20 before	4.9	1.6	52
	35 below road	3/27/05 7:40		7.4	2.5	
Peak 2 3/25/05	34 above road	3/29/05 2:00	0:30 after	2.9	0.6	176
	34 below road	3/29/05 2:30		8.1	1.6	
	35 above road	3/29/05 2:00	0:00	5.2	1.7	120
	35 below road	3/29/05 2:00		11.4	3.8	
Peak 1 5/08/05	34 above road	5/9/05 19:50	0:00	1.4	0.3	357
	34 below road	5/9/05 19:50		6.4	1.3	
	35 above road	5/9/05 18:10	1:00 after	5.7	1.9	70
	35 below road	5/9/05 19:10		9.7	3.2	
Peak 2 5/08/05	34 above road	5/10/05 10:50	0:50 after	1.6	0.3	283
	34 below road	5/10/05 11:40		6.1	1.2	
	35 above road	5/10/05 11:40	0:30 before	3.9	1.3	76
	35 below road	5/10/05 11:10		6.9	2.3	
5/17/05	34 above road	5/19/05 7:40	0:00	1.4	0.3	105
	34 below road	5/19/05 7:40		2.9	0.6	
	35 above road	5/19/05 6:20	0:00	2.0	0.7	29
	35 below road	5/19/05 6:20		2.6	0.9	
Average Values	34 above road		0:18 after (9)	2.4 (0.6)	0.5 (0.1)	196 (45)
	34 below road			6.6 (1.5)	1.3 (0.3)	
	35 above road		0:07 before (16)	5.1 (1.2)	1.7 (0.4)	66 (11)
	35 below road			8.7 (2.1)	2.9(0.7)	

Figure 8. Storm hydrographs for above and below the road at culverts 34 and 35 in the Claire Creek Watershed for the December 6th storm (a), the January 28th storm (b), the March 25th storm (c), the May 8th storm (d) and the May 17th storm (e) during the winter of 2004 – 2005.

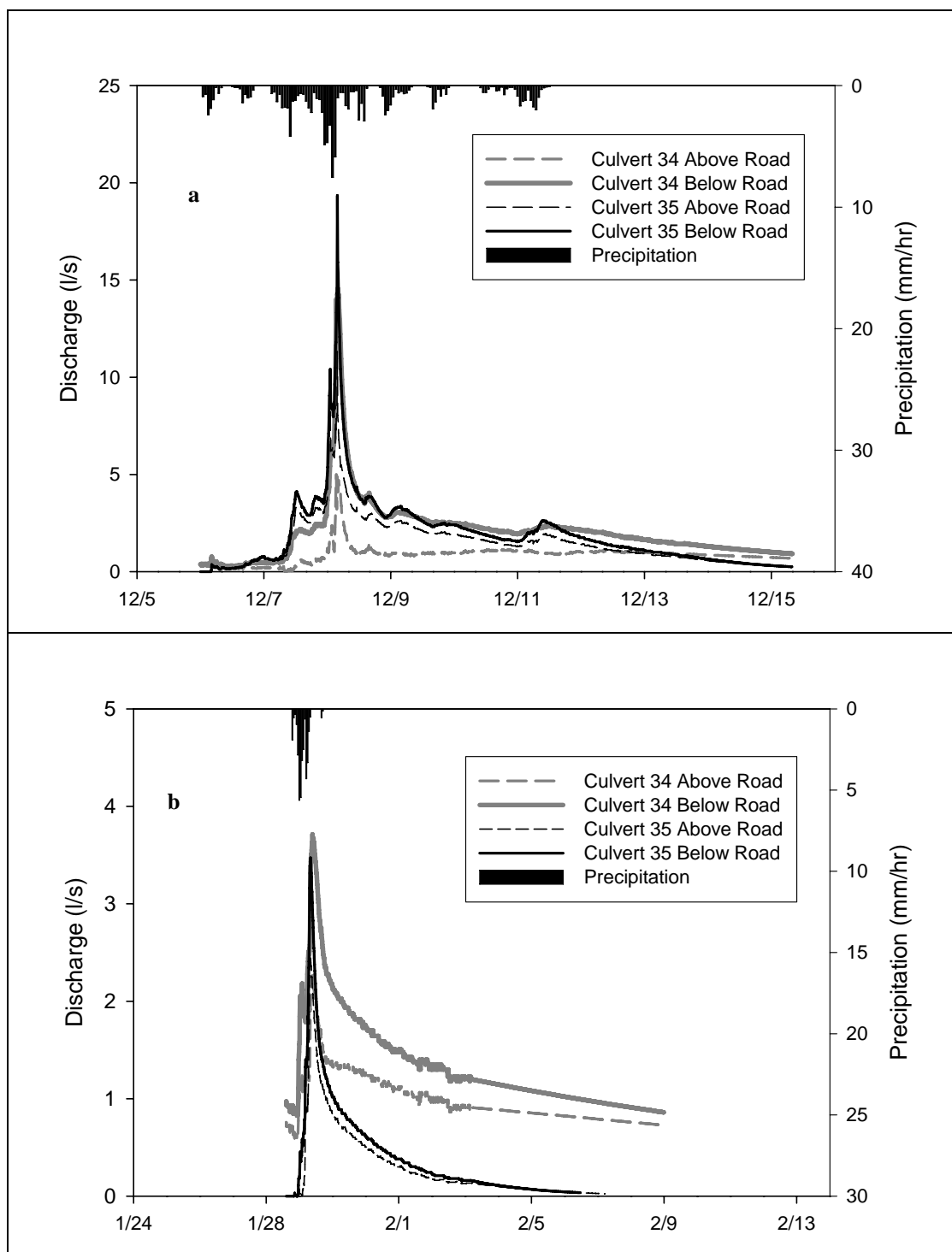


Figure 8 (continued). Storm hydrographs for above and below the road at culverts 34 and 35 in the Claire Creek Watershed for the December 6th storm (a), the January 28th storm (b), the March 25th storm (c), the May 8th storm (d) and the May 17th storm (e) during the winter of 2004 – 2005.

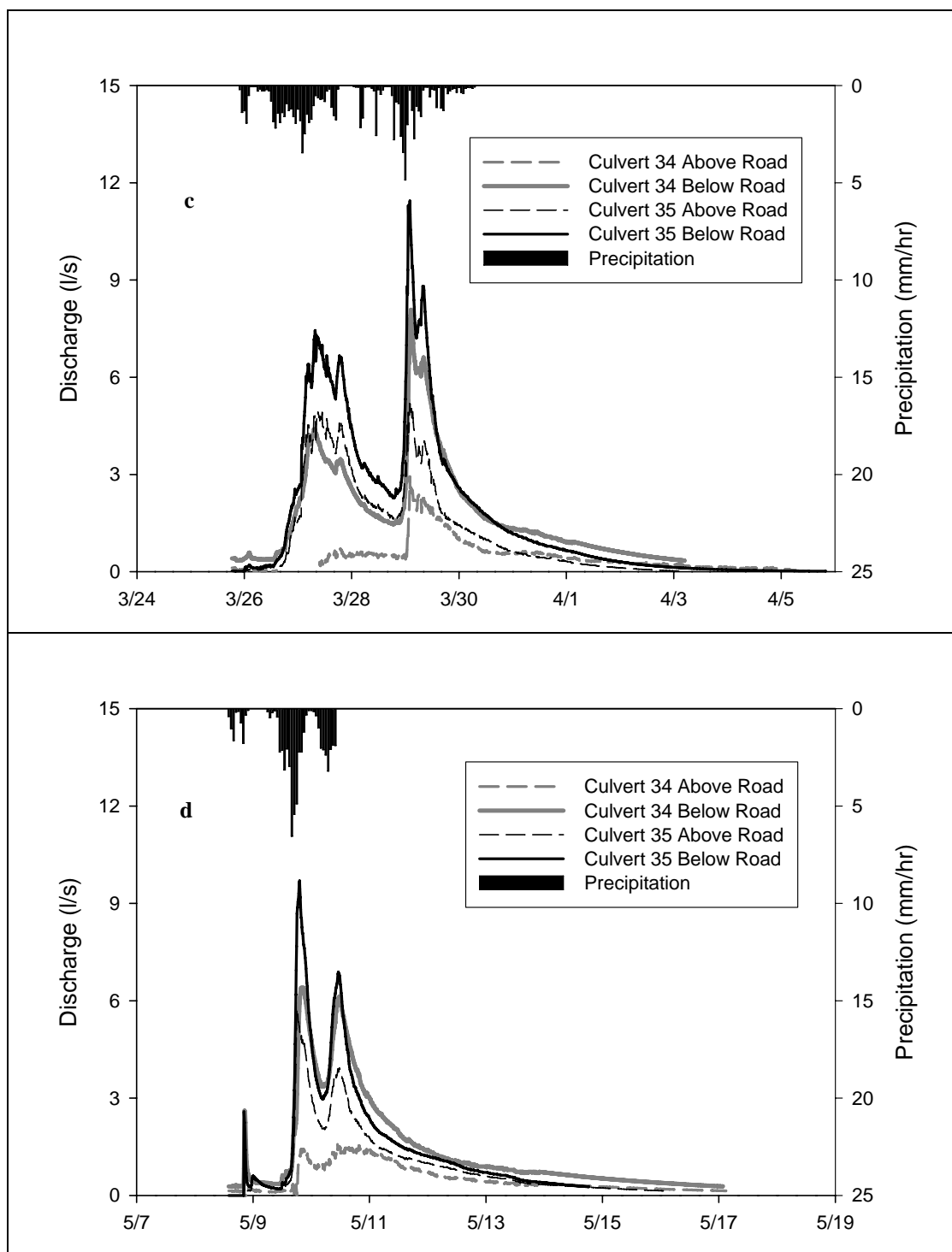
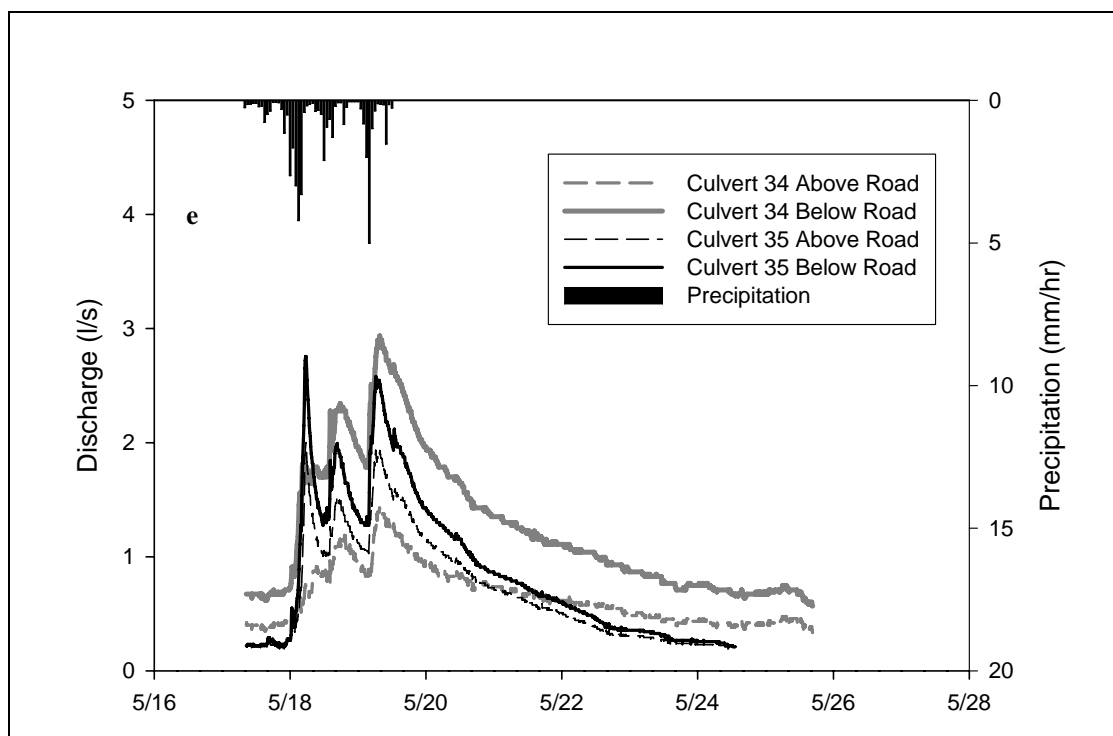


Figure 8 (continued). Storm hydrographs for above and below the road at culverts 34 and 35 in the Claire Creek Watershed for the December 6th storm (a), the January 28th storm (b), the March 25th storm (c), the May 8th storm (d) and the May 17th storm (e) during the winter of 2004 – 2005.



The increase in peakflow magnitude at each stream crossing culvert was positively correlated with rainfall. The correlation is strongest between the increase in peakflow and total storm precipitation (Table 6). For example, the greatest increase in peakflow was observed during the December 6th storm at culvert 34 (9.6 l/s) and corresponded to the storm with the greatest total rainfall (see Tables 4 and 5). The least increase in peakflow magnitude was observed at culvert 35 (0.6 l/s) during the May 17th storm, the storm with the second smallest total precipitation, and the smallest 24-hour rainfall intensity.

The percent increase in peakflow magnitude was less correlated to rainfall than the increase in peakflow magnitude. For example, the smallest percent increase in peakflow magnitude was associated with the smallest storm and the greatest percent increase in peakflow magnitude (457

percent) corresponded to the March 25th storm which had half the total precipitation of the largest storm.

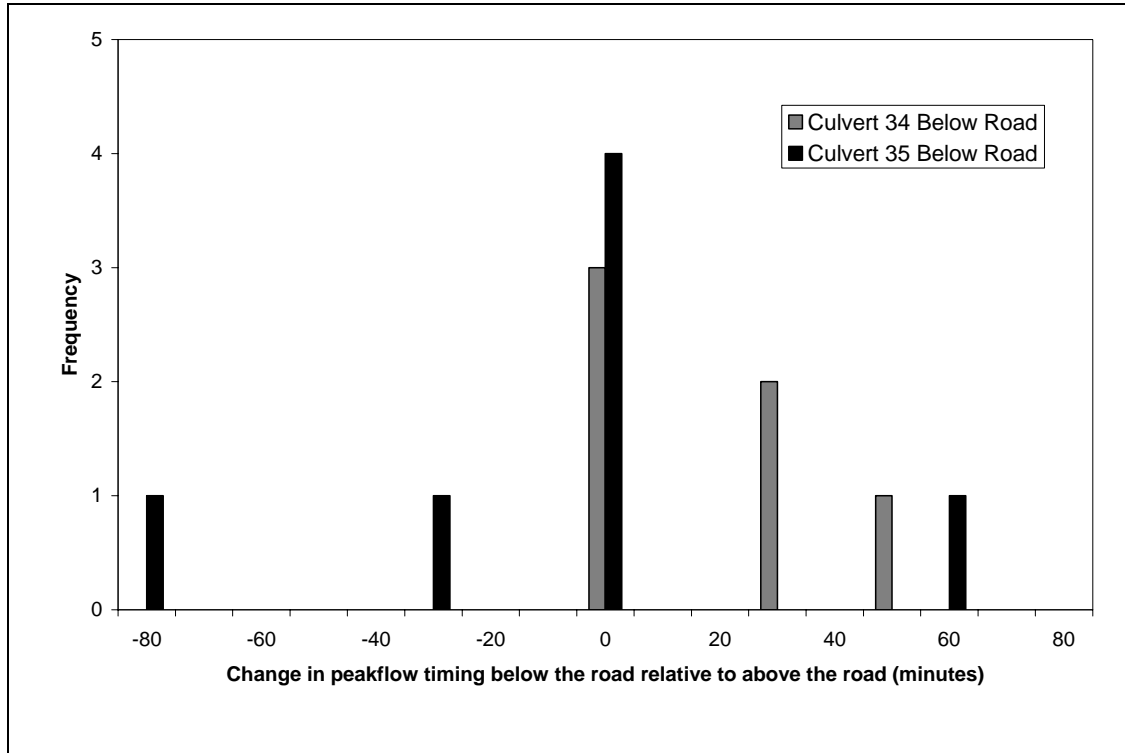
Table 6. Correlation coefficients between rainfall and the increase in peakflow above and below the road at culverts 34 and 35 in Claire Creek Watershed for five storms during the winter of 2004 – 2005.

	Location	Maximum 1-hr rain intensity	Maximum 24-hr rain intensity	Total rainfall
Increase in peakflow magnitude				
	Culvert 34	0.56	0.63	0.89
	Culvert 35	0.29	0.45	0.75
Percent increase in peakflow magnitude				
	Culvert 34	0.28	0.48	0.07
	Culvert 35	0.01	0.18	0.31

4.4.2 Peakflow Timing

To determine the effect of the road on peakflow timing, the timing of the peakflow for each storm above the culvert was compared to the timing of the peakflow below the culvert. The peakflow below the culvert occurred both before and after the peakflow above the culvert (Table 5). For the five storms that occurred, there were seven distinct peakflows. During these seven peakflows, there were 13 opportunities for the addition of ditchflow below the road to affect the peakflow timing of the stream above the road—six at culvert 34 and seven at culvert 35. Of the 13 opportunities, the road had no impact on timing for seven peakflows, advanced the timing for two peakflows, and delayed the timing for four peakflows. The greatest advance in peakflow timing was one hour and twenty minutes and occurred during the first peak of the March 25th storm at culvert 35 (Table 5). The greatest delay in peakflow timing was 60 minutes and occurred during the first peak of the May 8th storm at culvert 35. The average change in peakflow timing for all five storms was a delay of 18 minutes at culvert 34 and an advancement of seven minutes at culvert 35. The frequency of the change in timing is shown in Figure 9. There is no correlation between change in peakflow timing and total rainfall and maximum 1-hour or 24-hour rainfall intensities.

Figure 9. Frequency distribution of changes in peakflow timing due to the road at culverts 34 and 35 in the Claire Creek Watershed during the winter of 2004 – 2005. Positive values indicate a delay in peakflow timing; negative values indicate an advance in peakflow timing.



4.4.3 Quickflow Volume

To determine the effect of the road segments on quickflow volumes, the quickflow volume for the hydrograph above the road was compared to the quickflow volume for the hydrographs below the road. For all five storms and for both culverts the road increased the quickflow volume.

The quickflow volumes below culverts 34 and 35 were greater than quickflow volumes above culverts 34 and 35 (Table 7). The average quickflow volume above culvert 34 was 0.682×10^5 l and ranged from 0.985×10^5 to 0.262×10^5 l. The average quickflow volume below culvert 34 was 6.78×10^5 l and ranged from 10.9×10^5 to 4.09×10^5 l. The average quickflow above culvert 35 was 3.16×10^5 l and ranged from 0.936×10^5 to 5.63×10^5 l. The average quickflow below culvert 35 was 6.08×10^5 l and ranged from 12.5×10^5 to 1.64×10^5 l. On a unit area basis the quickflow volumes above and below culvert 34 averaged 1.4 and 13.5 mm, respectively and ranged from 2.0 and 21.8 mm, respectively to 0.5 and 8.2 mm, respectively. Unit area quickflow volumes above and below

culvert 35 averaged 10.5 and 20.3 mm, respectively and ranged from 18.8 and 41.8 mm, respectively to 3.1 and 5.5 mm, respectively.

An inconsistency was observed in the storms that produced the greatest and smallest quickflows above and below culverts 34 and 35. The largest quickflow volume above and below culvert 34 was observed during the May 8th and December 6th storms, respectively. The smallest quickflow volume above and below culvert 34 was observed during the May 17th and January 28th storms, respectively. The largest quickflow volumes above and below culvert 35 were observed during the March 25th storm, and the smallest quickflow above and below culvert 35 were observed during the January 28th storm.

The percent of increase in quickflow below the roads was not constant for the individual road segments for the different storms. At road segment 34, quickflow increased an average of 10 fold and the increase ranged from 660 percent to 1637 percent. The greatest percentage increase in quickflow occurred during the May 17th storm at culvert 34 when unit area quickflow volume above the road was 0.5 mm and quickflow volume below the road was 9.1 mm. At road segment 35 the average percent increase in quickflow was 87 percent and ranged from 68 to 120 percent.

On average, the stream above culvert 35 yielded more quickflow and unit area quickflow than the stream above culvert 34. However, on average the stream below culvert 35 yielded less quickflow but more unit area quickflow than the stream below culvert 34. Percent increase in quickflow volume at the culverts was not correlated to total rainfall, or either 1-hour or 24-hour rainfall intensities.

Table 7. Changes in quickflow volume above and below the road at culverts 34 and 35 in Oak Creek watershed during the winter of 2004 - 2005. Changes caused by the introduction of ditch flow into the stream channel. Standard error in parenthesis.

Storm	Location	Quickflow volume (l)	Quickflow unit area (mm)	Percentage increase in quickflow below the road (%)
12/06/04	Culvert 34 above road	94,300	1.9	1056
	Culvert 34 below road	1,090,000	21.8	
	Culvert 35 above road	488,000	16.3	68
	Culvert 35 below road	822,000	27.4	
1/28/05	Culvert 34 above road	53,800	1.1	660
	Culvert 34 below road	409,000	8.2	
	Culvert 35 above road	93,600	3.1	75
	Culvert 35 below road	164,000	5.5	
3/25/05	Culvert 34 above road	--	--	--
	Culvert 34 below road	--	--	
	Culvert 35 above road	563,000	18.8	120
	Culvert 35 below road	1,250,000	41.8	
5/08/05	Culvert 34 above road	98,500	2.0	668
	Culvert 34 below road	756,000	15.1	
	Culvert 35 above road	319,000	10.7	81
	Culvert 35 below road	578,000	19.3	
5/17/05	Culvert 34 above road	26,200	0.5	1637
	Culvert 34 below road	455,000	9.1	
	Culvert 35 above road	118,000	3.9	90
	Culvert 35 below road	224,000	7.5	
Average Values	Culvert 34 above road	68,200 (17,200)	1.4 (0.4)	1005 (230)
	Culvert 34 below road	678,000 (157,600)	13.5 (3.1)	
	Culvert 35 above road	316,000 (94,700)	10.5 (3.2)	87 (9)
	Culvert 35 below road	608,000 (200,400)	20.3 (6.7)	

4.4.4 Total Stormflow Volume

To determine the effect of the road on total runoff volume, the total volume for the hydrographs above culverts 34 and 35 was compared with the total volume for the hydrographs below culverts 34 and 35. For all five storms and for both culverts the effect of the road was to increase total stormflow (Table 8). The average total stormflow volume above culverts 34 and 35 was 7.04×10^5 and 6.93×10^5 l, respectively, and ranged from 3.71×10^5 to 11.2×10^5 l and 2.45×10^5 to 12.2×10^5 l, respectively. The average total stormflow volume below culverts 34 and 35 was 12.7×10^5 and 9.74×10^5 l, respectively and ranged from 8.98×10^5 to 18.3×10^5 l and 3.14×10^5 to 16.1×10^5 l, respectively. On a unit area basis total stormflow volumes above culverts 34 and 35 averaged 14.1 and 23.1 mm of runoff, respectively, and ranged from 7.4 to 22.4 mm and 8.2 to 40.7 mm, respectively. Unit area total stormflow volumes below culverts 34 and 35 averaged 25.4 and 32.5 mm, respectively, and ranged from 18.0 to 36.6 mm and 10.5 to 53.7 mm, respectively.

There was no consistent pattern between storm size and total stormflow above or below culverts 34 and 35. Greatest or smallest total stormflow above the culvert usually did not correspond to greatest or smallest total stormflow below the culvert, and the greatest or smallest total stormflow above or below one culvert did not correspond to the greatest or smallest total stormflow above or below the other culvert for the same storm. The January 28th storm produced the greatest total stormflow above culvert 34, but the December 6th storm produced the greatest total stormflow below culvert 34. The December 6th storm produced the greatest total stormflow above culvert 35, but the March 25th storm produced the greatest total stormflow below culvert 35. The May 8th storm produced the smallest total stormflow above culvert 34, but the May 17th storm produced the smallest total stormflow below culvert 34. The January 28th storm produced the smallest total stormflow above and below culvert 35.

The average percent increase in total stormflow below the road at culvert 34 was 99 percent and ranged from 20 to 170 percent (Table 8). The average percent increase in total stormflow below the road at culvert 35 was 38 percent and ranged from 25 to 69 percent. Neither the May 8th nor the

March 25th storm were the largest storms observed, yet they produced the largest percent increase in total runoff volume at culverts 34 and 35, respectively.

Table 8. Total stormflow above and below the road at culverts 34 and 35 in Oak Creek watershed during the winter of 2004 – 2005. Standard errors in parenthesis.

Storm	Location	Total stormflow volume (l)	Total stormflow unit area (mm)	Percent increase in total stormflow below the road (%)
12/06/04	Culvert 34 above road	853,000	17.1	115
	Culvert 34 below road	1,830,000	36.6	
	Culvert 35 above road	1,220,000	40.7	27
	Culvert 35 below road	1,550,000	51.7	
1/28/05	Culvert 34 above road	1,120,000	22.4	20
	Culvert 34 below road	1,340,000	26.8	
	Culvert 35 above road	245,000	8.2	28
	Culvert 35 below road	314,000	10.5	
3/25/05	Culvert 34 above road	--	--	--
	Culvert 34 below road	1,290,000	25.8	
	Culvert 35 above road	949,000	31.6	70
	Culvert 35 below road	1,610,000	53.7	
5/08/05	Culvert 34 above road	371,000	7.4	170
	Culvert 34 below road	1,000,000	20.0	
	Culvert 35 above road	620,000	20.7	38
	Culvert 35 below road	857,000	28.6	
5/17/05	Culvert 34 above road	470,000	9.4	91
	Culvert 34 below road	898,000	18.0	
	Culvert 35 above road	432,000	14.4	25
	Culvert 35 below road	541,000	18.0	
Average Values	Culvert 34 above road	704,000 (173,000)	14.1 (3.5)	99 (24)
	Culvert 34 below road	1,270,000 (163,000)	25.4 (3.3)	
	Culvert 35 above road	693,000 (176,000)	23.1 (5.9)	38 (7)
	Culvert 35 below road	974,000 (262,000)	32.5 (8.7)	

4.5 Road Effects for the Claire Creek Watershed

The discharge at the mouth of the Claire Creek Watershed (see map Figure 3) was measured during the winter of 2004 – 2005 in addition to discharge at culverts 34 and 35. The impact of the road on the hydrology of Claire Creek could not be determined in the absence of pre-road runoff data. However, a comparison of the hydrographs above and below culverts 34 and 35 and the hydrograph at the mouth of Claire Creek was made to show the watershed response in relation to the response measured at the road segments from the five storms.

4.5.1 Peakflow Magnitude

The peakflow magnitudes at the mouth of Claire Creek averaged 30 l/s and ranged from 49 l/s during the December 6th storm to 18 l/s during the May 17th storm (Table 9). The corresponding peakflows above culverts 34 and 35 averaged 2.4 l/s and 5.1 l/s respectively and ranged from 5.0 l/s and 11.3 l/s, respectively for the December 6th storm to 1.4 l/s and 2.0 l/s, respectively for the storm on May 17th. The peakflows below culverts 34 and 35 that included the effect of the road averaged 6.6 l/s and 8.7 l/s respectively and ranged from 14.6 l/s and 19.3 l/s for the December 6th storm to 2.9 l/s and 2.6 l/s respectively for the May 17th storm (see Table 5). As a general pattern, the peakflow magnitudes increased below culverts 34 and 35 and in relation to the storm size and watershed size as illustrated in Figure 10 a-e.

Table 9. Time of peakflow, real travel time of peakflows, peakflow magnitude, and quickflow volumes measured above and below culverts 34 and 35, and at the mouth of the Claire Creek Watershed during the winter of 2004 – 2005.

Storm	Location	Time of peakflow (hh:mm)	Change from watershed mouth (hh:mm)	Peakflow magnitude (l/s)	Unit area peakflow magnitude (l/s/ha)	Quickflow (l)	Unit area quickflow (mm)
12/06/04	Claire Creek	12/8/04 4:20	0	49	1.0	2,450,000	4.8
	34 above road	12/8/04 3:30	0:50 before	5.0	1.0	94,300	1.9
	34 below road	12/8/04 4:00	0:20 before	14.6	2.9	1,090,000	21.8
	35 above road	12/8/04 3:50	0:30 before	11.3	3.8	488,000	16.3
	35 below road	12/8/04 3:50	0:30 before	19.3	6.5	822,000	27.4
1/28/05	Claire Creek	1/29/05 9:40	0	22	0.4	805,000	1.6
	34 above road	1/29/05 9:30	0:10 before	2.3	0.5	53,800	1.1
	34 below road	1/29/05 9:30	0:10 before	3.7	0.7	409,000	8.2
	35 above road	1/29/05 8:10	1:30 before	2.5	0.8	93,600	3.1
	35 below road	1/29/05 8:10	1:30 before	3.5	1.2	164,000	5.5
Peak 1 3/25/05	Claire Creek	3/27/05 8:00	0	29	0.6	2,140,000	4.2
	34 above road	--	--	--	--	--	--
	34 below road	3/27/05 7:10	0:50 before	4.4	0.9	--	--
	35 above road	3/27/05 9:00	1:00 after	4.9	1.6	563,000	18.8
	35 below road	3/27/05 7:40	0:20 before	7.4	2.5	1,250,000	41.8
Peak 2 3/25/05	Claire Creek	3/29/05 2:40	0	32	0.6		
	34 above road	3/29/05 2:00	0:40 before	2.9	0.6		
	34 below road	3/29/05 2:30	0:10 before	8.1	1.6		
	35 above road	3/29/05 2:00	0:40 before	5.2	1.7		
	35 below road	3/29/05 2:00	0:40 before	11.4	3.8		
Peak 1 5/08/05	Claire Creek	5/9/05 20:30	0	33	0.6	1,880,000	3.7
	34 above road	5/9/05 19:50	0:40 before	1.4	0.3	98,500	2.0
	34 below road	5/9/05 19:50	0:40 before	6.4	1.3	756,000	15.1
	35 above road	5/9/05 18:10	2:20 before	5.7	1.9	319,000	10.7
	35 below road	5/9/05 19:10	1:20 before	9.7	3.2	578,000	19.3
Peak 2 5/08/05	Claire Creek	5/10/05 11:40	0	30	0.6		
	34 above road	5/10/05 10:50	0:50 before	1.6	0.3		
	34 below road	5/10/05 11:40	0	6.1	1.2		
	35 above road	5/10/05 11:40	0	3.9	1.3		
	35 below road	5/10/05 11:10	0:30 before	6.9	2.3		
5/17/05	Claire Creek	5/19/05 7:40	0	18	0.4	429,000	0.8
	34 above road	5/19/05 7:40	0	1.4	0.3	26,200	0.5
	34 below road	5/19/05 7:40	0	2.9	0.6	455,000	9.1
	35 above road	5/19/05 6:20	1:20 before	2.0	0.7	118,000	3.9
	35 below road	5/19/05 6:20	1:20 before	2.6	0.9	224,000	7.5
Average Values	Claire Creek		0	30.3	0.6	1,540,000	3.0
	34 above road		0:32 before	2.4	0.5	68,200	1.4
	34 below road		0:19 before	6.6	1.3	678,000	13.5
	35 above road		0:46 before	5.1	1.7	316,000	10.5
	35 below road		0:53 before	8.7	2.9	608,000	20.3

Figure 10. Storm hydrographs for above and below the road at culverts 34 and 35 and at the mouth of the Claire Creek Watershed for the December 6th storm (a), the January 28th storm (b), the March 25th storm (c), the May 8th storm (d) and the May 17th storm (e) during the winter of 2004 – 2005.

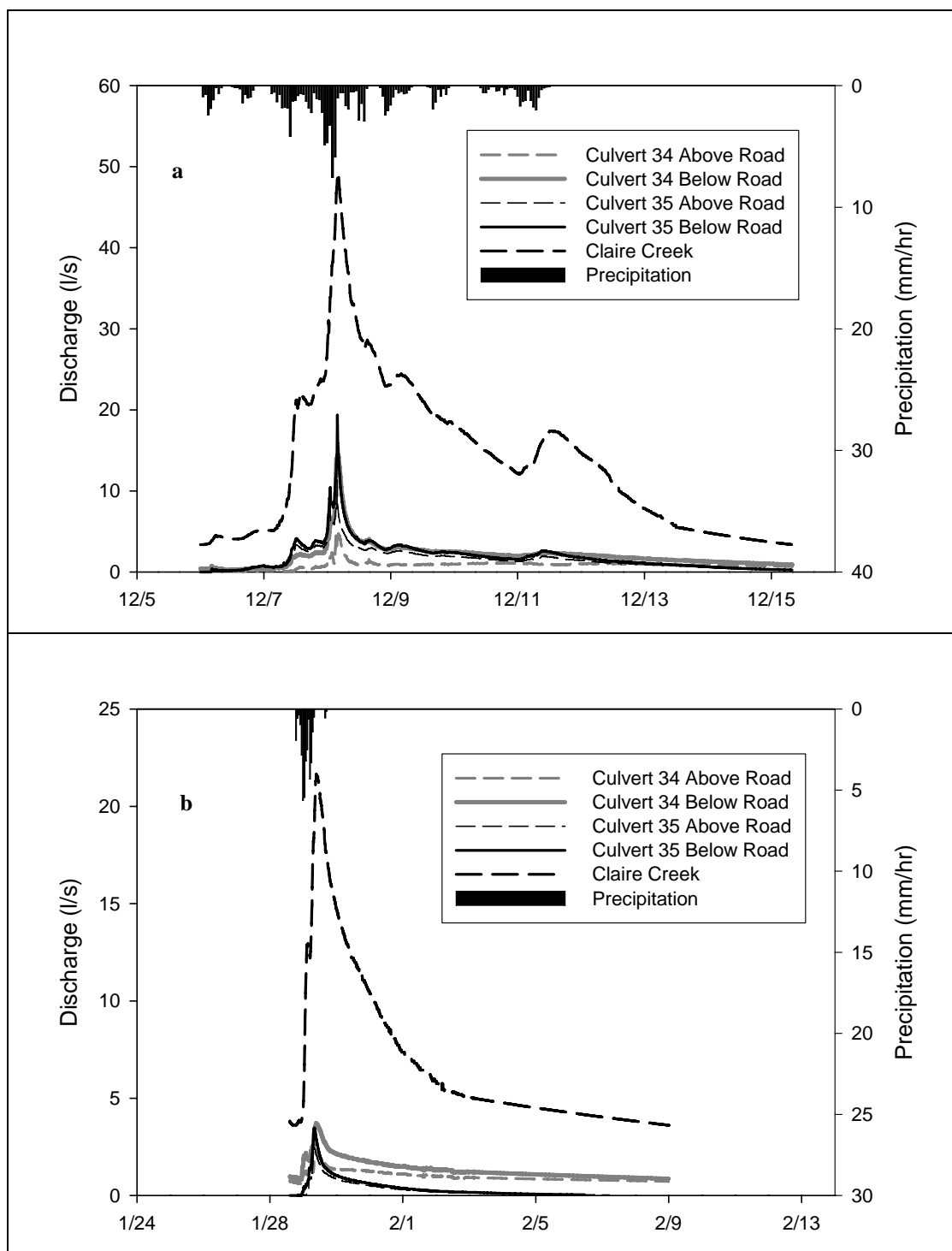


Figure 10 (continued). Storm hydrographs for above and below the road at culverts 34 and 35 and at the mouth of the Claire Creek Watershed for the December 6th storm (a), the January 28th storm (b), the March 25th storm (c), the May 8th storm (d) and the May 17th storm (e) during the winter of 2004 – 2005.

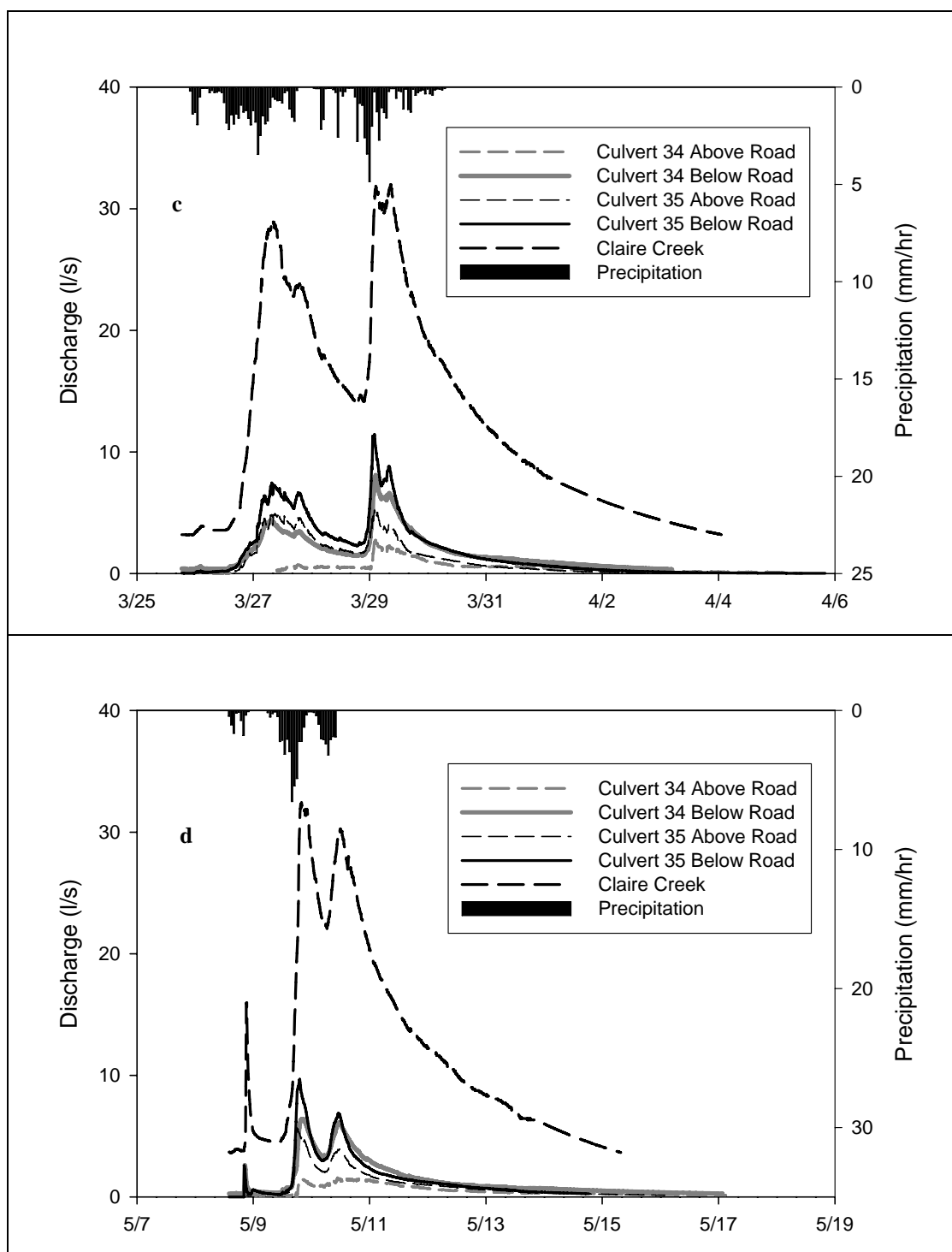
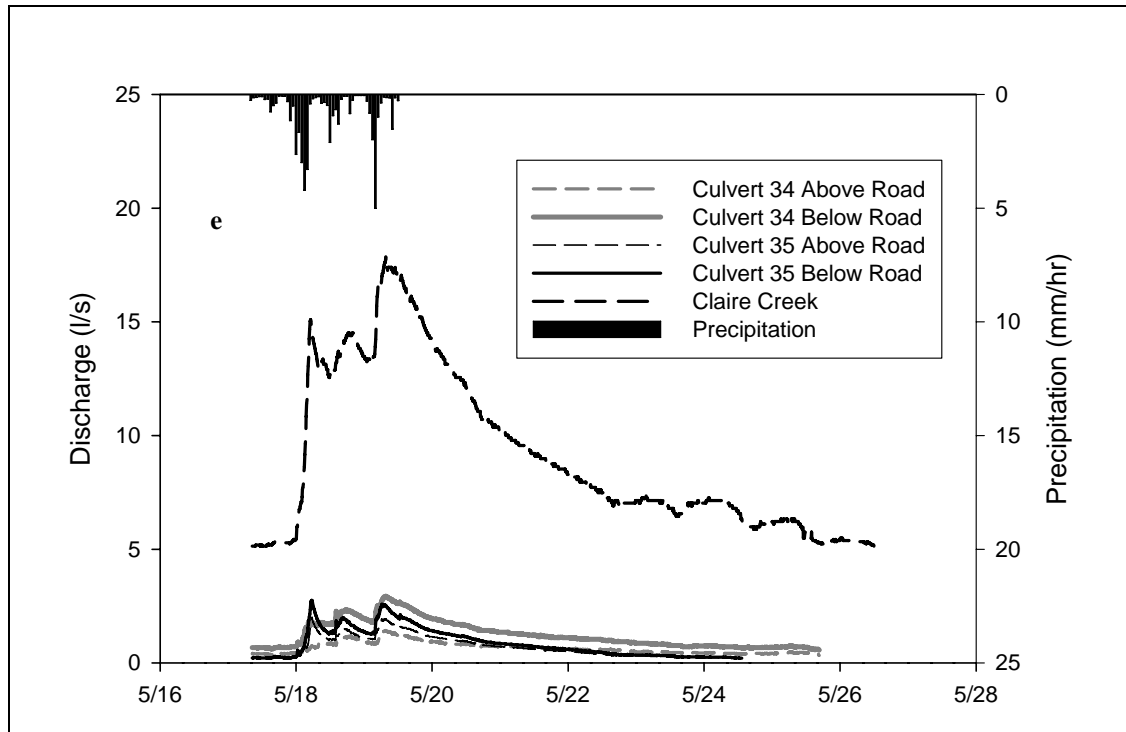


Figure 10 (continued). Storm hydrographs for above and below the road at culverts 34 and 35 and at the mouth of the Claire Creek Watershed for the December 6th storm (a), the January 28th storm (b), the March 25th storm (c), the May 8th storm (d) and the May 17th storm (e) during the winter of 2004 – 2005.



The generalization that peakflows increased with watershed size does not hold for the peakflows expressed on a unit area basis. The magnitude of the peakflows at the mouth of the Claire Creek Watershed averaged 0.6 l/s/ha and ranged from 1.0 l/s/ha during the December 6th storm to 0.3 l/s/ha for the May 17th storm (Table 9). The peakflows for the watersheds above culverts 34 and 35 averaged 0.5 l/s/ha and 1.7 l/s/ha respectively and ranged from 1.0 l/s/ha and 3.8 l/s/ha respectively for the December 6th storm to 0.3 l/s/ha and 0.7 l/s/ha respectively for the May 17th storm. The peakflows below culverts 34 and 35 that included the effect of the road averaged 1.3 l/s/ha and 2.9 l/s/ha respectively and ranged from 2.9 l/s/ha and 6.5 l/s/ha respectively for the December 6th storm and 0.6 l/s/ha and 0.9 l/s/ha respectively for the May 17th storm. The peakflows expressed on a per unit area basis increased as the watershed area decreased. Of the Claire Creek Watershed and the watersheds above culverts 34 and 35, unit area peakflows were greatest for the smallest watersheds

(above culvert 35) and smallest for the larger Claire Creek Watershed (see Table 2). The peakflows expressed on a per unit area basis still increased as an effect of the road at culverts 34 and 35.

4.5.2 Real Peakflow Travel Times

The timing of the peakflows above and below culverts 34 and 35 were compared to the timing of the peakflows at the mouth of Claire Creek, and the difference was estimated to be the real travel time of the peakflows. Seven peakflows were observed during this study and from these seven peakflows, there was 27 comparisons that could be made between the timing of peakflows above and below culverts 34 and 35 and the timing of the peakflows at the mouth of Claire Creek. A frequency distribution of the real travel times of peakflows from above and below culverts 34 and 35 to the mouth of Claire Creek are shown in Figure 11.

The peakflows that were observed above culvert 34 occurred before the peakflows at the mouth of Claire Creek five out of the six peakflows observed. The peakflows occurred at the same time for the single remaining peakflow observed. The real travel time of the peakflows from above culvert 34 to the mouth of Claire Creek ranged from 50 minutes to zero. The peakflows that were observed below culvert 34 occurred before the peakflows at the mouth of Claire Creek five out of the seven peakflows that were observed. The peakflows occurred at the same time for the two remaining peakflows observed. The real travel time of the peakflows from below culvert 34 to the mouth of Claire Creek ranged from 50 minutes to zero.

The peakflows that were observed above culvert 35 occurred before the peakflows at the mouth of Claire Creek five out of the seven peakflows observed. The peakflows occurred at the same time once, and the peakflows occurred above culvert 35 after the peakflow at Claire Creek once. The real travel time of the peakflows from above culvert 35 to the mouth of Claire Creek ranged from 140 minutes to a negative travel time of 60 minutes. The negative travel time resulted because the peakflow occurred first at the mouth of Claire Creek, and later above culvert 35. The peakflows that were observed below culvert 35 occurred before the peakflows at the mouth of Claire Creek for seven out of seven peakflows observed. The real travel time of the peakflows from below culvert 35 to the mouth of Claire Creek ranged from 90 minutes to 20 minutes.

The occurrences of real travel times of zero suggest that the peakflow traveled fast enough to be measured simultaneously at the culvert and the mouth of Claire Creek. Thus real travel times of zero are not physically possible. Likewise the occurrence of the negative travel time of the peakflow above culvert 35 is not physically possible.

In order to investigate whether patterns existed in the differences of real travel times of the peakflows, the real travel times were graphed against the magnitudes of the peakflows. The real travel times were graphed relative to the magnitude of the peakflow at Claire Creek (Figure 12a) and above and below the culverts (Figure 12b). No obvious patterns or trends were detected in the graphs showing the differences in the timing of peakflows.

Figure 11. Frequency distribution of the real travel times from above and below culverts 34 and 35 to the mouth of Claire Creek during the winter of 2004 – 2005.

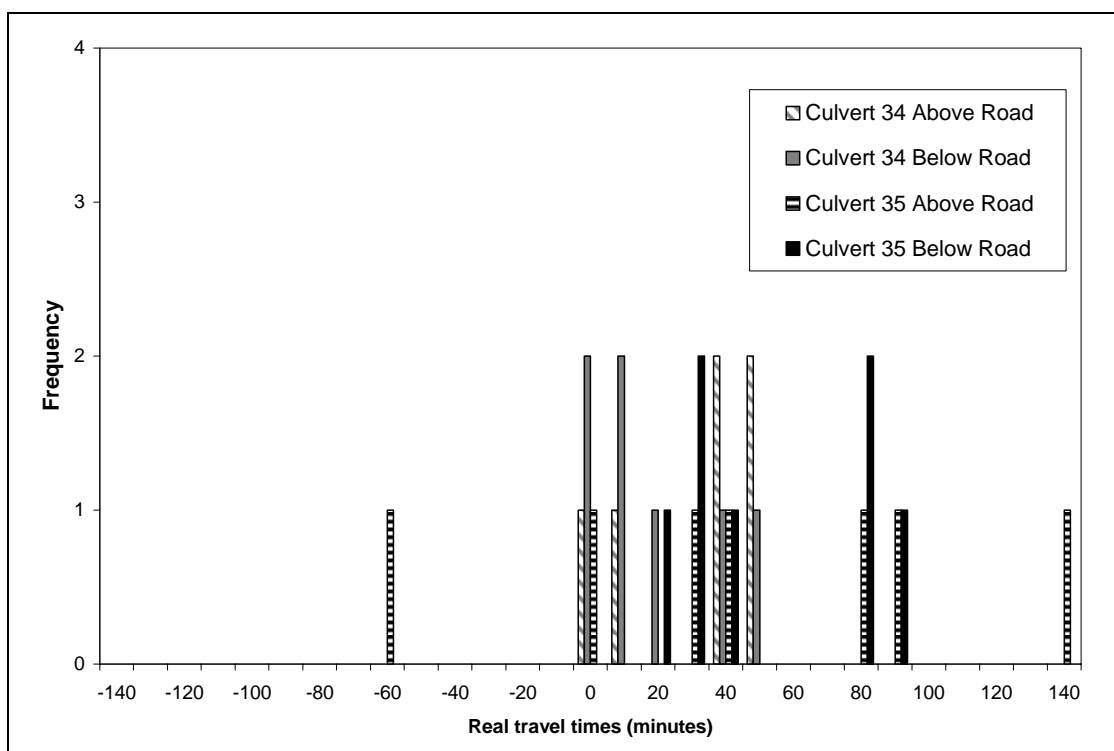
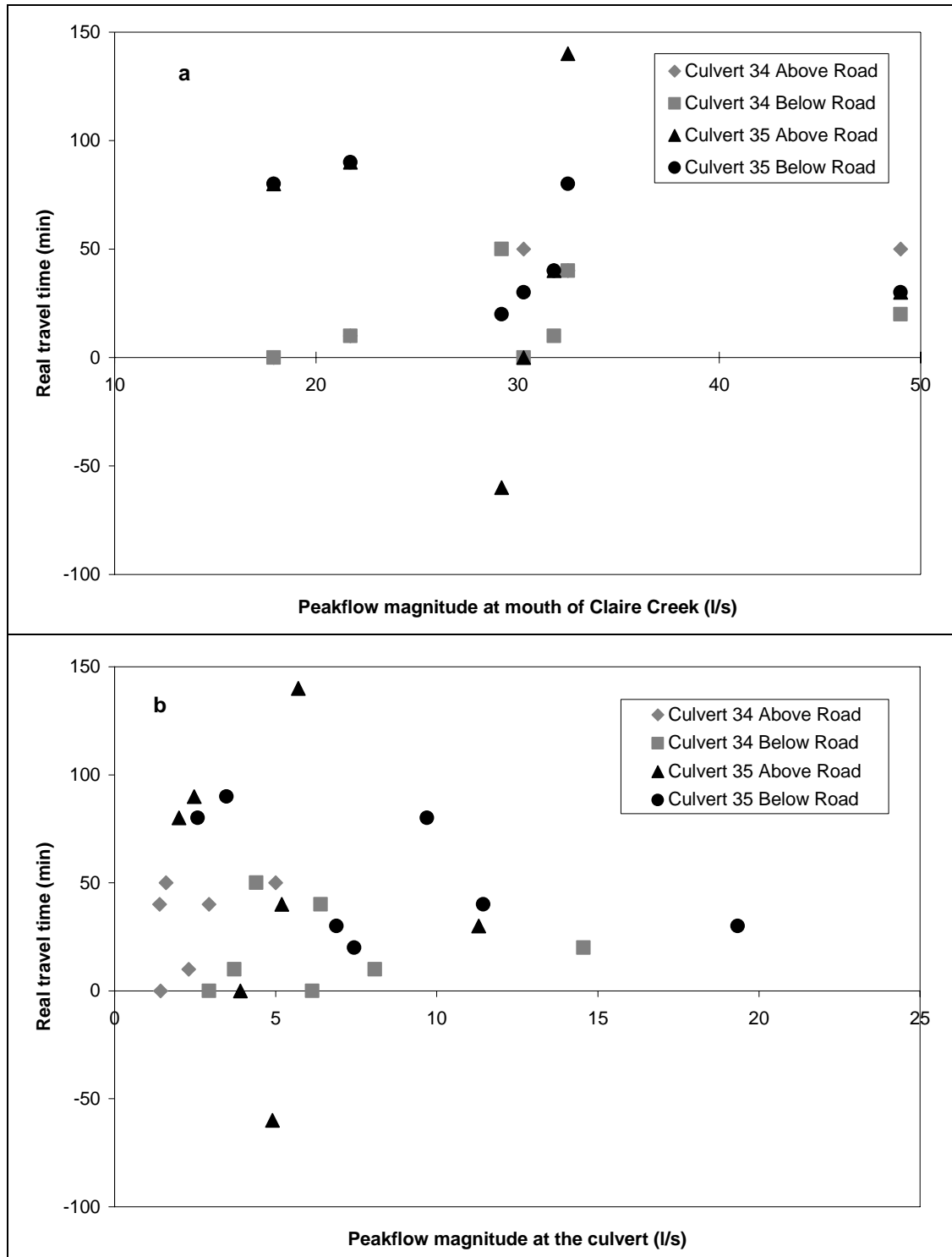


Figure 12. Scatterplots of real travel times from above and below culverts 34 and 35 to the mouth of Claire Creek relative to a) the magnitude of the peakflow at Claire Creek, and b) the magnitude of the peakflow at the culverts.



4.5.3 Quickflow Volume

The quickflow volumes at the mouth of Claire Creek were compared to the quickflow volumes above and below culverts 34 and 35. The volumes of quickflow from above and below culverts 34 and 35 were quantified and reported in a previous section of this thesis. Recall that for all five storms the volumes of quickflow that occurred below the culverts was greater than the volumes of quickflow that occurred above the culverts (Table 7). These findings are consistent with those of Toman (2004).

The quickflow volumes at the mouth of Claire Creek averaged 15.4×10^5 l and ranged from 24.5×10^5 l for the December 6th storm to 4.29×10^5 l for the May 17th storm (Table 9). The corresponding quickflow volumes above culverts 34 and 35 averaged 0.682×10^5 l and 3.16×10^5 l, respectively and ranged from 0.985×10^5 l and 5.63×10^5 l, respectively to 0.262×10^5 l and 0.936×10^5 l, respectively. The corresponding quickflow volumes from below culverts 34 and 35 averaged 6.78×10^5 l and 6.08×10^5 l, respectively and ranged from 10.9×10^5 l and 12.5×10^5 l, respectively to 4.90×10^5 l and 1.64×10^5 l, respectively. Expressed on a unit area basis, the unit area quickflow volumes at the mouth of Claire Creek averaged 3.0 mm and ranged from 4.8 mm to 0.8 mm. During each storm the unit area quickflow volumes at the mouth of the watershed were greater than the unit area quickflow volumes above culvert 34, but were smaller than the unit area quickflow volume above culvert 35 and below culverts 34 and 35.

The storms that produced the largest and smallest quickflow volumes at the mouth of Claire Creek were not the same as the storms that produced the largest and smallest quickflow volumes above and below culverts 34 and 35. As mentioned, the largest and smallest quickflow volumes measured at the mouth of Claire Creek were for the December 6th and May 17th storms, respectively. These storms did not consistently produce the largest and smallest quickflow volumes above and below culverts 34 and 35 (see Table 9). Thus the occurrence of the largest and smallest quickflow volumes measured at the mouth of the watershed may happen independent of the largest and smallest quickflow volumes above and below culverts 34 and 35.

4.5.4 Total Stormflow Volume

Total stormflow volume at the mouth of Claire Creek was compared to the total stormflow volume above and below culverts 34 and 35 for each storm. The average total stormflow volume at the mouth of Claire Creek was 82.4×10^5 l and ranged from 108×10^5 to 66.1×10^5 l. Total stormflow below the culverts represented a larger portion of total stormflow at the watershed mouth than the total stormflow above the culverts (Table 10). On average the total stormflow above and below culvert 34 represented 9 and 16 percent, respectively of total stormflow at the mouth of the Claire Creek Watershed. On average, the total stormflow above and below culvert 35 represented 8 and 11 percent, respectively, of the total stormflow at the mouth of the Claire Creek Watershed.

When the volumes of total stormflow are expressed on a unit area basis the area depth volume is often greater above and below culverts 34 and 35 than at the mouth of Claire Creek. The average unit area volume of total stormflow at the mouth of Claire Creek was 16.0 mm and ranged from 21.0 to 12.8 mm. The average unit area total stormflow volume above and below culvert 34 was 14.0 and 25.4 mm, respectively and ranged from 22.3 to 7.4 mm and 36.6 to 18.0 mm, respectively. The unit area total stormflow volume above and below culvert 35 was 23.1 and 32.5 mm, respectively and ranged from 40.7 to 8.2 mm and 53.6 to 10.5 mm, respectively.

The ranges of unit area total stormflow volumes observed above and below culverts 34 and 35 often exceeded the unit area total stormflow volume at the mouth of Claire Creek. Of the nine measurements of total volume made above culverts 34 and 35, four had unit area total stormflow volumes that were less than the unit area total volume at the mouth of the Claire Creek Watershed, and the remaining five had unit area total volumes that exceeded the unit area total volume at the mouth of the Claire Creek Watershed. Of the 10 measurements of total volume made below culverts 34 and 35, one had unit area total stormflow volumes that were less than the unit area total volume at the mouth of the Claire Creek Watershed, and the remaining nine had unit area total volumes that exceeded the unit area total volume at the mouth of the Claire Creek Watershed.

Table 10. Total stormflow volumes observed above and below culverts 34 and 35 and at the mouth of Claire Creek during winter of 2004 – 2005.

Storm	Location	Total volume (l)	Percent of total volume at mouth of watershed (%)	Unit area total volume (mm)	Percent of unit area total volume at mouth of watershed (%)
12/06/04	Claire Creek	10,800,000	100	21.0	100
	34 above road	853,000	8	17.1	81
	34 below road	1,830,000	17	36.6	174
	35 above road	1,220,000	11	40.7	193
	35 below road	1,550,000	14	51.8	246
1/28/05	Claire Creek	6,610,000	100	12.8	100
	34 above road	1,120,000	17	22.3	174
	34 below road	1,340,000	20	26.8	209
	35 above road	245,000	4	8.2	64
	35 below road	314,000	5	10.5	81
3/25/05	Claire Creek	9,860,000	100	19.1	100
	34 above road	--	--	--	--
	34 below road	1,290,000	13	25.8	135
	35 above road	949,000	10	31.6	165
	35 below road	1,610,000	16	53.6	280
5/08/05	Claire Creek	6,810,000	100	13.2	100
	34 above road	371,000	5	7.4	56
	34 below road	1,000,000	15	20.0	151
	35 above road	620,000	9	20.7	156
	35 below road	857,000	13	28.6	216
5/17/05	Claire Creek	7,140,000	100	13.9	100
	34 above road	470,000	7	9.4	68
	34 below road	898,000	13	18.0	130
	35 above road	432,000	6	14.4	104
	35 below road	541,000	8	18.0	130
Average Values	Claire Creek	8,240,000	100	16.0	100
	34 above road	704,000	9	14.0	95
	34 below road	1,270,000	16	25.4	160
	35 above road	693,000	8	23.1	137
	35 below road	974,000	11	32.5	191

4.6 Discharge at Finley Creek and Oak Creek

The peakflows in Claire Creek occurred before and after peakflows in Finley Creek. On average, peakflows occurred 9 minutes earlier at Claire Creek and 24 minutes earlier at Finley Creek than at the Oak Creek gauging station (Table 11). The magnitude of the maximum instantaneous peakflows was greater for Claire Creek than for Finley Creek for all five storms. However, Finley Creek had larger peakflow magnitudes when expressed on a unit area basis for four of the five storms. The same pattern held for quickflow volumes; quickflow volume was greatest for Claire Creek, but quickflow expressed as a unit area depth was greatest for Finley Creek (Table 12). On average, the magnitudes of the peakflows that occurred at Claire Creek and Finley Creek were only three and two percent, respectively, of the magnitudes of the peakflows that occurred at the Oak Creek gauging station. When these peakflows are expressed on a unit area basis, Claire and Finley Creek were 44 and 71 percent of the peakflows at the Oak Creek gauging station. The peakflow magnitudes and quickflow volumes were greatest for the December 6th storm and smallest for the May 17th storm.

Table 11. Maximum instantaneous peakflow magnitude and timing at the mouth of Claire Creek, Finley Creek, and Oak Creek watersheds from five storms during the winter of 2004 – 2005.

Storm	Location	Time of peakflow (hh:mm)	Change from Oak Creek (hh:mm)	Peakflow magnitude (l/s)	Percentage of peak at watershed mouth (%)	Unit area peakflow magnitude (l/s/ha)	Percentage of unit area peak at watershed mouth (%)
12/06/04	Oak Creek	12/8/04 5:00	0	1957	100	2.4	100
	Claire Creek	12/8/04 4:20	0:40 before	49	3	1.0	40
	Finley Creek	12/8/04 4:10	0:50 before	39	2	2.0	84
1/28/05	Oak Creek	1/29/05 9:40	0	521	100	0.6	100
	Claire Creek	1/29/05 9:40	0	22	4	0.4	67
	Finley Creek	1/29/05 8:40	1:00 before	13	3	0.7	106
Peak #1 3/25/25	Oak Creek	3/27/05 7:50	0	998	100	1.2	100
	Claire Creek	3/27/05 8:00	0:10 after	29	3	0.6	47
	Finley Creek	3/27/05 7:50	0	17	2	0.9	72
Peak #2 3/25/25	Oak Creek	3/29/05 3:00	0	1113	100	1.4	100
	Claire Creek	3/29/05 2:40	0:20 before	32	3	0.6	46
	Finley Creek	3/29/05 2:30	0:30 before	20	2	1.0	76
Peak #1 5/08/05	Oak Creek	5/9/05 21:10	0	643	100	0.8	100
	Claire Creek	5/9/05 20:30	0:40 before	32	5	0.6	81
	Finley Creek	5/9/05 21:00	0:10 before	14	2	0.7	93
Peak #2 5/08/05	Oak Creek	5/10/05 12:20	0	946	100	1.1	100
	Claire Creek	5/10/05 11:40	0:40 before	30	3	0.6	51
	Finley Creek	5/10/05 11:30	0:50 before	17	2	0.9	76
5/17/05	Oak Creek	5/19/05 6:30	0	438	100	0.5	100
	Claire Creek	5/19/05 7:40	1:10 after	18	4	0.3	65
	Finley Creek	5/19/05 7:00	0:30 after	6	1	0.3	58
Average Values	Oak Creek		0	945	100	1.1	100
	Claire Creek		0:09 before	30	4	0.6	57
	Finley Creek		0:24 before	18	2	0.9	81

Table 12. Quickflow volumes at the mouth of Claire Creek, Finley Creek, and Oak Creek watersheds from five storms during the winter of 2004 – 2005.

Storm	Location	Quickflow volume (l)	Percentage of quickflow volume at watershed mouth (%)	Unit area quickflow (mm)	Percentage of unit area quickflow at watershed mouth (%)
12/06/04	Oak Creek	93,500,000	100	11.3	100
	Claire Creek	2,450,000	3	4.8	42
	Finley Creek	1,640,000	2	8.4	74
1/28/05	Oak Creek	22,100,000	100	2.7	100
	Claire Creek	805,000	4	1.6	58
	Finley Creek	423,000	2	2.2	80
3/25/05	Oak Creek	102,000,000	100	12.4	100
	Claire Creek	2,140,000	2	4.2	34
	Finley Creek	1,560,000	2	8.0	64
5/08/05	Oak Creek	55,300,000	100	6.7	100
	Claire Creek	1,880,000	3	3.7	55
	Finley Creek	880,000	2	4.5	67
5/17/05	Oak Creek	20,500,000	100	2.5	100
	Claire Creek	429,000	2	0.8	34
	Finley Creek	--	--	--	--
Average Values	Oak Creek	58,700,000	100	7.1	100
	Claire Creek	1,540,000	3	3.0	44
	Finley Creek	1,130,000	2	5.7	71

4.7 Modeled Travel Time of Peakflows

The second objective of this study was to model the travel times of the peakflows from above and below culverts 34 and 35 to the mouth of Claire Creek with and without the effect of the road.

Travel times were modeled using two kinematic wave equations, and by treating the streams as one continuous reach, and as a series of discrete stream reaches. To model the road effect, only the peakflow inputs were changed in the equations, and all other parameters were held constant for peakflows above and below the road.

4.7.1 Modeled Travel Times

The differences in slopes between the culvert and the confluence and between the confluence and the mouth of Claire Creek necessitated that separate calculations of travel time be made for each of the three stream segments. Peakflows from culverts 34 and 35 were assumed to arrive simultaneously at the confluence and a range of travel times was modeled by varying the peakflow magnitude at the confluence and the amount of lateral inflow. Two different routing equations were used: the Chow equation (equation 12) and the Wong equation (equation 13). For each equation, travel times were modeled by treating each stream as one continuous channel and as a number of discrete channel segments. The Manning roughness coefficient, n , was set to 0.1 in both equations for all modeled travel times. This value was selected from a table of approximated roughness coefficients according to the type of channel, the amount of vegetation in the channel, and the size of the substrate material (Chow, 1959). Modeled travel times were shortest for the December 6th storm, the storm with the most runoff, and longest for the May 17th storm, the storm with the least runoff, regardless of the equation or channel method used. In this section modeled travel times will be presented for the stream between culvert 34 and the confluence, for the stream between culvert 35 and the confluence, and for Claire Creek between the confluence and the mouth of the watershed.

Modeled travel times from culvert 34 to the confluence using the Chow equation and treating the stream as one continuous channel are presented in Table 1. For the peakflows above culvert 34, the shortest modeled travel times ranged from 5.8 to 8.4 minutes; the longest modeled travel times ranged from 10.0 to 18.1 minutes; and the average modeled travel times ranged from 7.0 to 10.5 minutes. For the peakflows below culvert 34, the shortest modeled travel times ranged from 5.6 to 8.1 minutes; the longest modeled travel times ranged from 6.5 to 12.4 minutes; and the average modeled travel times ranged from 6.0 to 9.5 minutes. The shortest modeled travel time decreased the most between above and below culvert 34 during the May 17th storm and was a reduction of 0.3 minutes. The longest and average modeled travel times decreased the most between above and below culvert 34 during the December 6th storm and was a reduction of 3.5 minutes and 1 minute, respectively.

Table 13. Modeled travel times for peakflows above and below culvert 34 from the culvert to the confluence in the Claire Creek Watershed using the Chow (1988) and Wong (2001) kinematic wave equations and treating the stream as one continuous channel.

Storm	Chow Equation Modeled travel time (min)			Wong Equation Modeled travel time (min)		
	Shortest	Longest	Average	Shortest	Longest	Average
12/06/04						
Above culvert 34	5.8	10.0	7.0	7.3	10.0	8.2
Below culvert 34	5.6	6.5	6.0	6.0	6.5	6.3
1/28/05						
Above culvert 34	7.6	13.6	9.2	9.7	13.7	11.0
Below culvert 34	7.5	11.3	8.8	9.0	11.3	9.8
3/25/05 Peak #1						
Above culvert 34	--	--	--	--	--	--
Below culvert 34	7.0	10.5	8.2	8.4	10.5	9.2
3/25/05 Peak #2						
Above culvert 34	6.7	12.4	8.2	8.6	12.4	9.8
Below culvert 34	6.7	8.2	7.3	7.4	8.3	7.8
5/08/05 Peak #1						
Above culvert 34	6.7	12.1	8.1	8.5	12.1	9.7
Below culvert 34	6.7	9.1	7.5	7.7	9.1	8.2
5/08/05 Peak #2						
Above culvert 34	6.7	12.0	8.2	8.5	12.1	9.7
Below culvert 34	6.6	9.2	7.6	7.7	9.2	9.3
5/17/05						
Above culvert 34	8.4	18.1	10.5	11.2	18.1	13.2
Below culvert 34	8.1	12.4	9.5	9.7	12.4	10.7
Overall average						
Above culvert 34			8.5			10.3
Below culvert 34			7.8			8.8

The modeled travel times from culvert 34 to the confluence using the Wong equation and treating the stream as one continuous channel are also presented in Table 13. For the peakflows above culvert 34, the shortest modeled travel times range from 7.3 to 11.2 minutes; the longest modeled travel times range from 10.0 to 18.1 minutes; and the average modeled travel times ranged from 8.2 to 13.2 minutes. For the peakflows below culvert 34, the shortest modeled travel times ranged from 6.0 to 9.7 minutes; the longest modeled travel times ranged from 6.5 to 12.4 minutes; and the average modeled travel times ranged from 6.3 to 10.7 minutes. The decrease in modeled travel times between above and below culvert 34 was the largest during the December 6th storm. The

shortest modeled travel time was reduced by 1.3 minutes; the longest modeled travel time was reduced by 3.5 minutes; and the average modeled travel time was reduced by 1.9 minutes.

Using the Chow equation and treating the stream below culvert 34 as discrete channel segments resulted in an increase in the shortest and average modeled travel times and a decrease in the longest travel times when compared with the modeled travel times using the Chow equation and a single, continuous length of channel (Table 14). For the peakflows above culvert 34, the shortest modeled travel times ranged from 7.0 to 10.9 minutes; the longest modeled travel times ranged from 9.8 to 17.9 minutes; and the average modeled travel times ranged from 7.9 to 12.8 minutes. For the peakflows below culvert 34, the shortest modeled travel times ranged from 5.9 to 9.5 minutes; the longest modeled travel times ranged from 6.4 to 12.1 minutes; and the average modeled travel times ranged from 6.1 to 10.4 minutes. The decrease in modeled travel times between above and below culvert 34 was the largest during the December 6th storm. The shortest modeled travel time was reduced by 1.1 minutes; the longest modeled travel time was reduced by 3.4 minutes; and the average modeled travel time was reduced by 1.8 minutes.

Using the Wong equation, and treating the stream below culvert 34 as discrete channel segments resulted in a decrease in the shortest, longest, and average modeled travel times when compared with modeled travel times using the Wong equation and a single, continuous length of channel (Table 14). For the peakflows above culvert 34, the shortest modeled travel times ranged from 7.1 to 11.0 minutes; the longest modeled travel times ranged from 9.8 to 17.9 minutes; and the average modeled travel times ranged from 8.0 to 12.9 minutes. For the peakflows below culvert 34, the shortest modeled travel times ranged from 5.9 to 9.5 minutes; the longest modeled travel times ranged from 6.4 to 12.2 minutes; and the average modeled travel times ranged from 6.1 to 10.5 minutes. The decrease in modeled travel times between above and below culvert 34 was the largest during the December 6th storm. The shortest modeled travel time was reduced by 1.2 minutes; the longest modeled travel time was reduced by 3.4 minutes; and the average modeled travel time was reduced by 1.9 minutes.

The modeled travel times for the reach of stream from culvert 34 to the confluence given the two equations, treating the stream as one long reach or a series of shorter reaches, with and without the influence of the road and for the five storms ranged from an absolute minimum of 5.6 minutes to an absolute maximum of 18.1 minutes. On average, there was no difference in modeled travel times between one continuous reach and a series of discrete reaches. On average, the Wong equation results in slightly longer modeled travel times that were made with and without the road than the Chow equation, but only by 1 to 2 minutes out of travel times of 8 to 10 minutes. On average, the effect of the road was to decrease the modeled travel times by about 1 minute out of 8 to 10 minutes.

Table 14. Modeled travel times for peakflows above and below culvert 34 from the culvert to the confluence in the Claire Creek Watershed using the Chow (1988) and Wong (2001) kinematic wave equations and treating Claire Creek as discrete channel segments.

Storm	Chow Equation Modeled travel time (min)			Wong Equation Modeled travel time (min)		
	Shortest	Longest	Average	Shortest	Longest	Average
12/06/04						
Above culvert 34	7.0	9.8	7.9	7.1	9.8	8.0
Below culvert 34	5.9	6.4	6.1	5.9	6.4	6.1
1/28/05						
Above culvert 34	9.3	13.3	10.6	9.4	13.3	10.7
Below culvert 34	8.7	11.0	9.6	8.7	11.0	9.6
3/25/05 Peak #1						
Above culvert 34	--	--	--	--	--	--
Below culvert 34	8.1	10.3	8.9	8.2	10.3	9.0
3/25/05 Peak #2						
Above culvert 34	8.3	12.1	9.5	8.4	12.2	9.6
Below culvert 34	7.2	8.0	7.6	7.2	8.1	7.6
5/08/05 Peak #1						
Above culvert 34	8.2	11.8	9.4	8.3	11.8	9.4
Below culvert 34	7.4	8.8	8.0	7.5	8.9	8.0
5/08/05 Peak #2						
Above culvert 34	8.3	11.8	9.4	8.3	11.8	9.5
Below culvert 34	7.5	9.0	8.1	7.5	9.0	8.1
5/17/05						
Above culvert 34	10.9	17.9	12.8	11.0	17.9	12.9
Below culvert 34	9.5	12.1	10.4	9.5	12.2	10.5
Overall average						
Above culvert 34			9.9			10.0
Below culvert 34			8.4			7.3

Modeled travel times from culvert 35 to the confluence using the Chow equation and treating the stream as one continuous stream reach are presented in Table 15. For the peakflows above culvert 35, the shortest modeled travel times ranged from 5.4 to 8.2 minutes; the longest modeled travel times ranged from 7.8 to 15.7 minutes; and the average modeled travel times ranged from 6.2 to 10.1 minutes. For the peakflows below culvert 35, the shortest modeled travel times ranged from 5.5 to 8.4 minutes; the longest modeled travel times ranged from 6.3 to 14.2 minutes; and the average modeled travel times ranged from 6.2 to 10.1 minutes. When the Chow equation was used and the stream was treated as one continuous stream reach the shortest modeled travel times for peakflows below culvert 35 are longer than the shortest travel times modeled for peakflows above culvert 35. The biggest difference in modeled travel times between above and below culvert 35 for the shortest modeled travel time occurred during the first peak of the March 25th storm, and was an increase of 0.2 minutes. The biggest difference in the longest and average modeled travel times occurred during the second peak of the March 25th storm, and was a reduction of 2.9 minutes and 0.7 minutes, respectively.

Table 15. Modeled travel times for peakflows above and below culvert 35 from the culvert to the confluence in the Claire Creek Watershed using the Chow (1988) and Wong (2001) kinematic wave equations and treating Claire Creek as one continuous channel.

Storm	Chow Equation Modeled travel time (min)			Wong Equation Modeled travel time (min)		
	Shortest	Longest	Average	Shortest	Longest	Average
12/06/04						
Above culvert 35	5.4	7.8	6.2	6.3	7.9	6.9
Below culvert 35	5.5	6.3	5.9	5.9	6.3	6.1
1/28/05						
Above culvert 35	7.7	14.4	9.4	9.9	14.4	11.3
Below culvert 35	7.8	12.6	9.3	9.6	12.6	10.6
3/25/05 Peak #1						
Above culvert 35	6.5	11.0	7.8	8.1	11.0	9.3
Below culvert 35	6.7	9.3	7.6	7.7	9.3	8.4
3/25/05 Peak #2						
Above culvert 35	6.5	10.7	7.7	8.0	10.7	9.0
Below culvert 35	6.5	7.8	7.0	7.1	7.8	7.4
5/08/05 Peak #1						
Above culvert 35	6.4	10.2	7.6	7.8	10.2	8.7
Below culvert 35	6.4	8.3	7.1	7.2	8.4	7.7
5/08/05 Peak #2						
Above culvert 35	6.7	11.8	8.1	8.4	11.8	9.6
Below culvert 35	6.8	9.6	7.7	7.9	9.6	8.6
5/17/05						
Above culvert 35	8.2	15.7	10.1	10.6	15.7	12.2
Below culvert 35	8.4	14.2	10.1	10.5	14.2	11.8
Overall average						
Above culvert 34			8.1			9.6
Below culvert 34			7.8			8.7

Modeled travel times from culvert 35 to the confluence using the Wong equation and treating the stream as one continuous stream reach are also presented in Table 15. For the peakflows above culvert 35, the shortest modeled travel times ranged from 6.3 to 10.6 minutes; the longest modeled travel times ranged from 7.9 to 15.7 minutes; and the average modeled travel times ranged from 6.9 to 12.2 minutes. For the peakflows below culvert 35, the shortest modeled travel times ranged from 5.9 to 10.5 minutes; the longest modeled travel times ranged from 6.3 to 14.2 minutes; and the average modeled travel times ranged from 6.1 to 11.8 minutes. The biggest differences in modeled travel times between above and below culvert 35 occurred during the second peak of the March 25th storm.

The shortest modeled travel time decreased by 0.9 minutes; the longest modeled travel time decreased by 2.9 minutes; and the average modeled travel time decreased by 1.6 minutes.

Using the Chow equation and treating the stream below culvert 35 as discrete channel segments resulted in an increase in the modeled shortest and average travel times and decreased the longest travel times relative to the travel times modeled using the stream as one continuous reach (Table 16). For the peakflows above culvert 35, the shortest modeled travel times ranged from 6.3 to 10.4 minutes; the longest modeled travel times ranged from 7.8 to 15.7 minutes; and the average modeled travel times ranged from 6.9 to 12.0 minutes. For the peakflows below culvert 35, the shortest modeled travel times ranged from 5.8 to 10.3 minutes; the longest modeled travel times ranged from 6.3 to 14.1 minutes; and the average modeled travel times ranged from 6.1 to 11.6 minutes. The biggest difference in modeled travel times between above and below culvert 35 occurred during the second peak of the March 25th storm. The shortest modeled travel time decreased by 0.9 minutes; the longest modeled travel time decreased by 2.9 minutes; and the average modeled travel time decreased by 1.4 minutes.

Table 16. Modeled travel times for peakflows above and below culvert 35 from the culvert to the confluence in the Claire Creek Watershed using the Chow (1988) and Wong (2001) kinematic wave equations and treating Claire Creek as discrete channel segments.

Storm	Chow Equation Modeled travel time (min)			Wong Equation Modeled travel time (min)		
	Shortest	Longest	Average	Shortest	Longest	Average
12/06/04						
Above culvert 35	6.3	7.8	6.9	6.3	7.9	6.9
Below culvert 35	5.8	6.3	6.1	5.9	6.3	6.1
1/28/05						
Above culvert 35	9.7	14.3	11.2	9.8	14.4	11.2
Below culvert 35	9.4	12.5	10.5	9.4	12.5	10.5
3/25/05 Peak #1						
Above culvert 35	7.9	10.9	8.9	8.0	11.0	9.0
Below culvert 35	7.6	9.3	8.3	7.7	9.3	8.3
3/25/05 Peak #2						
Above culvert 35	7.9	10.7	8.8	7.9	10.7	8.9
Below culvert 35	7.0	7.8	7.4	7.0	7.8	7.4
5/08/05 Peak #1						
Above culvert 35	7.7	10.2	8.6	7.7	10.3	8.6
Below culvert 35	7.1	8.3	7.6	7.2	8.3	7.7
5/08/05 Peak #2						
Above culvert 35	8.3	11.8	9.4	8.3	11.8	9.4
Below culvert 35	7.8	9.5	8.5	7.8	9.6	8.5
5/17/05						
Above culvert 35	10.4	15.7	12.0	10.5	15.7	12.0
Below culvert 35	10.3	14.1	11.6	10.4	14.1	11.7
Overall average						
Above culvert 34			9.4			9.4
Below culvert 34			8.6			8.8

Using the Wong equation and treating the stream below culvert 35 as discrete channel segments decreased the shortest, longest, and average modeled travel times compared with a single continuous stream reach (Table 16). For the peakflows above culvert 35, the shortest modeled travel times ranged from 6.3 to 10.4 minutes; the longest modeled travel times ranged from 7.9 to 15.7 minutes; and the average modeled travel times ranged from 6.9 to 12.0 minutes. For the peakflows below culvert 35, the shortest modeled travel times ranged from 5.9 to 10.4 minutes; the longest modeled travel times ranged from 7.9 to 14.1 minutes; and the average modeled travel times ranged from 6.1 to 11.7 minutes. The biggest difference in modeled travel times between above and below

culvert 35 all occurred during the second peak of the March 25th storm. The shortest modeled travel time decreased by 0.9 minutes; the longest modeled travel time decreased by 2.9 minutes; and the average modeled travel time decreased by 1.5 minutes.

The modeled travel times for the reach of stream from culvert 35 to the confluence given the two equations, treating the stream as one long reach or a series of shorter reaches, with and without the influence of the road and for the five storms ranged from an absolute minimum of 5.4 minutes to an absolute maximum of 15.7 minutes. On average, the difference in modeled travel times between one continuous reach and a series of discrete reaches was about 1 minute out of 8 to 10 minutes. On average, the Wong equation results in slightly longer modeled travel times than the Chow equation for made with and without the road, but only by 1 to 2 minutes out of travel times of 8 to 10 minutes. On average, the effect of the road was to decrease the modeled travel times by about 1 minute out of 8 to 10 minutes.

After the travel times were modeled for the streams between culverts 34 and 35 and their confluence, travel times were modeled for Claire Creek between the confluence and the mouth of the watershed (see map, Figure 4). Modeled travel times using the Chow equation and treating the stream as one continuous stream reach from the confluence of the streams to the watershed mouth are presented in Table 17. For the peakflows from above the culverts, the shortest modeled travel times ranged from 10.9 to 16.3 minutes; the longest modeled travel times ranged from 16.9 to 32.7 minutes; and the average modeled travel times ranged from 12.8 to 20.2 minutes. For the peakflows from below the culverts, the shortest modeled travel times did not change; the longest modeled travel times ranged from 12.6 to 26.8 minutes; and the average modeled travel times ranged from 11.6 to 19.3 minutes. The biggest difference in modeled travel times between above and below the culverts occurred during the second peak of the March 25th storm. The longest modeled travel time decreased by 6.6 minutes; and the average modeled travel time decreased by 1.5 minutes.

Table 17. Modeled travel times for peakflows above and below culverts 34 and 35 in the Claire Creek Watershed from the confluence to the mouth using the Chow (1988) and Wong (2001) kinematic wave equations and treating Claire Creek as one continuous channel.

Storm	Chow Equation Modeled travel time (min)			Wong Equation Modeled travel time (min)		
	Shortest	Longest	Average	Shortest	Longest	Average
12/06/04						
Above the culverts	10.9	16.9	12.8	10.9	13.2	11.8
Below the culverts	10.9	12.6	11.6	10.9	11.7	11.3
1/28/05						
Above the culverts	15.1	27.6	18.4	15.1	19.3	16.6
Below the culverts	15.1	23.5	17.8	15.1	18.3	16.3
3/25/05 Peak #1						
Above the culverts	--	--	--	--	--	--
Below the culverts	13.4	19.2	15.4	13.4	15.7	14.4
3/25/05 Peak #2						
Above the culverts	12.9	22.3	15.6	13.0	16.2	14.1
Below the culverts	12.9	15.7	14.1	13.0	14.2	13.5
5/08/05 Peak #1						
Above the culverts	12.8	21.5	15.3	12.8	15.9	14.0
Below the culverts	12.8	17.0	14.4	12.8	14.6	13.6
5/08/05 Peak #2						
Above the culverts	13.2	23.4	16.0	13.2	16.7	14.5
Below the culverts	13.2	18.5	15.1	13.2	15.4	14.1
5/17/05						
Above the culverts	16.3	32.7	20.2	16.3	21.4	18.0
Below the culverts	16.3	26.8	19.3	16.3	19.9	17.7
Overall average						
Above the culvert			16.4			14.8
Below the culvert			15.4			14.4

Modeled travel times using the Wong equation and treating the stream as one continuous channel from the confluence of the streams to the mouth of the watershed are also presented in Table 17. For the peakflows from above the culverts, the shortest modeled travel times ranged from 10.9 to 16.3 minutes; the longest modeled travel times ranged from 13.2 to 21.4 minutes; and the average modeled travel times ranged from 11.8 to 18.0 minutes. For the peakflows from below the culverts, the shortest modeled travel times did not change; the longest modeled travel times ranged from 11.7 to 19.9 minutes; and the average modeled travel times ranged from 11.3 to 17.7 minutes. The biggest difference in modeled travel times between above and below the culverts occurred during the second

peak of the March 25th storm. The longest modeled travel time decreased by 2.0 minutes; and the average modeled travel time decreased by 0.6 minutes.

Using the Chow equation and treating the stream below the confluence as discrete channel segments resulted in an increase in the shortest travel times and a decrease for the longest and average travel times, compared with travel times modeled with a single, continuous stream reach (Tables 18). For the peakflows from above the culverts, the shortest modeled travel times ranged from 11.2 to 16.7 minutes; the longest modeled travel times ranged from 13.3 to 21.3 minutes; and the average modeled travel times ranged from 12.0 to 18.3 minutes. For the peakflows from below the culverts, the shortest modeled travel times did not change; the longest modeled travel times ranged from 12.0 to 20.0 minutes; and the average modeled travel times ranged from 11.5 to 18.0 minutes. The biggest difference in modeled travel times between above and below the culverts occurred during the second peak of the March 25th storm. The longest modeled travel time decreased by 2.0 minutes; and the average modeled travel time decreased by 0.6 minutes.

Table 18. Modeled travel times for peakflows above and below culverts 34 and 35 in the Claire Creek Watershed from the confluence to the mouth using the Chow (1988) and Wong (2001) kinematic wave equations and treating Claire Creek as discrete channel segments.

Storm	Chow Equation Modeled travel time (min)			Wong Equation Modeled travel time (min)		
	Shortest	Longest	Average	Shortest	Longest	Average
12/06/04						
Above the culverts	11.2	13.3	12.0	11.2	13.3	12.0
Below the culverts	11.2	12.0	11.5	11.2	11.9	11.5
1/28/05						
Above the culverts	15.5	19.3	16.8	15.5	19.4	16.9
Below the culverts	15.5	18.4	16.6	15.5	18.5	16.7
3/25/05 Peak #1						
Above the culverts	--	--	--	--	--	--
Below the culverts	13.7	15.9	14.6	13.8	16.0	14.7
3/25/05 Peak #2						
Above the culverts	13.3	16.3	14.4	13.3	16.4	14.4
Below the culverts	13.3	14.2	13.8	13.3	14.5	13.8
5/08/05 Peak #1						
Above the culverts	13.1	16.0	14.2	13.2	16.1	14.2
Below the culverts	13.1	14.8	13.8	13.2	14.8	13.9
5/08/05 Peak #2						
Above the culverts	13.5	16.7	14.7	13.6	16.8	14.8
Below the culverts	13.5	15.5	14.4	13.6	15.6	14.4
5/17/05						
Above the culverts	16.7	21.3	18.3	16.7	21.5	18.4
Below the culverts	16.7	20.0	18.0	16.7	20.1	18.0
Overall average						
Above the culverts			15.1			15.5
Below the culverts			14.7			15.0

Using the Wong equation and treating the stream below the confluence as discrete channel segments resulted in an increase in the travel times, compared with travel times modeled with a single, continuous stream reach (Tables 18). For peakflows from above the culverts, the shortest modeled travel times ranged from 11.2 to 16.7 minutes; the longest modeled travel times ranged from 13.3 to 21.5 minutes; and the average modeled travel times ranged from 12.0 to 18.4 minutes. For peakflows from below the culverts, the shortest modeled travel times did not change; the longest modeled travel times ranged from 11.9 to 20.1 minutes; and the average modeled travel times ranged from 11.5 to 18.0 minutes. The biggest difference in modeled travel times between above and below

the culverts occurred during the second peak of the March 25th storm. The longest modeled travel time decreased by 1.9 minutes; and the average modeled travel time decreased by 0.6 minutes.

5. DISCUSSION

The impact of the #600 road on peakflow magnitude, peakflow timing, quickflow volumes, and total stormflow volumes is discernable at culverts 34 and 35. However, discerning the impact of the road on peakflow magnitude, peakflow timing, quickflow volumes and total stormflow volumes at the mouth of the Claire Creek Watershed is more difficult because the hydrology of the watershed in the absence of the road is not known and because the hydrological behavior of the non-monitored portion of the Claire Creek Watershed is not known. The real travel times of peakflows varied between storms and monitoring locations, which suggested that real travel times of peakflows may not be an appropriate tool to detect the effect of roads at the mouth of the watershed. Modeled peakflow travel times decreased, which indicates that the road might affect the peakflow travel time.

5.1 Road Effects at the Culverts

The impact of the road at the culverts was to increase the peakflow magnitude, quickflow volume, and total stormflow volume below culverts 34 and 35 (Table 19). The impact of the road on peakflow timing was less consistent. The peakflows in the streams above culverts 34 and 35 were advanced, remained unchanged, and were delayed by the addition of ditchflow.

Table 19. The average change in peakflow timing and the average percent increases in peakflow magnitude, quickflow volume and total stormflow below culverts 34 and 35 in the Claire Creek Watershed during the winter of 2004 – 2005. Percent increase is in parenthesis.

Culvert	Peakflow timing	Peakflow magnitude (l/s)	Quickflow volume (mm)	Total stormflow (mm)
34 above road	--	2.4	1.4	14.1
34 below road	18 minutes after	6.6 (196)	13.5 (1005)	25.4 (99)
35 above road	--	5.1	10.5	23.1
35 below road	7 minutes before	8.7 (66)	20.3 (87)	32.5 (38)

5.1.1 Peakflow Magnitude

The results of this study indicate that the road affects the peakflow magnitude at the stream crossing culverts. Peakflow magnitudes increased below culverts 34 and 35 for all seven of the observed peaks as a result of the addition of ditchflow by an average of 196 and 66 percent, respectively. Peakflow magnitude above and below culvert 35 during the winter of 2004 – 2005 were

similar to the peakflow magnitude observed during the winter 2002 – 2003 (Toman, 2004), and the average percent increase in peakflow magnitude was slightly higher in the present study. Toman observed an average percent increase of 43 percent, and the present study observed an average percent increase of 66 percent. Both winters were characterized by storms with return intervals of less than 1 year.

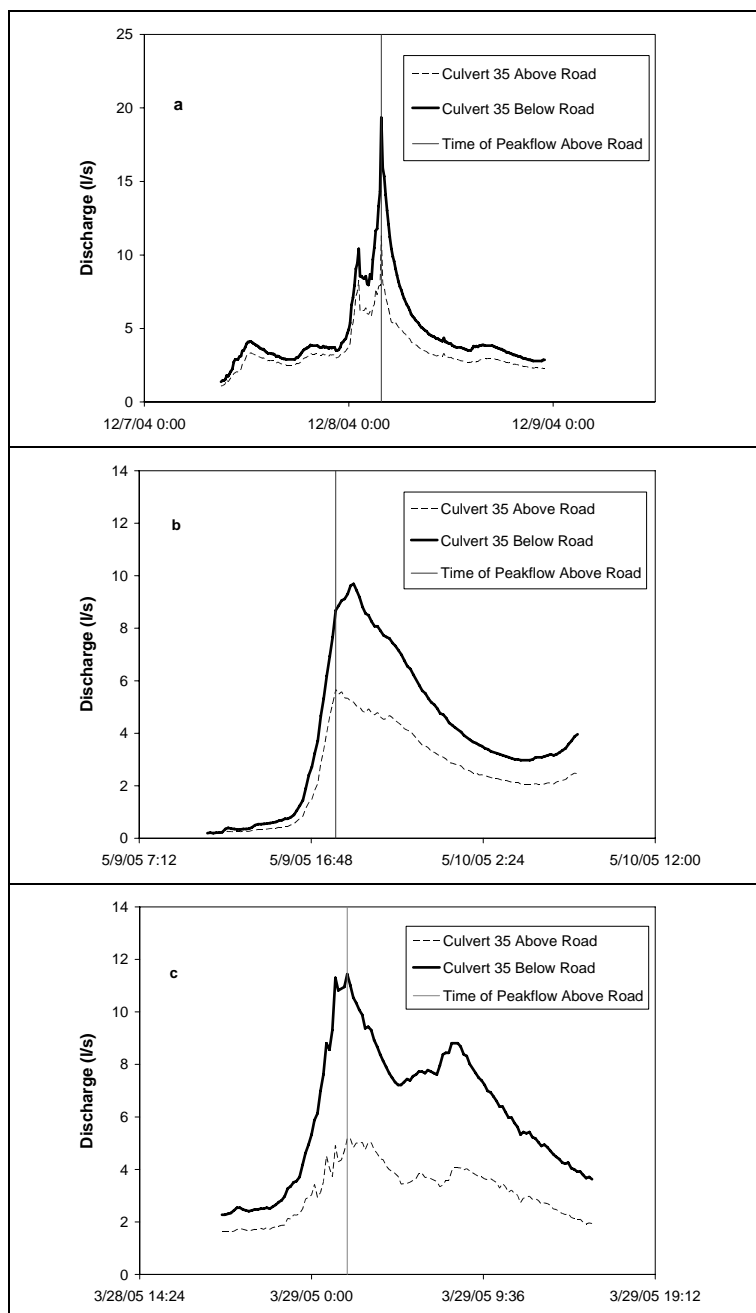
5.1.2 Peakflow Timing

The effect of the road on peakflow timing was less consistent than the effect of the road on peakflow magnitude below culverts 34 and 35. If peakflows occurred above the culvert either before or simultaneously with peakflows below the culvert, the peakflow timing of the stream was not advanced by ditch flow (Figure 13a and b). However, if peakflows occurred below the culvert prior to peakflows above the culvert, the ditch flow did advance the peakflow timing of the stream by contributing to the rising limb (Figure 13c). Fifteen percent of the peakflows at culverts 34 and 35 were advanced by the addition of ditchflow, 54 percent were unchanged, and 31 percent were delayed by the addition of ditchflow. Large, intense storms did not cause the greatest changes in peakflow timing below the road. For the storm with the largest total precipitation and the most intense 1-hour and 24-hour rainfall (December 6th), the peakflow timing was delayed by 30 minutes below culvert 34 and was unchanged below culvert 35 (Table 5). In addition, peakflow timing below culverts 34 and 35 remained unchanged for the storms that had the greatest percent increase in peakflow magnitude. Thus, the impact of the road on peakflow timing below the culverts varies with the most common response being no change.

The changes in peakflow timing observed in this study are within the range observed in the Oak Creek Watershed (Toman, 2004). Toman (2004) reported that, on average, the peakflow occurred below the culverts 1.0 hour before the peakflow above the culvert and that the difference ranged from an advance in timing of 14.3 hours to a delay in timing of 16.0 hours. In the present study the peakflows below the culverts occurred, on average, 4.6 minutes after the peakflows above the culverts and that difference ranged from an advance in timing of 1.3 hours to a delay in timing of 1.0 hour.

A comparison of the change in peakflow timing at culverts 34 and 35 observed by Toman (2004) and by the present study reveal that the change in peakflow timing at these two culverts was greater during the present study. Toman (2004) experienced an equipment malfunction at culvert 34 and was unable to present runoff data for culvert 34. In the present study the average change in peakflow timing below culvert 34 was a delay of 18 minutes and ranged from an advance of 0 minutes to a delay of 50 minutes. Toman (2004) observed that, on average, the peakflow below culvert 35 occurred 0.5 hours before the peakflow above culvert 35 and that the difference ranged from an advance in timing of 1.0 hours to no change. In the present study the average change in peakflow timing below culvert 35 was an advance of 7 minutes and ranged from an advance of 80 minutes to a delay of 60 minutes (Table 5).

Figure 13. The peakflow timing of the streams above and below the road at Culvert 35 for three storms in the winter of 2004-2005. Peakflow timing above the road was observed to be the same as below the road (a), to occur before peakflow below the road (b), and to occur after peakflow below the road (c).



5.1.3 Quickflow Volume

An increase in quickflow volume at the road is another effect of the road. Quickflow volumes below culverts 34 and 35 were greater than the quickflow volumes above culverts 34 and 35 for all five storms and of the hydrology parameters that were measured quickflow was the parameter most affected by the road (Table 19). The large impact of the road on quickflow was due, at least in part, to the assignment of all ditchflow to quickflow.

The increase in quickflow below culvert 34 was not identical to the increase in quickflow below culvert 35. Quickflow measured in the stream above culvert 35 were greater than the quickflow measured in the stream above culvert 34 (see Table 7). However, quickflow measured below culvert 34 were greater than the quickflow measured below culvert 35. For all five storms the increase in quickflow below culvert 34 was much greater than the increase in quickflow below culvert 35, which indicates that the road had a greater impact on quickflow at culvert 34 than at culvert 35.

Toman (2004) reported that quickflow increased below the road by an average of 52 percent and that the increase ranged from 0 to 517 percent. In the present study, quickflow volumes below culverts 34 and 35 increased by an average of 495 percent and ranged from 68 to 1637 percent (Table 7). One reason that the range of increase in quickflow below the culverts observed in this study is greater than the range reported by Toman (2004) is that different culverts were monitored. Toman (2004) did not include culvert 34, which generated a greater percent increase in quickflow than any of the culverts included in her study. If only culvert 35 is considered, which averaged an increase of 87 percent in quickflow below the culvert, that increase is within the range observed by Toman (2004).

5.1.4 Total Stormflow Volume

The impact of the road was to increase total stormflow below culverts 34 and 35. The average percent increase in total stormflow was less than the increase in peakflow magnitude or quickflow (Table 19). There was no consistent pattern between the total stormflow above and below each culvert or from culvert to culvert within the same storm. For example, the January 28th storm—the storm with the least rainfall—produced the greatest total stormflow above culvert 34 and the smallest total stormflow above and below culvert 35 (Table 10).

These temporal disparities suggest that some factor other than the road is also affecting the hydrology of the areas upslope of the culverts. Differences in rainfall patterns, soil storage, or preferential flow paths could affect the total stormflow as well as the road. Tromp-van Meerveld (2004) studied a trench that extended to the bedrock of a hillslope and reported that subsurface runoff came from different parts of the hillslope depending on antecedent soil moisture and total storm precipitation. In the present study, the periods without rainfall between the storms varied, so it is expected that the antecedent soil moisture would be different for each storm as was the total rainfall.

Total stormflow is a function of input within the watershed. A road can change the input into the watershed only if it transports water from one watershed to the other. Thus, the increase of total stormflow directly below the road in this study does not indicate an increase in water within the watershed. The water that enters the stream at the culverts would normally enter the stream lower in the watershed if the road were not there. Therefore, the impact of the road on total stormflow is most discernable and likely to affect the hydrology of a watershed right at the road, and the impact would be less discernable at the mouth of the watershed.

5.1.5 Culvert 34 versus Culvert 35

The road affected peakflow magnitudes, quickflow volumes, and total stormflow at both culverts, but the effect was greater at culvert 34 (Table 19). The fact that impacts were greater for all three parameters at culvert 34 indicates that something about the watershed upslope of culvert 34 makes it consistently more susceptible to road effects than the watershed upslope of culvert 35. However, in a study of multiple culverts within the Oak Creek Watershed, Toman (2004) found no correlation in the variability between culverts and elevation, length of the ditch, upslope contributing area, average cutslope height, road gradient, average hillslope gradient, average soil depth, contributing road surface area, topographic index, total contributing area, and instantaneous maximum flow or total stormflow. The ditch associated with the segment of road between culverts 34 and 35 flows for most of the year, even during the dry season. This suggests that the road intercepts a perennial, subsurface preferential flow pathway. During storms this flow carries more subsurface flow than the surrounding hillslope and it all drains to culvert 34. This is, most likely, why the

increases in peakflow magnitude, quickflow volumes, and total stormflow were always greater at culvert 34 than at culvert 35.

During storms, the peakflow magnitude and quickflow volume observed in the stream above culvert 35 were greater than those observed in the stream above culvert 34. The subsurface flow pathway intercepted by the road between culverts 34 and 35 appears to enter the ditch within two meters of culvert 35. The proximity of the subsurface flow pathway to the stream above culvert 35 may explain why peakflow magnitudes and quickflow volumes were always greater above culvert 35 during storms. It also may explain why the increases in peakflow magnitudes and quickflow volumes below culvert 35 are not as great as the increases below culvert 34. The road may be intercepting stream flow that would otherwise have flowed in the stream below culvert 35 and redirecting it to the stream below culvert 34.

5.2 Travel Time of Peakflows

The travel times modeled by either the Chow or Wong equation, and by treating the stream as one continuous reach or as a number of discrete reaches, were relatively consistent, and for simplicity the discussion will use the results from the Wong equation and the continuous channel. The Wong equation was chosen because it has inputs for both the upstream and downstream discharge. As a result, the modeled travel times are expected to be closer representations of the travel time of peakflows than the Chow equation, as the discharge is expected to increase downstream.

5.2.1 Modeled Travel Times

With one exception, the #600 road decreased the shortest, longest, and average modeled travel times of peakflows in the stream between culvert 34 and the confluence and culvert 35 and the confluence for both the Chow and Wong equation, and when the stream was treated as one continuous reach or a series of discrete reaches (Tables 13 – 16). The shortest modeled travel times of peakflows above culvert 35 were less than the modeled travel time of peakflows below culvert 35 when travel times were modeled using the Chow equation and the continuous channel method. The modeled travel time increased for peakflows below culvert 35 as a result of the assumption that the peakflows from culvert 34 and 35 arrive simultaneously at the confluence. To meet that assumption, the

downstream discharge in the stream below culvert 35 had to be decreased to compensate for the increase in peakflow observed below culvert 34 (Equations 15 and 16). Decreasing the downstream discharge in the stream below culvert 35 resulted in a longer modeled travel time. Thus, the exception to the pattern of decreased travel times being modeled for peakflows below the culverts was a result of the assumptions applied to the travel time equation.

The shortest modeled travel times assumed that all of the lateral inflow happened above the confluence, thus the #600 road does not affect the shortest modeled travel times from the confluence to the mouth of the watershed. In Equation 14, any change in peakflow magnitude below the road would be mitigated by a decrease in lateral inflow, q , along the channels upstream of the confluence to ensure that the initial upstream discharge is never greater than the discharge measured at the mouth of Claire Creek. As a result, the initial upstream discharge would be constant regardless of changes in peakflows above and below the culverts, as would the modeled travel time.

In contrast, the longest modeled travel times were made by assigning all of the lateral inflow to occur downstream of the confluence. Thus, the initial upstream discharge is equal to the collective peakflow magnitude from culverts 34 and 35. Peakflow magnitudes always increased below culverts 34 and 35 and resulted in a decrease in the amount of lateral inflow that occurs downstream of the confluence and a reduction in the modeled travel time in Claire Creek. Just as the #600 road always increased peakflow magnitudes, it always decreased the longest and average modeled travel times. Even though this impact was consistent, the changes in travel times were minor.

The modeled travel times of peakflows were first examined for the stream reach below the confluence. The December 6th storm had the greatest peakflow magnitudes. The collective peakflow magnitude above culverts 34 and 35 was 16.3 l/s, and the collective peakflow magnitude below culverts 34 and 35 was 33.9 l/s (see Table 5). Although the collective peakflow magnitude below the culverts is more than 100 percent greater than the collective peakflow magnitude above the culverts, the travel time modeled with the average amount of lateral inflow in Claire Creek is only reduced by 4 percent (from 11.8 to 11.3 minutes). Thus the road reduced the average modeled travel time for the peakflows in this storm by only 0.5 minutes (see Table 17). The second peak of the March 25th storm

had the greatest percent increase in collective peakflow magnitude (140 percent). It also had the largest reduction in the average modeled travel time in Claire Creek: 5 percent (from 14.1 to 13.5 minutes), a difference of 0.6 minutes. These examples demonstrate that large increases in peakflow magnitude below the roads do not decrease the modeled travel times in Claire Creek by a large amount.

Above the confluence, where the slopes were greater, the changes in modeled travel time were also minor when compared to the increase in peakflow magnitude. During the December 6th storm, the peakflow at culvert 34 and 35 increased by 190 and 70 percent, respectively, the average modeled travel times were reduced by 24 and 12 percent, respectively. The 24 percent reduction at culvert 34 correlates to a decrease in travel time of 1.9 minutes (from 8.2 to 6.3 minutes) and the 12 percent reduction at culvert 35 correlates to a decrease in travel time of 0.8 minutes (from 6.9 to 6.1 minutes).

Combining the modeled travel times for the stream between culvert 34 and the confluence, and from the confluence to the mouth of Claire Creek produces an estimate of the travel time from culvert 34 to the mouth of Claire Creek. The estimated travel time for the peakflows above the culvert can then be compared to the travel times for the peakflows below the culvert (Table 20). The overall average travel time for the peakflows from above culvert 34 to the mouth of Claire Creek is 25.1 minutes, and ranged from an absolute minimum travel time of 18.2 minutes to an absolute maximum travel time of 39.5 minutes. The overall average travel time for the peakflows from below culvert 34 to the mouth of Claire Creek is 23.2 minutes, and ranged from an absolute minimum travel time of 16.9 minutes to an absolute maximum travel time of 32.3 minutes.

The process was repeated for the modeled travel times for the stream between culvert 35 and the confluence, and from the confluence to the mouth to estimate total travel times for peakflows above and below the culvert (Table 20). The overall average travel time for the peakflows from above culvert 35 to the mouth of Claire Creek is 24.4 minutes, and ranged from an absolute minimum travel time of 17.2 minutes to an absolute maximum travel time of 37.1 minutes. The overall average travel time for the peakflows from below culvert 35 to the mouth of Claire Creek is 23.1 minutes, and

ranged from an absolute minimum travel time of 16.8 minutes to an absolute maximum travel time of 34.1 minutes.

Table 20. Modeled travel times for peakflows from above and below culverts 34 and 35 to the mouth of Claire Creek using the Wong (2001) kinematic wave equation and treating Claire Creek as one continuous channel.

Storm	Culvert 34 to mouth Modeled travel time (min)			Culvert 35 to mouth Modeled travel time (min)		
	Shortest	Longest	Average	Shortest	Longest	Average
12/06/04						
Without the road	18.2	23.2	20.0	17.2	21.1	18.7
With the road	16.9	18.2	17.6	16.8	18.0	17.4
1/28/05						
Without the road	24.8	33.0	27.6	25.0	33.7	27.9
With the road	24.1	29.6	26.1	24.7	30.9	26.9
3/25/05 Peak #1						
Without the road						
With the road	21.8	26.2	23.6	21.1	25.0	22.8
3/25/05 Peak #2						
Without the road	21.6	28.6	23.9	21.0	26.9	23.1
With the road	20.4	22.5	21.3	20.1	22.0	20.9
5/08/05 Peak #1						
Without the road	21.3	28.0	23.7	20.6	26.1	22.7
With the road	20.5	23.7	21.8	20.0	23.0	21.3
5/08/05 Peak #2						
Without the road	21.7	28.8	24.2	21.6	28.5	24.1
With the road	20.9	24.6	23.4	21.1	25.0	22.7
5/17/05						
Without the road	27.5	39.5	31.2	26.9	37.1	30.2
With the road	26.0	32.3	28.4	26.8	34.1	29.5
Overall average						
Without the road			25.1			24.4
With the road			23.2			23.1

For each storm the modeled peakflow travel times from above culverts 34 and 35 to the mouth of Claire Creek were never more than ten minutes longer than the travel time from below the appropriate culvert to the mouth of Claire Creek. Often the difference in modeled travel times below the culverts was less than five minutes. Since the sampling interval of the capacitance rods and pressure transducers was ten minutes, the change in modeled travel times would be smaller than the ability of this study to detect.

As mentioned, the kinematic wave equations were selected so that all of the stream reach parameters could be held constant while only the peakflow magnitudes were changed to model the effect of adding ditch runoff into the streams at stream crossing culverts. The addition of ditch runoff increased peakflow magnitudes by an average of 145 percent at culverts 34 and 35, and on average the modeled travel time decreased by 1 to 2 minutes. The small change in modeled travel times relative to the large increase in peakflow magnitudes suggests that some other factor is influencing the arrival of peakflows at the mouth of the watershed more than the addition of ditchflow.

5.2.2 Real and Modeled Travel Times

Real and modeled travel times were calculated for peakflows from above and below culverts 34 and 35 to the mouth of Claire Creek with and without the road effect. Real travel times were not correlated to changes in peakflow magnitude at culverts 34 and 35 or at the mouth of the watershed. The modeled travel times were impacted by the change in peakflow magnitude resulting from the #600 road.

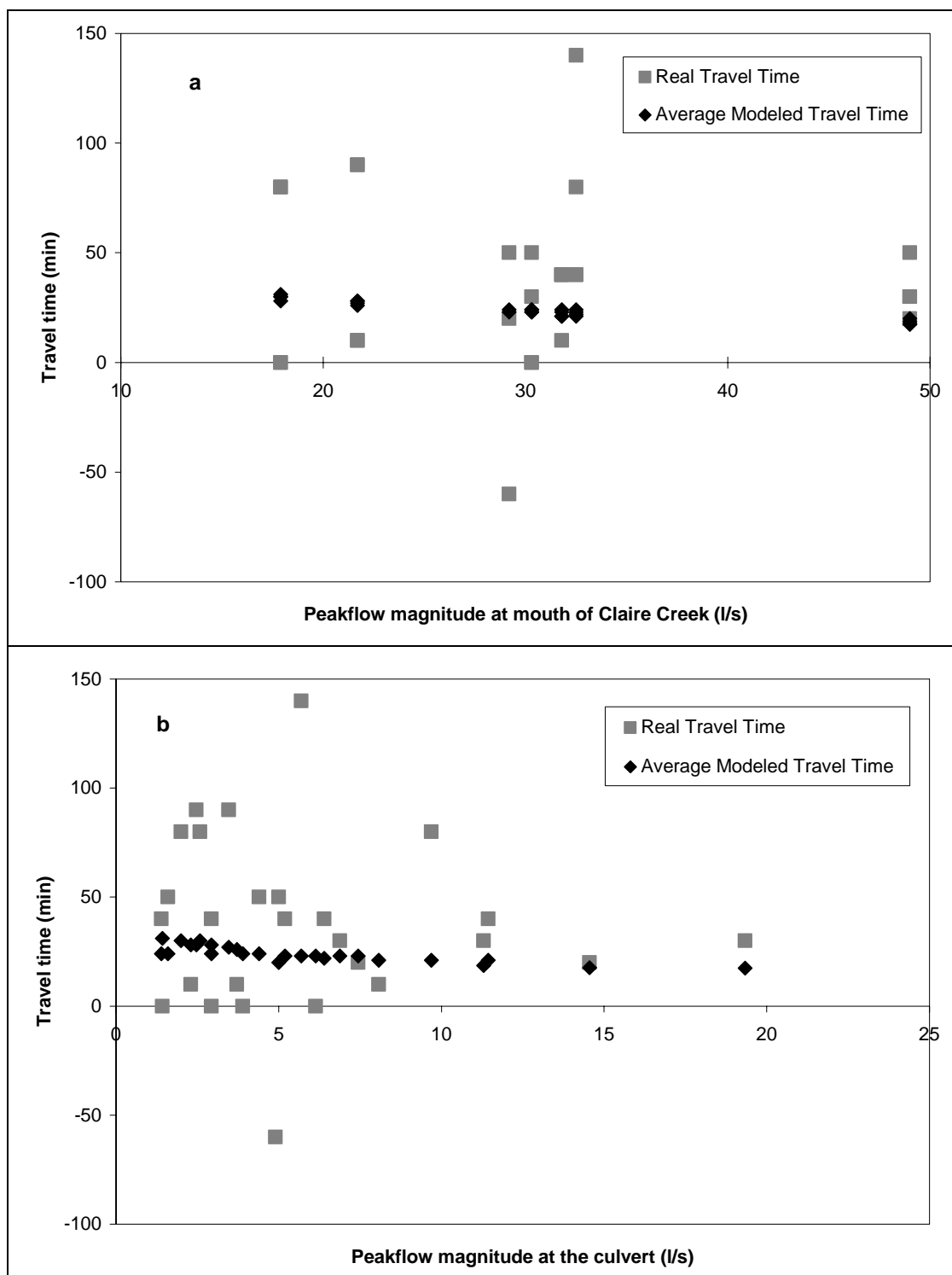
Although the correlation between the real travel times of peakflows and peakflow magnitudes above and below the culverts and at the mouth of Claire Creek is poor (Figure 12a and 12b), the real travel times are useful to illustrate that peakflows at the culverts may occur independent of peakflows at the mouth of the watershed. For example, two storms produced peakflows that occurred simultaneously at the culvert monitoring locations and at the mouth of the Claire Creek Watershed (Table 9). The rapid wave velocities, or celerities, that would have been required in order for the peaks to occur simultaneously are not possible. In another example, during the first peak of the March 25th storm, the peakflow above culvert 35 happened 60 minutes after the peakflow at the mouth of Claire Creek, resulting in a peakflow with a negative real celerity. Additionally, large increases in peakflow magnitude at the stream crossing culvert were not consistently reflected in the real travel times of peakflows. For example, in the December 6th storm, the peakflow magnitude below culvert 35 increased by 8 l/s, but the real travel time of the peakflow was not changed.

In contrast, the road impact on modeled travel times of peakflows was consistent in that the modeled travel times decreased in relation to increasing peakflow magnitudes. As a result the

modeled travel times had less variability than the real travel times of peakflows relative to the peakflow magnitude observed at the mouth of Claire Creek (Figure 14a) and above and below culverts 34 and 35 (Figure 14b).

The disparity between modeled and real travel times suggests that the kinematic wave failed to model runoff in Claire Creek and that some other factor is having a larger effect on the runoff at the mouth of the Claire Creek. If a decrease in travel time of a peakflow from a stream crossing culvert to the mouth of the watershed was dependant on the increase in peakflow magnitude caused by the addition of ditch runoff, it is expected that the modeled and real travel times would be similar. Factors such as spatial and temporal rainfall variability (Goodrich et al., 1995; Bidin and Chappell, 2003) and the distribution of subsurface preferential flow paths in soil and bedrock profiles have been reported to impact the arrival of peakflows at the mouth of a watershed (Whipkey, 1965; Mosley, 1979; McDonnell, 1990; Anderson et al., 1997). These factors and other hydrologic pathways throughout the watershed may have influenced the peakflow timing at the mouth of Claire Creek more than the addition of the ditchflow at culverts 34 and 35.

Figure 14. Scatterplots of real travel times and average modeled travel times of peakflows from culverts 34 and 35 to the mouth of Claire Creek relative to a) peakflow magnitude observed at the mouth of Claire Creek, and b) peakflow magnitude observed above and below culverts 34 and 35 during the winter of 2004 – 2005.



5.3 Instantaneous Peakflow versus Near Peakflow

Much of this paper has dealt with the magnitude and timing of peakflows observed at monitoring locations within the Claire Creek Watershed. The peakflow was previously defined as the maximum instantaneous discharge at a given monitoring location. However, the term is somewhat misleading, as the peaks actually occur over a prolonged period of time.

When viewed for the duration of an entire storm, the peak appears as a single moment on the hydrograph. However, an analysis of the hydrographs from the mouth of Claire Creek reveals that the discharge was 'near peak' for some time. Near peak is the term used to define that portion of the hydrograph beginning when the discharge increased to within 1 l/s of the peak discharge, continuing through the peak, and ending when the discharge had receded and was no longer within 1 l/s of the peak discharge (Equation 19):

$$nearpeak = (Q_{max} - Q_i) \leq 1 l/s \quad (19)$$

where Q_{max} is the peakflow (l/s), and Q_i is the discharge at time i (l/s). For example, the discharge at Claire Creek peaked at 49 l/s during the December 6th storm. The near peak began at 03:50am when the discharge was first measured to be greater than 48 l/s, and ended at 04:30am when the discharge was last measured to be greater than 48 l/s (Table 21). The duration of the near peak for the December 6th storm was then 40 minutes, and during that time the discharge changed by less than 1 l/s.

The length of the near peak period has implications for the effect of the #600 road in altering the peakflow timing at the mouth of Claire Creek. The greatest change in modeled travel time of 7.2 minutes happened during the May 17th storm, which also had the longest near peak of 9 hours and 10 minutes. The flow at the mouth increased by one liter per second over the course of 2 hours and 40 minutes and then required another 6 hours and 10 minutes to decrease by one liter per second. It is difficult to discern whether the advancement of 7.2 minutes had any noteworthy effect on the hydrology at the mouth of Claire Creek. The change in modeled travel time for peakflows above and below the road was never greater than 10 minutes during any of the five storms, and the near peaks for all but one of the storms lasted more than 90 minutes.

A change of 10 minutes in the arrival of the peakflows at the mouth of the watershed correlates to discharge magnitudes that were not dissimilar to the observed peakflow. The greatest change in peakflow magnitude within the ten minute interval was observed during the December 6th storm and was 0.6 l/s. For all other storms the change in peakflow was less than 0.3 l/s. Thus, the change in peakflow timing and peakflow magnitude that result from the road was small and does not appear to affect the hydrology at the mouth of Claire Creek.

Table 21. Time and duration of ‘near peak’ at the mouth of Claire Creek for five storms during the winter of 2004 – 2005.

Storm	Time of near peak (hh:mm)			Duration (hh:mm)
	Begin	Peak	End	
12/06/04	03:50	04:20	04:30	0:40
01/28/05	08:30	9:40	12:10	3:40
03/25/05 #1	05:40	08:00	10:10	4:30
03/25/05 #2	02:10	02:40	03:50	1:40
05/08/05 #1	19:30	20:30	21:20	1:50
05/08/05 #2	10:30	11:40	13:00	2:30
05/17/05	05:00	07:40	14:10	9:10

5.4 Sensitivity of Kinematic Waves to Equation Parameters

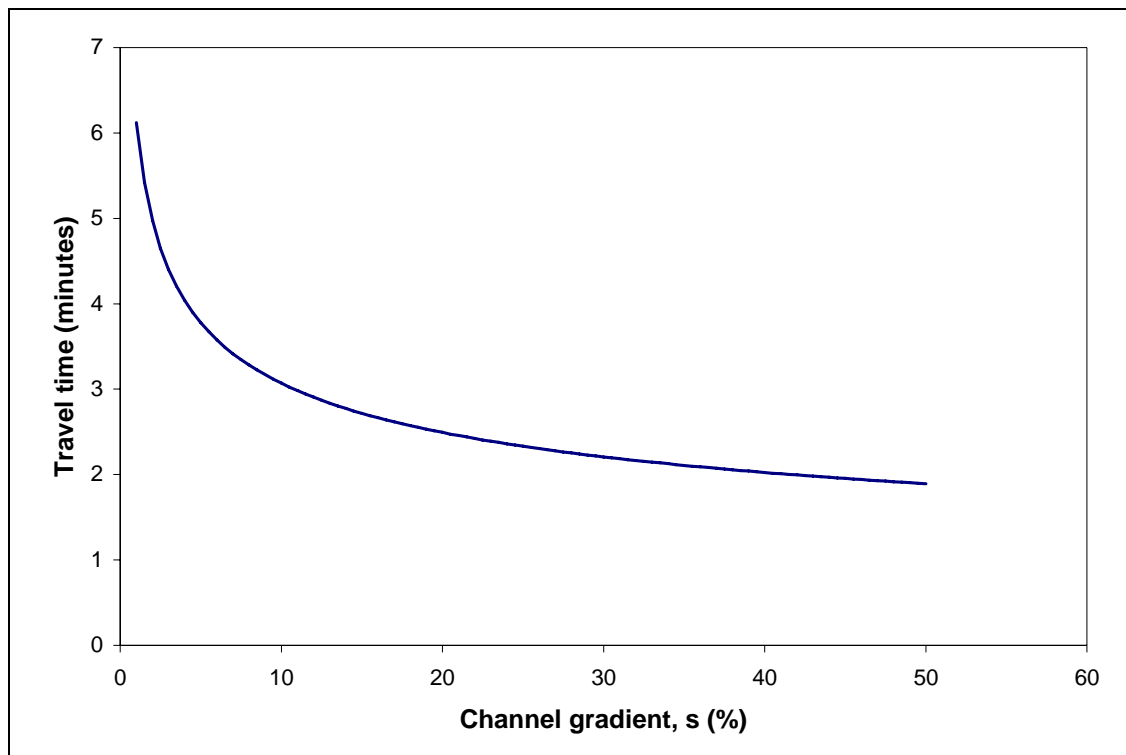
A sensitivity analysis for parameters in the Wong (2001) equation was conducted to determine how much the modeled travel times would have changed for Claire Creek as the channel slope, roughness coefficient, and the discharge at the confluence were changed. The channel slope was measured in the field and is known, and the roughness coefficient and discharges used in the equation were approximated.

5.4.1 Channel Slope

The channel slopes in Claire Creek were measured with a hand level and a stadia rod. Recognizing that the accuracy of the measurements is limited, a sensitivity analysis of channel slope was conducted. The analysis revealed that the modeled travel time is inversely related to the channel slope, though the relationship is not linear. Travel times are most effected by changes in slope at lower gradients (Figure 15). For example, using the Wong (2001) equation and the continuous

channel segment method for the December 6th storm, the average modeled travel time of the peakflow above the culvert is 11.8 minutes. Reducing the channel slope from 11.3 to 9.3 percent results in a modeled travel time of 12.5 minutes, a difference of 0.7 minutes. If the change was from 9.3 to 7.3 percent, the modeled travel time would be 13.4 minutes, an additional increase of 0.9 minutes. Thus, modeled travel times are more effected as slopes decrease. Since the channel slope did not change in the modeled travel times for the above and below the culvert peakflows, any inaccuracy would be equally applied to both peakflows. As a result, the difference in the timing between the peakflows above and below the culverts would be consistent.

Figure 15. Graph showing relationship between channel slope and average modeled travel times from the confluence of the streams below culverts 34 and 35 to the mouth of the Claire Creek Watershed for the December 6th, 2004 storm, using the Wong (2001) equation and continuous method.



5.4.2 Manning Roughness Coefficient

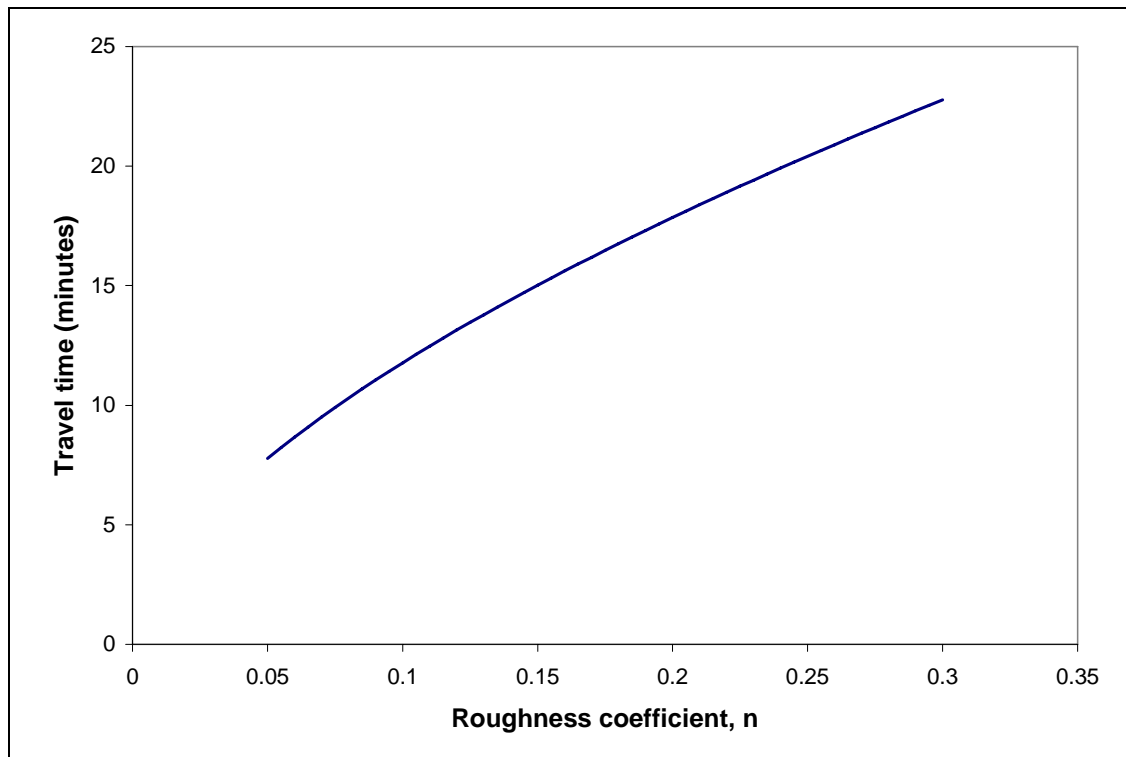
Some of the uncertainty in the modeled travel times of the peakflows arises from the value used as the roughness coefficient in equation 12 and 13. The Manning roughness coefficient selected for the all three stream reaches was 0.1. The table and diagrams used in selecting that value, while quite specific for channels with low stream slopes, are more generalized for steep stream channels in forested headwaters (Chow, 1959).

Past studies have taken different approaches to applying the Manning equation on steep slopes. Jarrett (1984) conducted experiments on channels with slopes up to five percent to develop an equation that predicts the roughness coefficient of slope with gradients up to 4 percent. Jarrett (1984) found that his equation produced more variability in the roughness coefficient on streams with gradients above 6 percent. A subsequent study (Marcus et al., 1992) used the Jarrett equation to predict a roughness coefficient of small mountain streams with gradients up to 18 percent. Marcus et al. (1992) found that the Jarrett equation overestimated the roughness coefficient by an average of 32 percent. Working with slopes up to 16 percent, Loukas and Dalezios (2000) assigned a constant roughness coefficient of 0.1, rather than use the Jarrett equation. Loukas and Dalezios (2000) recognized that the slopes at their study site were beyond the validity range of Jarrett's equation. Cowan (1956) provides a subjective method of determining the roughness coefficient from channel character, degree of irregularity, variability in cross section size and shape, effect of obstructions, vegetation, and the degree of meandering.

The Loukas and Dalezios (2000) study was conducted in the Coast Mountains of British Columbia, which have a similar topography to the Oregon Coast Range. Furthermore, assigning a constant roughness coefficient and channel slope modeled similar response times when compared to equations that varied these two parameters linearly and nonlinearly (Loukas and Dalezios, 2000). Thus, the roughness coefficient for Claire Creek was assumed to be 0.1 in agreement with the value used by Loukas and Dalezios (2000). Then, after assuming this value, the Cowan method was used in which the value was still determined to be 0.1. Assigning greater roughness values would have

increased the modeled travel times for both above and below the culverts (Figure 16), but it would not have changed the difference in travel time from above and below the culverts.

Figure 16. Graph of relationship between roughness coefficient, n , and average modeled travel time of kinematic wave from the confluence of the streams below culverts 34 and 35 to the mouth of the Claire Creek Watershed for the December 6th, 2004 storm, using the Wong (2001) equation and continuous method.



5.4.3 Lateral Inflow

Kinematic wave equations rely on the assumption that the lateral inflow remains constant through the longitudinal profile of the stream (Singh, 1996; Wong, 2001). This assumption is unlikely to occur in a natural system. For example, there are specific locations along the channel where other small, first order streams drain into the streams below culvert 34 and 35 as well as Claire Creek. As a result, the lateral inflow could be lumped and not constant. Most of the small channels flowing into Claire Creek are located near the confluence. Thus, the modeled travel times would be expected to decrease if more discharge is entering Claire Creek along the upper channel lengths, instead of near the mouth of the watershed, or if the increase was allocated equally along the entire

channel. Also, the amount of lateral inflow associated with the peakflow would probably be smaller at the lower portion of the watershed, where soils are assumed to be deeper and slopes are less steep. If such is the case, the modeled travel times reported here may be slight overestimations of the actual travel times, but again the difference in the modeled travel time for peakflows above and below the culverts would remain consistent.

5.4.4 Discharge at the Confluence

The discharge value at the confluence—the initial upstream discharge in the modeled travel times below the confluence, and the downstream discharge in modeled travel time above the confluence—is the parameter with the most uncertainty. It also had the least effect on the modeled travel time. Recall that estimates of the discharge at the confluence were made from the collective peakflow magnitudes observed above and below culverts 34 and 35, and by varying the lateral inflow to the stream channel. Consequently, a range of discharge values at the confluence was calculated.

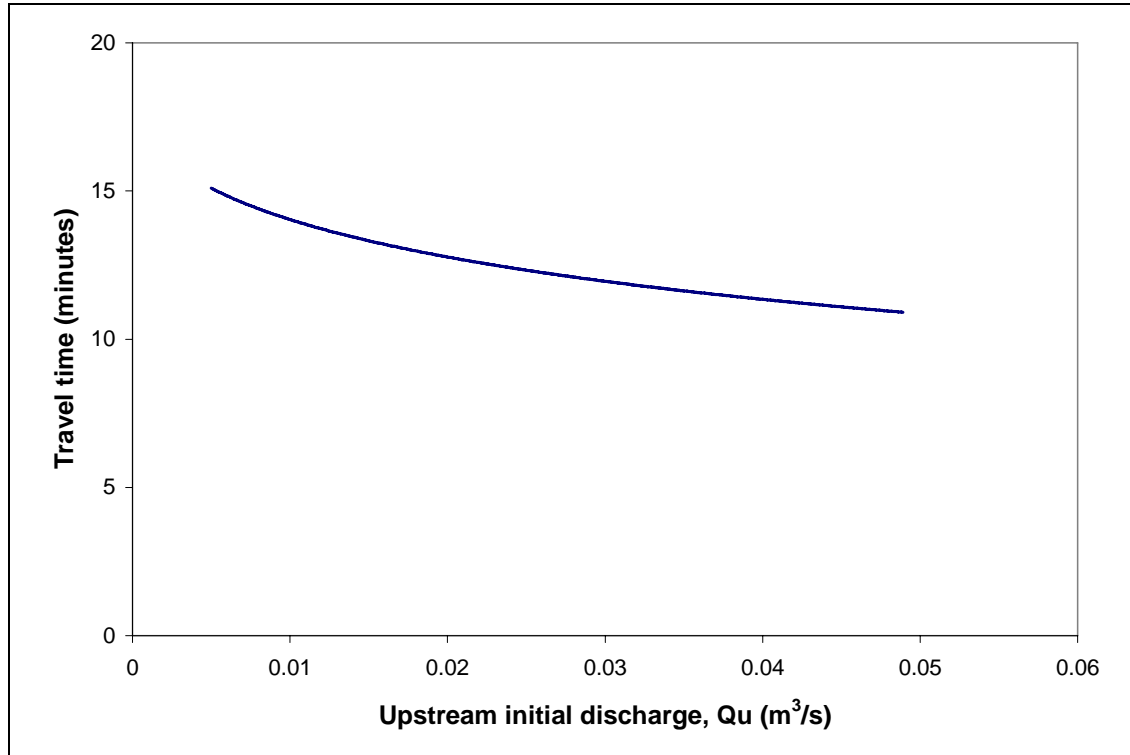
In modeling the range of discharge values at the confluence, the assumption was made that the peakflows from each road segment would arrive simultaneously at the confluence of streams 34 and 35. This assumption was made to model the greatest road effect possible. However, for several of the storms this assumption may not have been valid, which would affect the discharge at the confluence. Using the January 28th storm as an example, peakflow below culvert 35 was observed at 8:10am, while peakflow below culvert 34 was observed at 9:30am; a difference of 80 minutes. The stream below culvert 34 is 318 meters from the culvert to the confluence and has an average slope of 37 percent (Table 1). The stream below culvert 35 is 393 meters from the culvert to the confluence and has an average slope of 34 percent. Even though the stream between culvert 34 and the confluence is shorter and steeper than the stream between culvert 35 and the confluence, it is not likely that the peakflow from culvert 34 would overcome the 80 minute time lag and arrive at the confluence simultaneously with the peakflow from culvert 35. In fact, the average modeled travel times for the stream below culverts 34 and 35 was 9.2 and 11.0 minutes, respectively. Thus, the 80 minute difference in the arrival of the peakflows from culvert 34 and 35 would be preserved. Furthermore, the average travel time modeled from the confluence to the mouth of Claire Creek (a

distance of 538 meters) was 16.3 minutes. It is probable that the peakflow measured below culvert 35 would have passed from the watershed before the peakflow measured below culvert 34 arrived at the confluence. As a result, the range of initial upstream discharges at the confluence would have decreased, and the modeled travel times of the peakflows would increase.

The peakflows at culverts 34 and 35 never occurred simultaneously, but the smallest difference in peakflow timing between culverts was observed during the December 6th storm. The peakflow occurred below culvert 35 ten minutes before the peakflow below culvert 34. Although, this instance represents the most likely opportunity for the peakflows to arrive at the confluence simultaneously, it still probably did not happen, as the modeled travel times for each channel suggest that the time difference would have been preserved (Table 13, 15). Thus, even when peakflows below culvert 34 occurred at almost the same time as the peakflow below culvert 35, the peakflows may not have arrived simultaneously at the confluence.

Although there is an effect on the modeled travel times if an incorrect discharge value is used in equation 12 or 13, the effect is small. As shown in Figure 17, an overestimation of the discharge at the confluence would have to be large in order to have a significant impact on the modeled travel time. For example, the discharge at the confluence during the December 6th storm had to be greater than the collective discharge from below culverts 34 and 35 ($0.034 \text{ m}^3/\text{s}$) but less than the discharge observed at the mouth of Claire Creek ($0.049 \text{ m}^3/\text{s}$). Those discharge values correspond to modeled travel times from the confluence to the mouth of Claire Creek ranging from 10.9 to 11.7 minutes. Thus, any error introduced by inputting an inappropriate discharge value at the confluence would translate to an error in travel times of no greater than 0.8 minutes.

Figure 17. Graph of initial upstream discharge at the confluence of the streams below culverts 34 and 35, and the modeled travel times from the confluence to the mouth of the Claire Creek Watershed for the December 6th, 2004 storm, using the Wong (2001) equation and continuous method.



6. CONCLUSION

At each of the stream crossing culverts in this study, the road effect is clearly discernable on some of the parameters measured. The addition of runoff from inboard ditches increased peakflow magnitudes, quickflow volumes, and total flow volumes in the streams immediately beneath each of the culverts. A consistent change in peakflow timing was not discernable immediately below the culverts. Peakflows above the culverts were advanced, unchanged, and delayed by the addition of runoff from the ditch. The change in peakflow timing above and below the road did not correlate well with change in peakflow magnitude.

Though the hydrological effects of the road on the watershed mouth are unknown because pre-construction runoff data is not available, modeling the travel time of peakflows using kinematic wave equations suggests that the #600 road affects peakflows at the mouth of Claire Creek. Increasing the peakflow magnitude at stream crossing culverts through the addition of ditch runoff resulted in shorter travel times relative to the travel times without the addition of ditch runoff. However, even under assumptions that simulate the greatest possible road effect the difference in the modeled travel times of the peakflows was small.

The change to real peakflow travel times above and below the road does not correlate to changes in peakflow magnitude at the stream crossing culvert or peakflow magnitude at the mouth of Claire Creek. The disparity between the modeled and real travel times suggests that factors including the spatial and temporal variability in rainfall or the hydrologic process occurring throughout the watershed are influencing the runoff at the mouth of Claire Creek more than the addition of ditch runoff.

Determining if a road is altering the hydrology at the mouth of a watershed, specifically the peakflow magnitude and timing, is difficult. Further research, is needed in order to understand the interaction between rainfall and runoff processes of a forested watershed before the road effect can be determined with significance. Future studies would be benefited by measuring rainfall and stream runoff at a higher spatial resolution than was used in this study.

7. LITERATURE CITED

- Abdul, A.S., and R.W. Gillham, 1984. Laboratory studies of the effects of the capillary fringe on streamflow generation. *Water Resources Research*, 20(6): 691-698.
- Amann, J.R., 2004. Sediment production from forest roads in the upper Oak Creek watershed of Oregon Coast Range. M.S. Thesis, Oregon State University, Corvallis 90 pp.
- American Society of Civil Engineers, 1996. River hydraulics. Technical engineering and design guides as adapted from the US Army Corps of Engineers, No. 18, 144 pp.
- Anderson, S.P., Dietrich, W.E., Montgomery, D.R., Torres, R., Conrad, M.E., and K. Loague, 1997. Subsurface flow paths in a steep, unchanneled catchment. *Water Resources Research*, 33(12): 2637-2653.
- Beschta, R.L. Pyles, M.R., Skaugset, A.E. and C.G. Surfleet, 2000. Peakflow responses to forest practices in the western Cascades of Oregon, USA, *Journal of Hydrology (Amsterdam)*, 233: 102-120.
- Betson, R.P., 1964. What is watershed runoff? *Journal of Geophysical Research*, 69(8): 1541-1552.
- Bidin, K., and N.A. Chappell, 2003. First evidence of a structured and dynamic spatial pattern of rainfall within a small humid tropical catchment. *Hydrology and Earth System Sciences*, 7(2): 245-253.
- Bilby, R.E., Sullivan, K, and S.H. Duncan, 1989. The generation and fate of road-surface sediment in forested watersheds in southwestern Washington. *Forest Science*, 35: 453-468.
- Bowling, L.C. and D.P. Lettenmaier, 1997. Evaluation of the effects of forest roads on streamflow in Hard and Ware Creeks, Washington. Timber Fish and Wildlife Report TFW-SH20-97-001, Department of Civil Engineering, University of Washington, Seattle, 189 pp.
- Brooks, K.N., Ffolliott, P.F., Gregersen, H.M., and L.F. DeBano, 1997. Hydrology and the management of watersheds. Iowa State University Press, Ames, Iowa, 502 pp.
- Brown, V.A., McDonnell, J.J., Burns, D.A., and C. Kendall, 1999. The role of event water, a rapid shallow flow component, and catchment size in summer stormflow. *Journal of Hydrology*, 217: 171-190.
- Buttle, J.M., 1994. Isotope hydrograph separations and rapid delivery of pre-event water from drainage basins. *Progress in Physical Geography*, 18: 16-41.
- Chow, V.T., 1959. Open-channel hydraulics. McGraw Hill Inc., New York, 680 pp.
- Chow, V.T., Maidment, D.R., and L.W. Mays, 1988. Applied Hydrology. McGraw Hill Inc., New York, 572 pp.
- Cowan, W.L., 1955. Estimating hydraulic roughness coefficients. *Agricultural Engineering*, 57: 473-475.
- Croke, J. and S. Mockler, 2001. Gully initiation and road-to-stream linkage in a forested catchment, southeastern Australia. *Earth Surface Processes and Landforms*, 26: 205-217.

- Donahue, J.P., and A.F. Howard, 1987. Hydraulic design of culverts on forest roads. *Canadian Journal of Forest Research*, 17: 1545-1551.
- Dunne, T., and R.D., Black, 1970. An experimental investigation of runoff production in permeable soils. *Water Resources Research*, 6(2): 478-490.
- Gburek, W.J., and D.E. Overton, 1973. Subcritical kinematic flow in a stable stream. *Journal of Hydraulics Division, American Society of Civil Engineers*, 99: 1433-1447.
- Gilbert, E.H., 2002. A characterization of road hydrology in the Oregon Coast Range. M.S. Thesis, Oregon State University, Corvallis, 82 pp.
- Goard, D.L., 2004. Characterizing the spatial distribution of short duration, high intensity rainfall in the central Oregon Coast Range. M.S. Thesis, Oregon State University, Corvallis, 114 pp.
- Goodrich, D.C., Faures, J.M., Woolhiser, D.A., Lane, L.J. and S. Sorooshian, 1995. Measurement and analysis of small-scale convective storm rainfall variability. *Journal of Hydrology*, 173(1): 283-308.
- Harr, R.D., Harper, W.C., Krygier, J.T., and F.S. Hsieh, 1975. Changes in storm hydrographs after road building and clear-cutting in the Oregon coast range. *Water Resources Research*, 11: 436-444.
- Harr, R.D., 1977. Water flux in soil and subsoil on a steep forested slope. *Journal of Hydrology* 33: 37-58.
- Hewlett, J.D., and A.R. Hibbert, 1967. Factors affecting the response of small watersheds to precipitation in humid areas. pp. 275-290. In: W.E. Sopper and H.W. Lull (eds) *Forest Hydrology*. Pergamon Press, N.Y., NY.
- Hillel, D., 1998. *Environmental soil physics*. Academic Press, San Diego, 771 pp.
- Horton, J.H., and R.H. Hawkins, 1965. Flow path of rain from the soil surface to the water table. *Soil Science* 100: 377-383.
- Horton, R.E., 1933. The role of infiltration in the hydrologic cycle. *EOS, American Geophysical Union Transactions*, 14: 446-460.
- Ice, G.G., Neary, D.G., and P.W. Adams, 2004. Effects of wildfire on soils and watershed processes. *Journal of Forestry*, 102(6): 16-20.
- Jarrett, R.D., 1984. Hydraulics of high-gradient streams. *Journal of Hydraulic Engineering*, 110 (11): 1519-1539.
- Jones, J.A., and G.E. Grant, 1996. Peak flow responses to clear-cutting and roads in small and large basins, western Cascades, Oregon, *Water Resources Research*, 32: 959-974.
- Jones, J.A., 2000. Hydrologic processes and peak discharge response to forest removal, regrowth, and roads in ten small experimental basins, western Cascades, Oregon. *Water Resources Research*, 36(9): 2621-2642.
- Keppeler, E. and Brown, D., 1998. Subsurface drainage processes and management impacts, USDA Forest Service General Technical Report PSW-GTR-168.

- King, J.G., and L.C. Tennyson, 1984. Alteration of streamflow characteristics following road construction in north central Idaho. *Water Resources Research*, 20(8): 1159-1163.
- Lighthill, M.J., and G.B. Whitham, 1955. Kinematic waves. *Proceedings of the Royal Society of London*, 229 (1178): 281-316.
- Longwood, F.R., 1940. A land use history of Benton County, Oregon. M.F. Thesis, Oregon State University, Corvallis, 146 pp.
- Loukas, A., and N.R. Dalezios, 2000. Response time of forested mountainous watersheds in humid regions. *Nordic Hydrology*, 31 (3): 149-168.
- Luce, C.H., and T.W. Cundy, 1994. Parameter identification for a runoff model for forest roads. *Water Resources Research*, 30(4): 1057-1069.
- MacArthur, R. and J.J. DeVries, 1993. Introduction and application of kinematic wave routing techniques using HEC-1. US Army Corps of Engineers, Institute for Water Resources, Hydrologic Engineering Center, 53 pp., www.hec.usace.army.mil
- Marbet, C.E., 2003. Hydrology of five forest roads in the Oregon Coast range. M.S. Thesis, Oregon State University, Corvallis, 94 pp.
- Marcus, W.A., Roberts, K., Harvey, L., and G. Tackman, 1992. An evaluation of methods for estimating Manning's n in small mountain streams. *Mountain Research and Development*, 12 (3): 227-239.
- McDonnell, J.J., 1990. A rationale for old water discharge through macropores in a steep, humid catchment. *Water Resources Research*, 26: 2821-2832.
- Megahan, W.F., 1972. Subsurface flow interception by a logging road in mountains of central Idaho. *National Symposium on Watersheds in Transition*, American Water Resources Association and Colorado State University, pp. 350-356.
- Megahan, W.F. and J.L. Clayton, 1983. Tracing subsurface flow on roadcuts on steep, forested slopes. *Soil Science Society of America Journal*, 47(6): 1063-1067.
- Mosley, M.P., 1979. Streamflow generation in a forested watershed, New Zealand. *Water Resources Research* 15:795-806.
- Oregon Department of Forestry, 1996. Forest roads, drainage and sediment delivery in the Kilchis river watershed, Report for the Tillamook Bay National Estuary Project.
- Oregon Department of Forestry, 2004. Forest Practice Administrative Rules and Forest Practices Act, Chapter 629.
- Parizek, R.R., 1971. Impact of highways on the hydrogeologic environment. In: *Environmental geomorphology: A proceedings volume of the First Annual Geomorphology Symposia Series*, Binghamton, NY, Oct. 1970, edited by D.R. Coates. State University of New York, Binghamton, NY.

- Pearce, A.J., Stewart, M.K., and M.G. Sklash, 1986. Storm runoff generation in humid headwater catchments 1. Where does the water come from? *Water Resources Research* 22(8): 1263-1272.
- Pinder, G.F., Jones, J.F., 1969. Determination of the ground-water component of peak discharge from the chemistry of total runoff. *Water Resources Research* 5(2): 438-445.
- Pritchett, W.L., 1979. Properties and management of forest soils. John Wiley & Sons, New York.
- Ragan, R.M., 1967. An experimental investigation of partial area contributions. Proceedings of the General Assembly of the International Association of the Science of Hydrology. Berne, 1968, pp. 241 – 251.
- Rantz, S.E., 1982. Measurement and computation of streamflow: volume 1. Measurement of stage and discharge, United States Department of the Interior, Geological Survey.
- Reid, L.M., and T. Dunne, 1984. Sediment production from forest road surfaces, *Water Resources Research*, 20: 1753-1761.
- Robinson and Chamberlain, 1960. Trapezoidal flumes for open-channel flow measurement. *Transactions of the ASAE*, 3(2): 120-128.
- Rothacher, J., 1965. Streamflow from small watersheds on the western slope of the Cascade Range of Oregon. *Water Resources Research* 1(1): 125-134.
- Rothacher, J., 1970. Increases in water yield following clear-cut logging in the Pacific Northwest. *Water Resources Research* 6(2): 653-658.
- Singh, V.P., 1996. Kinematic wave modeling in water resources: environmental hydrology. Wiley and Sons, New York, 1424 pp.
- Skaugset, A., and M.M. Allen, 1998. Forest road sediment and drainage monitoring project report for private and state lands in western Oregon, Report to Oregon Department of Forestry, Oregon State University.
- Sklash, M.G., and R.N. Farvolden, 1979. The role of groundwater in storm runoff. *Journal of Hydrology*, 43: 45-65.
- Tague, C., and L. Band, 2001. Simulating the impact of road construction and forest harvesting on hydrologic response. *Earth Surface Processes and Landforms*, 26: 135-151.
- Thomas, R.B., and W.F. Megahan, 1998. Peak flow responses to clear-cutting and roads in small and large basins, western Cascades, Oregon: a second opinion. *Water Resources Research*, 34: 3393-3403.
- Toman, E.M., 2004. Forest Road Hydrology: The Influence of Forest Roads on Stream Flow at Stream Crossings. M.S. Thesis, Oregon State University, Corvallis, Oregon, 79 pp.
- Torres, R., Dietrich, W.E., Montgomery, D.R., Anderson, S.P., and K. Loague, 1998. Unsaturated zone processes and the hydrologic response of a steep, unchanneled catchment. *Water Resources Research*, 34(8): 1865-1879.

- Tromp-van Meerveld, H.J., 2004. Hillslope hydrology: From patterns to processes. Ph.D. dissertation, Oregon State University, Corvallis, Oregon.
- United States Department of Agriculture-Forest Service, 2004. Forest service performance and accountability report, fiscal year 2004. <http://www.fs.fed.us/plan/par/2004/>
- Veldhuisen, C. and P. Russell, 1999. Forest road drainage and erosion infiltration in four west-Cascade watersheds. TFW Monitoring Report: TFW-MAG1-99-001.
- Wemple, B.C., 1994. Hydrologic integration of forest roads with stream networks in two basins, western Cascades, Oregon. M.S. Thesis, Oregon State University, Corvallis, Oregon, 88 pp.
- Wemple, B.C., Jones, J.A., and G.E. Grant, 1996. Channel network extension by logging roads in two basins, western Cascades, Oregon. *Water Resources Bulletin*, 32: 1195-1207.
- Wemple, B.C., 1998. Investigations of runoff production and sedimentation on forest roads. Ph.D. Dissertation, Oregon State University, Corvallis, Oregon, 168 pp.
- Wemple, B.C., Swanson, F.J., and J.A. Jones, 2001. Forest roads and geomorphic process interactions, Cascade Range, Oregon. *Earth Surface Processes and Landforms*, 26: 191-204.
- Wemple, B.C., and J.A. Jones, 2003. Runoff production on forest roads in a steep, mountain catchment. *Water Resources Research*, 39(8): 1220-1237 doi:10.1029/2002WR001744.
- Weyman, D.R., 1970. Throughflow on hillslopes and its relation to the stream hydrograph. *Bulletin of the International Association of Scientific Hydrology*, 15 (2): 25-33.
- Weyman, D.R., 1973. Measurement of the downslope flow of water in a soil. *Journal of Hydrology*, 20: 267-288.
- Whipkey, R.Z., 1965. Subsurface stormflow from forested slopes. *Bulletin of the International Association of Scientific Hydrology*, 2: 74-85.
- Wolman, M.G., 1954. A method for sampling coarse river-bed material: *Transactions of the American Geophysical Union*, 35: 951-956.
- Woolhiser, D.A., and J.A. Liggett, 1967. Unsteady one-dimensional flow over a plane – the rising hydrograph. *Water Resources Research*, 3(3): 753-771.
- Wong, T.S.W., 2001. Formulas for travel time in channel with upstream flow. *Journal of Hydrologic Engineering* 6(5): 416-422.
- Ziegler, A.D. and T.W. Giambelluca, 1997. Importance of rural roads as source areas for runoff in mountainous areas of northern Thailand. *Journal of Hydrology*, 196: 204-229.
- Ziemer, R.R., 1981. Storm flow response to road building and partial cutting in small streams of Northern California. *Water Resources Research*, 17(4): 907-917.